Modeling Dissolved Phosphorus Exports in Lake Erie Watersheds

Final Report

LEPF Grant 397-10

Submitted to:

Gail Hesse, Executive Director
Ohio Lake Erie Commission
111 E. Shoreline Drive
Sandusky, Ohio 44870

Prepared by:

Remegio Confesor Jr.
National Center for Water Quality Research
Heidelberg University
310 East Market Street
Tiffin, Ohio 44883

March 30, 2012

This project was funded in part through the Lake Erie Protection Fund. The LEPF is supported by the voluntary contributions of Ohioans who purchase the *Erie…Our Great Lake* license plate featuring the Marblehead lighthouse.

Modeling Dissolved Phosphorus Exports in Lake Erie Watersheds

Abstract

The recurrence of massive harmful algal blooms (HABs) in the western basin of Lake Erie since the mid-1990s is largely attributed to excessive loads of sediment and phosphorus (P) from the Maumee and Sandusky rivers. Data from the National Center for Water Quality Research (NCWQR) show that the dissolved P load has been increasing since the mid-1990s, corresponding to the reappearance of HABs in Lake Erie. The use of watershed models such as the Soil and Water Assessment Tool (SWAT) is a vital component in exploring the selection and optimal placement of best management practices (BMPs) to reduce nonpoint source pollution (e.g., dissolved phosphorus) from agricultural lands.

SWAT decently simulated the flow, sediments, dissolved P, total P and nitrite+nitrate from Rock Creek, Honey Creek, Sandusky River, and Maumee River. SWAT was successfully used to evaluate the effects of changes in mode of fertilizer application: switching from broadcast to incorporation and from incorporation to broadcast. Simulations showed that broadcasting fertilizer instead of incorporating tremendously increased the dissolved P, while incorporating the fertilizer instead of broadcasting decreased dissolved P. SWAT has a great potential in aiding selection and placement of BMPs to reduce dissolved P exports from the Lake Erie watersheds.

Table of Contents

Abstract i
Introduction 1
Study Objectives 1
The SWAT Model 2
Methods 3
  The Project Watersheds 3
  The SWAT Setup 4
  SWAT modification 5
  Sensitivity Analysis 6
  Calibration and Validation 8
Results 9
  Sensitivity Analysis 9
  SWAT Phosphorus output at low and high flows 12
    SWAT 2009 version 451 and 477 12
    SWAT 2009 version 488 12
  Calibration and validation results 13
  Effects of fertilizer application method 15
Summary and Conclusions 20
References 21
Appendix 1. ASABE Paper No. 1111060 23
Appendix 2. Sensitivity analysis results for Honey Creek, Sandusky, and Maumee 36
Appendix 3. Calibration graph results 43
Appendix 4. Validation graph results 60

Modeling Dissolved Phosphorus Exports in Lake Erie Watersheds

Introduction

The Great Lakes Water Quality Agreement (GLWQA) between the United States and Canada set a target load of 11,000 metric tons/yr of total phosphorus (P) for Lake Erie (US EPA, 1978). The coordinated efforts to control point source pollution resulted in a 60% decrease of total P loading into Lake Erie between the late 1960's and early 1980's (Hartig et al., 2007). As a consequence, algal bloom biomass declined in Lake Erie, especially the blue-green alga (cyanobacterium) *Aphanizomenon flos-aquae* (Nicholls et al., 1977; Makarawicz and Bertram, 1991). However, late-summer algal blooms (e.g., *Microcystis*) have been occurring again with increasing frequency and severity since the mid-1990's (Hartig et al., 2007). This recurrence of harmful algal blooms in Lake Erie is largely attributed to nutrient loading from its tributaries, especially the Maumee and Sandusky watersheds in northwest and north central Ohio. Land use in these watersheds is predominantly agricultural, with unit area nutrient losses comparable to other Midwestern croplands and maybe among the highest in the United States (Baker et al., 2008). The National Center for Water Quality Research (NCWQR) at Heidelberg University in Tiffin, Ohio, has been monitoring daily water quality adjacent to USGS flow gauging stations in the major watersheds draining to Lake Erie for up to 35 years. The NCWQR's data show that sediment and particulate phosphorus runoff to the lake has been reduced since the 1970's. However, the dissolved P load has been increasing in all the monitored Lake Erie tributaries since the mid-1990's.

Researchers have been exploring the selection and optimal placement of best management practices (BMPs) to reduce nonpoint source pollution from agricultural lands (Veith et al., 2003; Gitau et al., 2004; Maringanti et al., 2009). One vital component in these studies is the use of watershed models, specifically the Soil and Water Assessment Tool (SWAT). The SWAT phosphorus output at the subwatershed reaches includes organic P (*Porg*) and mineral P (*Pmin*) and does not explicitly have dissolved reactive phosphorus (*Pdis*). Total P (*Ptot*) is calculated as the sum of *Porg* and *Pmin*. In stream water quality monitoring projects, *Ptot* and *Pdis* are the P forms usually measured, and particulate P (*Ppar*) is then calculated as the difference between *Ptot* and *Pdis*. With the exception of *Ptot*, the different SWAT phosphorus forms and the observed values from stream monitoring cannot be directly compared. Thus, there seems to be a disconnection between the SWAT phosphorus output and stream water quality measurements. Furthermore, *Pmin* includes both dissolved and particulate P and is conventionally assumed to be equal to *Pdis*. While this assumption is valid during low flows, it is probably incorrect during storm events. To appropriately use SWAT in studying the increased *Pdis* exports from the Lake Erie watersheds, SWAT's performance in simulating dissolved phosphorus must be assessed in these watersheds.

Study Objectives

The main goal of this project was to modify SWAT to accurately account for the dissolved reactive phosphorus. The specific objectives are: (1) Add a *Pdis* output variable at the watershed reaches in SWAT, (2) Calibrate and validate the modified SWAT with observed data from the Rock Creek, Honey Creek, Sandusky, and Maumee watersheds, (3) Assess the effect of

fertilizer application method (broadcast vs. surface-applied) and timing (fall vs. spring) on nutrient exports from the above watersheds.

The SWAT Model

SWAT was developed by the United States Department of Agriculture - Agricultural Research Service (USDA-ARS) "to predict the impact of land management practices on water, sediment and agricultural chemical yields in large complex watersheds with varying soils, land use and management conditions over a long period of time" (Neitsch et al., 2005). SWAT is physically based, uses readily available inputs, is computationally efficient, and is a continuous model that operates on a daily time step. A Geographic Information Systems (GIS) interface (e.g., AVSWAT, ArcSWAT) is used to enter and designate land use, soil, weather, groundwater, water use, management, pond and stream water quality data, and the simulation period (Di Luzio et al., 2001). GIS input files include a digital elevation model (DEM), land use/land cover and soil properties layers, and a weather database (Figure 1). In a spatially distributed model, the processes (e.g. landscape, hydrologic, and plant growth) should be implemented in the smallest spatial area possible to increase accuracy and minimize uncertainty. Thus, in SWAT, the entire watershed is divided into subbasins and each subbasin is further divided into unique combinations of land use and soil properties. This smallest spatial unit is called the hydrologic response unit (HRU) (Figure 2).

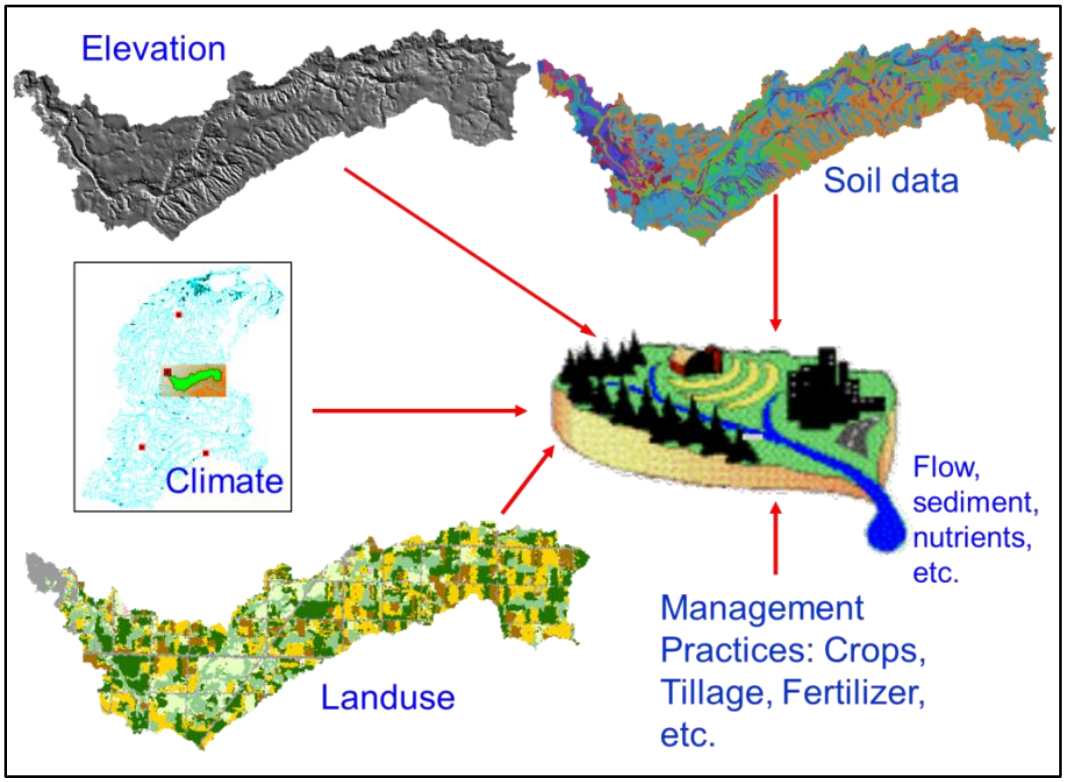

Figure 1. SWAT input and output diagram.

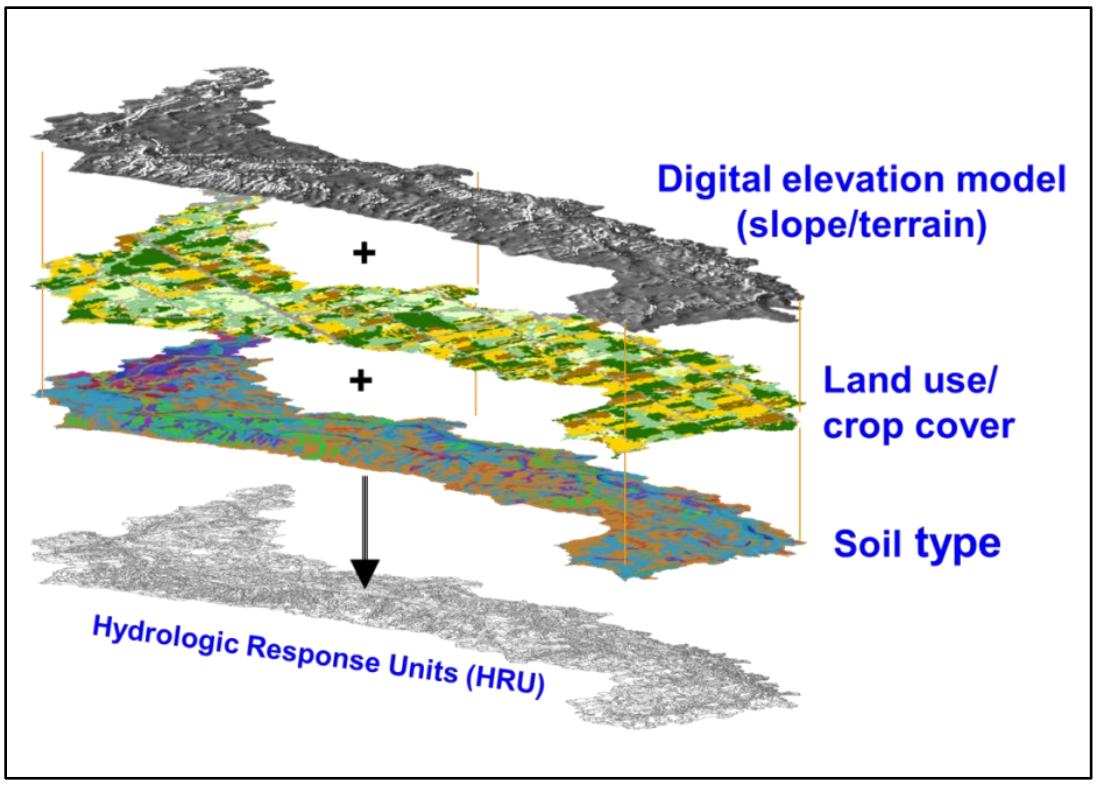

Figure 2. Calculation of the hydrologic response unit (HRU).

Methods

The Project Watersheds

The project area is located in northwest Ohio and includes the Maumee River (drainage area = 6,388 km^2 at 41°30' 00"N and 83°42' 46" W), Sandusky River (drainage area = 3,239 km^2 at 41°18' 28"N and 83°09' 32" W), Honey Creek (drainage area = 386 km^2 at 41° 01' 20" N and 83°06' 35" W) and Rock Creek (drainage area = 90 km^2 at 41° 06' 49" N and 83°10' 06" W) subbasins (Figure 3). These areas are characterized by a humid continental climate (four distinct seasons) and a relatively flat terrain. Daily average temperatures at Tiffin, OH near the confluence of Rock Creek and the Sandusky River, ranged from -8.6°C to -0.1°C in January and 17°C to 29°C in July for the period 1971-2000 (Loftus et al., 2006). Precipitation is distributed throughout the year, and from 1971 to 2000 average annual precipitation was 941.8 mm. Occasional droughts, blizzards, and tornadoes also occur. Agricultural practices in these four watersheds are similar and are typical of agricultural production in Northwest Ohio. The most common agricultural crops are corn, soybeans, and wheat. Four- to five-year crop rotations are sometimes followed with fallow fields usually planted to alfalfa. No-till, strip-till, and mulch-till are used for most (about 90%) soybean and wheat areas. About 80% of corn acreage is chisel plowed; the soil is not inverted but less than 30% of plant residue cover is left on the ground surface.

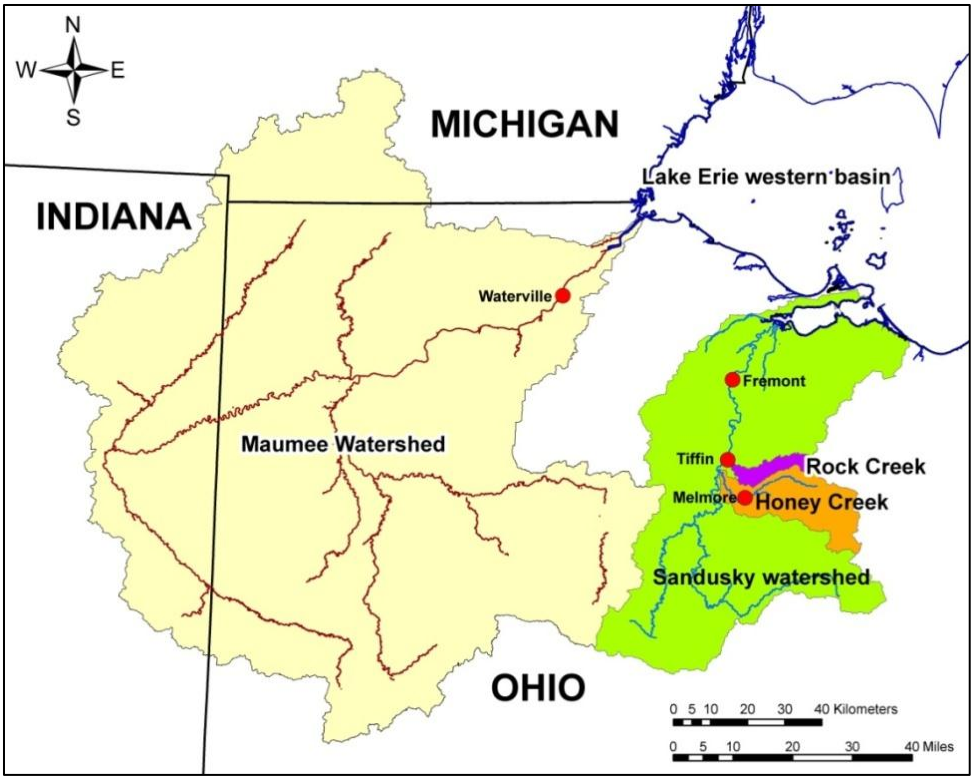

Figure 3. The project watersheds.

The SWAT Setup

GIS Data. The 10-m digital elevation models (DEM), soil data (Soil Survey Geographic (SSURGO) Database and statewide data (STATSGO)), daily rainfall and minimum/maximum temperature, and other geographic information system (GIS) layers were acquired from the websites of federal agencies (USGS, USDA, NOAA, etc.). These data were initially tested in ArcSWAT (version 2.3.4 for SWAT2005) and eventually in ArcSWAT (versions 93.5 to 96.7a for swat2009) to setup SWAT.

HRU calculation. Three metrics were used to calculate the HRU: threshold values of landuse area within the subwatershed area, soil type within a certain landuse, and slope class within a certain soil type. These values can be expressed as percent or actual area. The Sandusky watershed was split into 373 subbasins ranging from 100 to 2000 hectares to a total of 719 HRUs. Threshold values for HRU delineation in the Sandusky watershed were 20% landuse/crop cover, 33 % soil type, and 33% slope. These values indicate that landuses/crop cover that were less than 20% of the subwatershed area, the soil types that were less than 33% in a landuse, and the slopes that were less than 33% in a soil type, were all excluded. The remaining combinations of crop cover, soil types, and slopes were the HRUs and their areas were adjusted and weighted to reflect the original subwatershed area. The Rock Creek watershed was divided into168 subbasins (approximately 10 to 100 ha) and a total of 471 HRUs with a 25% landuse/crop cover, 25 % soil type, and 40% slope thresholds . The Honey Creek watershed was divided into 567 subbasins (19 ha to 180 ha). The dominant HRU option was chosen resulting in one HRU in one subwatershed. Due its very large area, the Maumee watershed was delineated into 225 subbasins and 1378 HRUs. The HRUs were set at 400/400/400 hectares threshold.

Crop rotation and management practices. Four-year crop rotations for each HRU in the Sandusky, Honey Creek, and Rock Creek watersheds were established using the crop cover GIS layers for 2006-2009 with corn, wheat, and soybean as the three dominant crop types. GIS layers for 2007-2010 were used in the Maumee watershed. Agricultural management practices include:

1. Corn crop: soil was chisel plowed and fertilizer (11-52-00, 130 kg/ha) was applied in fall. SWAT was programmed in such a way that 20% of the fertilizer remains at the soil surface even if the fertilizer was incorporated. In early spring anhydrous ammonia (100 kg/ha) was applied before seeding and was applied (100 kg/ha) again 1 month after seeding. Corn was harvested in fall approximately 5 months after seeding.
2. Corn double cropped with soybeans: soil was chisel-plowed and fertilizer (11-52-00, 210 kg/ha) was broadcast in fall. SWAT was programmed in such a way that 20% of the fertilizer remains at the soil surface even if the fertilizer was incorporated. In early spring anhydrous ammonia (100 kg/ha) was applied before seeding and was applied (100 kg/ha) again 1 month after seeding. Corn was harvested in fall approximately 5 months after seeding. The following spring, the SWAT generic no-till operation was done before seeding of the beans. The beans were then harvested in fall, 5 months after seeding.
3. Soybean crop: SWAT generic no-till with fertilizer (11-52-00, 95 kg/ha) broadcast (100% at the soil surface) before seeding in spring. The beans were harvested in fall about 5 months after seeding.
4. Wheat crop: SWAT generic no-till with fertilizer broadcast (100% at the soil surface) in fall (18-46-00, 130 kg/ha) before seeding. Fertilizer was broadcast (11-52-00, 150 kg/ha) again in early spring. Wheat was harvested from early to mid-July.

SWAT modification

At the start of this study, the official SWAT2009 release was version 446 and the FORTRAN source codes were available from http://swatmodel.tamu.edu/software/swat-model. We used the development version 451 in this study and modified some subroutine codes to account for the dissolved and inorganic form of phosphorus. The original equations in the subroutine virtual (FORTRAN file *virtual.f*) that summarize *Porg* and *Pmin* for subbasins with multiple HRUs were:

$$varoute(5,ihout) = (sub_yorgp(sb) + sub_sedps(sb)) * sub_ha \quad (1)$$

or simply put:

organic P in subbasin reach = surface runoff organic P + sediment-attached stable mineral P in the runoff

$$varoute(7,ihout) = (sub_solp(sb) + sub_gwsolp(sb) + sub_sedpa(sb)) * sub_ha \quad (2)$$

Equation (2) means that:

mineral P in subbasin reach = surface runoff soluble (or dissolved) P + ground water soluble P + sediment-attached active P in the runoff

It can be seen in equation (2) that *Pmin* is composed of soluble P and sediment-attached mineral P. The appropriate equation for *Ppar* to denote total particulate P and *Pdr* to denote soluble P, assuming that the dissolved organic P is negligible compared to *Ppar*, should be:

*Ppar = varoute(5,ihout) = (sub_yorgp(sb) + sub_sedps(sb) + sub_sedpa(sb)) * sub_ha* (4)

or, the particulate P in subbasin reach is equal to the surface runoff organic P plus the sediment-attached stable mineral P and the sediment-attached active P in the runoff.

*Pdr = varoute(7,ihout) = (sub_solp(sb) + sub_gwsolp(sb)) * sub_ha* (5)

or, the dissolved P is equal to the surface runoff soluble P plus the ground water soluble P.

To achieve the first objective of this study, we did not modify the original SWAT equations (1) and (2) into equations (4) and (5) but added a variable "*varoute(29,:)*" through the equation:

*varoute(29,ihout) = (sub_solp(sb) + sub_gwsolp(sb)) * sub_ha* (6)

Equation (6) was added in order to compare *Pmin* and *Pdr* with SWAT's original equations. **It should be noted that equations (4) and (5) replaced equations (1) and (2) in in newer SWAT2009 releases starting from version 477 on April 25, 2011**. However, equations (1) and (2) still remain unchanged in SWAT2000 and SWAT2005. The SWAT2009 version 488 was used in the sensitivity analysis, calibration, and validation in all four study watersheds.

Sensitivity Analysis

Sensitivity analysis using the "one-factor-at-a-time" (OAT) method described by Van Griensven et. al. (2002) was done for fifty-five parameters (Table 1). Selection of these parameters was based from previous sensitivity and calibration studies (van Liew et al., 2005; van Griensven et al., 2006). In this method, the value of each parameter is changed one-at-a-time and the objective function is calculated. The objective functions are the root mean square error (RMSE) of the observed data and the SWAT simulation output for flow, sediments, *Ptot*, *Pdis*, and NO_2+NO_3. It is assumed that the change in the output for each SWAT model run is attributed to the changes in the parameter values. Given number *n* of parameters (α), the sensitivity of the *ith* parameter to a perturbation Δ is

$$d(\alpha_i \mid \alpha) = \frac{[y(\alpha_i,\ldots,\alpha_{i-1},\alpha_i+\Delta,\alpha_{i+1},\ldots,\alpha_n) - y(\alpha)]}{\Delta} \quad (7)$$

where, $y(\alpha)$ is the model output of interest. Five values (minimum, 25th percentile, mean, 75th percentile, maximum) of each parameter were evaluated and SWAT was initially run with these 5 set of values. The minimum and maximum limits of the parameters were fixed to ensure realistic and acceptable values representative of the watershed characteristics. Each parameter was then changed 4 times and run with 5 sets of values of the rest of parameters. For example: the minimum value of parameter "a" was run with the 25th percentile, mean, 75th percentile, and maximum values of the other parameters; then the 25th percentile value of parameter "a" was run with the minimum, mean, 75th percentile, and maximum values of the other parameters, and so on. There were a total of 1,105 SWAT runs (4 parameter changes x 5 sets of parameter values x 55 parameters + 5 initial runs) for this process.

Table 1. SWAT parameters used in the sensitivity analysis.

Parameter	Min	Max	Encode[1]	Definition	Process Affected
SMTMP	-5	5	Value	Snow melt base temperature (°C)	Water Balance
SFTMP	-5	5	Value	Snowfall temperature (°C)	Water Balance
SMFMN	1.4	8	Value	Min melt factor for snow (mm/°C day)	Water Balance
SMFMX	1.4	8	Value	Max melt factor for snow (mm/°C day)	Water Balance
TIMP	0.01	1	Value	Snow pack temperature lag factor	Water Balance
ESCO	0.4	1	Value	Soil Evaporation compensation factor	Water Balance
SURLAG	1	20	Value	Surface Runoff lag coefficient	Runoff
ADJ_PKR	0.5	1.5	Value	Peak rate adjustment for sediment routing in the trib.	Runoff
RCN	0.25	1.5	Value	Nitrogen concentration in Rainfall (mg N/L)	Nutrient Cycling
SDNCO	0.8	1.4	Value	Denitrification threshold water content	Nutrient Cycling
N_UPDIS	1	100	Value	Nitrogen uptake distribution parameter	Nutrient Cycling
P_UPDIS	1	100	Value	Phophorus uptake distribution parameter	Nutrient Cycling
NPERCO	0.01	0.7	Value	Nitrate percolation coefficient	Nutrient Cycling
PPERCO	10	17.5	Value	Phosphorus percolation coefficient	Nutrient Cycling
PHOSKD	80	350	Value	Phosphorus partitioning coefficient	Nutrient Cycling
PSP	0.2	0.6	Value	Phosphorus availability index	Nutrient Cycling
PRF	0.75	1.25	Value	Peak rate adjustment for sediment routing in the main	Runoff
SPCON	0.0001	0.01	Value	Linear parameter for max sediment re-entrained	Runoff
SPEXP	1	2	Value	Exponential for calculating sediment re-entrained	Runoff
CH_K1	0.025	25	Value	Effective hydraulic conductivity in tributary channels	Runoff
CH_N1	0.016	0.15	Value	Manning's n for tributary channels	Runoff
USLE_C	0.75	1.25	Ratio	USLE C factor for water erosion	Geomorphology
SLSUBSN	0.75	1.25	Ratio	Average Slope Length (m)	Geomorphology
HRUSLP	0.75	1.25	Ratio	Average slope steepness (m/m)	Geomorphology
CANMX	0.01	5	Value	Maximum canopy storage (mm H_20)	Runoff
OVN	0.008	0.5	Value	Manning's n for overland flow	Runoff
CN2	0.75	1.25	Ratio	Initial SCS Curve Number for soil moisture II	Runoff
USLE_P	0.2	0.8	Value	USLE equation support practice factor	Geomorphology
SOLCRK	0.01	0.5	Value	Crack volume potential	Soil
SOL_AWC	0.75	1.25	Ratio	Available water capacity (mm/mm)	Soil
SOL_K	0.75	1.25	Ratio	Saturated hydraulic conductivity (mm/h)	Soil
USLE_K	0.75	1.25	Ratio	Soil Erodibility factor	Geomorphology
SOLSOLP	5	100	Value	Initial soluble P concentration in soil (mg P/kg soil)	Nutrient Cycling
SOL_ORGP	90	250	Value	Initial organic P concentration in soil (mg P/kg soil)	Nutrient Cycling
GWDELAY	0.5	10	Value	Groundwater delay time(days)	Groundwater
ALPHABF	0.1	0.99	Value	Baseflow alpha factor (days)	Groundwater
GWQMN	5	300	Value	Water depth in shallow aquifer for return flow (mm)	Groundwater

Table 1. SWAT parameters…continued.

Parameter	Min	Max	Encode	Definition	Process Affected
GWREVAP	0.02	2	Value	Groundwater "revap" coefficient (days)	Groundwater
REVAPMN	10	300	Value	Threshold depth for "revap" to occur (mm)	Groundwater
SHAL_N	0.001	1	Value	Initial concentration of NO^{-3} in shallow aquifer (mgP/L)	Groundwater
GWSOLP	0.001	1	Value	Concentration of soluble P in shallow aquifer (mgP/L)	Groundwater
CH_N2	0.016	0.15	Value	Manning's n for main channel	Channel
CH_K2	0.025	25	Value	Effective hydraulic conductivity in the main channel	Channel
CH_COV1	0.01	0.99	Value	Channel erodibility factor	Channel
CH_COV2	0.01	0.99	Value	Channel cover factor	Channel
AI_0	10	100	Value	Ratio of chlorophyll to algal biomass	In-stream nutrient
AI_2	0.01	0.02	Value	Fraction of algal biomass that is phosphorus	In-stream nutrient
MUMAX	1	3	Value	Maximum specific algal growth rate (day^{-1})	In-stream nutrient
RHOQ	0.05	0.5	Value	Algal respiration rate (day^{-1})	In-stream nutrient
K_N	0.01	0.3	Value	Half-saturation constant for nitrogen	In-stream nutrient
K_P	0.001	0.05	Value	Half-saturation constant for phosphorus	In-stream nutrient
RS1	0.15	1.82	Value	Local algal settling rate	In-stream nutrient
RS2	0.01	0.1	Value	Benthic source rate for dissolved phosphorus	In-stream nutrient
RS5	0.001	0.1	Value	Organic phosphorus settling rate	In-stream nutrient
BC4	0.01	0.7	Value	Mineralization constant rate of organic P to dissolved P	In-stream nutrient

[1] Encoding type: Value – parameter value was derived from the range of values (min to max) to run SWAT; ratio - the parameter's default value was multiplied by the ratio from this range.

Calibration and Validation

We modified and employed the automatic calibration method proposed by Confesor and Whittaker (2007) in this study. The 55 parameters used in the sensitivity analysis were to be optimized in the calibration process. The calibration (January 1, 2006 to December 31, 2009) and validation (January 1, 2002 to December 31, 2005) periods were set for four years. The objective functions were to minimize the average Root Mean Square Error (RMSE) of the observed vs. simulated variables (i.e., flow, sediment, *Ptot*, *Pdis*, and NO_2+NO_3). The RMSE was defined as:

$$RMSE = \left[\frac{1}{n} \sum_{i=1}^{n} \left(Q_{obs,i} - Q_{sim,i} \right)^2 \right]^{0.5}$$

where, n is the number of daily time steps, $Q_{obs,i}$ is the observed variable at time i, and $Q_{sim,i}$ is the simulated variable at time i. The Nash-Sutcliffe model efficiency (NSE, Nash and Suttcliffe, 1970) was used to evaluate SWAT's overall performance at calibration and validation:

$$NSE = 1 - \left[\frac{\frac{1}{n} \sum_{i=1}^{n} \left(Q_{obs,i} - Q_{sim,i} \right)^2}{\frac{1}{n} \sum_{i=1}^{n} \left(Q_{obs,i} - \bar{Q}_{obs} \right)^2} \right]$$

where, $\bar{Q}_{obs}$ is average of the observed daily variable and all the other variables are as previously defined. The Nash-Sutcliffe efficiency ranges from negative infinity to 1, with 1 indicating a perfect fit.

The computational scheme with five objective functions used in this study was implemented in an IBM server with two quad-core processors. SWAT and the multiobjective evolutionary algorithm (the nondominated-sorting genetic algorithm, NSGA; Deb et al., 2002) were created in Fortran as shared libraries callable in R. The implementation NSGA was simplified by using the genetic algorithm package (genalg) of the R statistical language (R-Development Core Team, 2011). SWAT's source code was modified and was called as a subroutine so that the values of the parameters of each solution were read instead of the values from the input files previously generated by ArcSWAT. The population size (unique combinations of the parameters) was 120 and the autocalibration was stopped after 200 iterations. Thus, there were a total of 24,000 (120 population size x 200 iterations) SWAT runs in the calibration of each watershed. The daily range of values was calculated from the simulation results of the 120 optimized combinations of the parameters.

Results

Sensitivity Analysis

The results of the sensitivity analysis for Rock Creek without in-stream processing are shown in Table 2. The parameters were ranked according their sensitivity to flow, sediments, *Ptot*, *Pdis*, and NO_2+NO_3. It is not surprising that the parameters affecting in-stream processing are the least sensitive (ranked lower) compared with the other parameters since the in-stream processing was switched off. It is noteworthy that the five SWAT output variables seem to be most sensitive to the changes in curve number (CN2). The curve number is a function of soil permeability, landuse, and antecedent moisture. CN2 is used to calculate runoff and infiltration from a storm event and it directly affects the transport of nutrients and sediment from the field. Thus, the hydrology of the model seems to be the major driving factor that influences SWAT output. As expected, the sediment output was sensitive to changes of the parameters (e.g., CH_N2, HRUSLP, USLE_K, USLE_P, SPEXP) that influence morphological, channel, and runoff processes. *Ptot* and *Pdis* were highly sensitive to the parameters (e.g., PSP, SOLSOLP, GWSOLP, SOL_ORGP, PHOSKD) that affect phosphorus nutrient cycling.

The parameters affecting in-stream processing did not influence the flow and sediment outputs when SWAT was set to model in-stream processing (Table 3). However, the *Ptot*, *Pdis*, and NO_2+NO_3 outputs were sensitive to changes of these parameters. The curve number (CN2) was still the overall most sensitive parameter. With the exception of BC4 (mineralization constant rate of organic P to dissolved P), the in-stream parameters were not as sensitive to the parameters governing morphological, nutrient cycling, and runoff processes. Similar trends were observed in the Honey Creek, Sandusky, and Maumee models. Results of the sensitivity analysis in these watersheds are presented in Appendix 2.

Table 2. SWAT sensitivity ranking of 55 parameters for Rock Creek WITHOUT in-stream processing.

Rank	FLOW	SED	TOTP	SRP	NO23
1	CN2	CN2	PSP	PHOSKD	SOL_AWC
2	ALPHABF	CH_N2	CN2	CN2	SOLCRK
3	ESCO	HRUSLP	HRUSLP	SOL_AWC	CN2
4	SOL_AWC	PRF	USLE_P	GWQMN	SDNCO
5	SURLAG	USLE_K	USLE_K	PSP	TIMP
6	SOLCRK	USLE_P	SOLSOLP	SOLSOLP	ALPHABF
7	CH_K2	SOL_AWC	SOL_AWC	TIMP	GWQMN
8	GWQMN	SPEXP	USLE_C	P_UPDIS	NPERCO
9	REVAPMN	SOLCRK	ALPHABF	GWSOLP	ESCO
10	GWDELAY	USLE_C	CH_K2	REVAPMN	SMFMN
11	SMFMN	ESCO	SOL_ORGP	ALPHABF	REVAPMN
12	CH_N2	ADJ_PKR	SOLCRK	CH_K2	HRUSLP
13	TIMP	OVN	ADJ_PKR	SMFMN	CH_K2
14	CH_K1	SLSUBSN	TIMP	GWDELAY	RCN
15	ADJ_PKR	SURLAG	SURLAG	HRUSLP	SURLAG
16	SMFMX	SPCON	CANMX	SOLCRK	CANMX
17	SLSUBSN	ALPHABF	OVN	PPERCO	GWDELAY
18	SDNCO	CH_N1	P_UPDIS	GWREVAP	SOL_K
19	OVN	CH_K2	PHOSKD	ESCO	CH_N2
20	CANMX	SDNCO	SMFMN	USLE_P	CH_K1
21	CH_N1	SMFMN	SLSUBSN	SURLAG	GWREVAP
22	GWREVAP	CH_K1	ESCO	USLE_K	SLSUBSN
23	HRUSLP	CANMX	CH_N1	CH_N2	SMFMX
24	RCN	GWQMN	GWQMN	SDNCO	ADJ_PKR
25	SOL_K	TIMP	CH_N2	ADJ_PKR	N_UPDIS
26	N_UPDIS	REVAPMN	SDNCO	CH_K1	OVN
27	NPERCO	RCN	PPERCO	SOL_K	CH_N1
28	USLE_K	GWDELAY	REVAPMN	SLSUBSN	USLE_K
29	USLE_C	SMFMX	CH_K1	USLE_C	USLE_P
30	USLE_P	GWREVAP	GWDELAY	OVN	USLE_C
31	P_UPDIS	NPERCO	RCN	SMFMX	P_UPDIS
32	SOLSOLP	SOL_K	SMFMX	CH_N1	SOLSOLP
33	PSP	CH_COV1	GWREVAP	CANMX	PSP
34	PPERCO	CH_COV2	SOL_K	SOL_ORGP	PHOSKD
35	PHOSKD	P_UPDIS	GWSOLP	RCN	PPERCO
36	SOL_ORGP	N_UPDIS	NPERCO	N_UPDIS	SOL_ORGP
37	SMTMP	SOLSOLP	N_UPDIS	NPERCO	SHAL_N
38	SFTMP	PSP	PRF	PRF	GWSOLP
39	PRF	PHOSKD	SPEXP	SPEXP	PRF
40	SPCON	PPERCO	SPCON	SPCON	SPEXP
41	SPEXP	SOL_ORGP	CH_COV1	CH_COV1	SPCON
42	SHAL_N	SMTMP	CH_COV2	CH_COV2	CH_COV1
43	GWSOLP	SFTMP	SMTMP	SMTMP	CH_COV2
44	CH_COV1	SHAL_N	SFTMP	SFTMP	SMTMP
45	CH_COV2	GWSOLP	SHAL_N	SHAL_N	SFTMP
46	AI_0	AI_0	AI_0	AI_0	AI_0
47	AI_2	AI_2	AI_2	AI_2	AI_2
48	MUMAX	MUMAX	MUMAX	MUMAX	MUMAX
49	RHOQ	RHOQ	RHOQ	RHOQ	RHOQ
50	K_N	K_N	K_N	K_N	K_N
51	K_P	K_P	K_P	K_P	K_P
52	RS1	RS1	RS1	RS1	RS1
53	RS2	RS2	RS2	RS2	RS2
54	RS5	RS5	RS5	RS5	RS5
55	BC4	BC4	BC4	BC4	BC4

Table 3. SWAT sensitivity ranking of 55 parameters for Rock Creek WITH in-stream processing.

Rank	FLOW	SED	TOTP	SRP	NO23
1	CN2	CN2	PSP	PSP	SOL_AWC
2	ALPHABF	CH_N2	CN2	CN2	SOLCRK
3	ESCO	HRUSLP	HRUSLP	BC4	SDNCO
4	SOL_AWC	PRF	USLE_P	HRUSLP	TIMP
5	SURLAG	USLE_K	USLE_K	USLE_P	CN2
6	SOLCRK	USLE_P	SOLSOLP	SOLSOLP	ALPHABF
7	CH_K2	SOL_AWC	SOL_AWC	USLE_K	CANMX
8	GWQMN	SPEXP	USLE_C	SOL_AWC	GWQMN
9	REVAPMN	SOLCRK	ALPHABF	CH_N2	SMFMN
10	GWDELAY	USLE_C	CH_K2	PHOSKD	AI_0
11	SMFMN	ESCO	SOL_ORGP	ALPHABF	ESCO
12	CH_N2	ADJ_PKR	ADJ_PKR	CH_K2	MUMAX
13	TIMP	OVN	SOLCRK	TIMP	HRUSLP
14	CH_K1	SLSUBSN	SURLAG	USLE_C	NPERCO
15	ADJ_PKR	SURLAG	OVN	SOL_ORGP	RS1
16	SMFMX	SPCON	P_UPDIS	SOLCRK	REVAPMN
17	SDNCO	ALPHABF	TIMP	P_UPDIS	SURLAG
18	SLSUBSN	CH_N1	PHOSKD	SURLAG	GWDELAY
19	OVN	CH_K2	SLSUBSN	MUMAX	CH_K2
20	CANMX	SDNCO	CH_N2	ADJ_PKR	SOL_K
21	GWREVAP	SMFMN	ESCO	AI_0	RCN
22	CH_N1	CH_K1	SMFMN	ESCO	CH_K1
23	HRUSLP	CANMX	SDNCO	SMFMN	CH_N2
24	SOL_K	GWQMN	CH_N1	OVN	USLE_P
25	RCN	TIMP	GWQMN	AI_2	GWREVAP
26	N_UPDIS	REVAPMN	RS5	GWQMN	SLSUBSN
27	NPERCO	GWDELAY	PPERCO	RS1	USLE_K
28	USLE_K	RCN	MUMAX	SLSUBSN	SMFMX
29	USLE_C	SMFMX	RHOQ	SDNCO	RHOQ
30	P_UPDIS	GWREVAP	REVAPMN	REVAPMN	K_N
31	USLE_P	NPERCO	AI_0	PPERCO	ADJ_PKR
32	SOLSOLP	SOL_K	CANMX	CH_N1	USLE_C
33	PSP	CH_COV1	CH_K1	RHOQ	BC4
34	PHOSKD	CH_COV2	RCN	GWSOLP	OVN
35	PPERCO	P_UPDIS	GWDELAY	RS5	N_UPDIS
36	SOL_ORGP	N_UPDIS	AI_2	GWDELAY	CH_N1
37	SMTMP	SOLSOLP	BC4	CANMX	SOLSOLP
38	SFTMP	PSP	GWREVAP	NPERCO	PSP
39	PRF	PHOSKD	SMFMX	RCN	AI_2
40	SPCON	PPERCO	NPERCO	K_N	P_UPDIS
41	SPEXP	SOL_ORGP	RS1	GWREVAP	PPERCO
42	SHAL_N	SMTMP	K_N	SOL_K	PHOSKD
43	GWSOLP	SFTMP	GWSOLP	SMFMX	K_P
43	GWSOLP	SFTMP	GWSOLP	SMFMX	K_P
44	CH_COV1	SHAL_N	SOL_K	CH_K1	GWSOLP
45	CH_COV2	GWSOLP	N_UPDIS	N_UPDIS	SOL_ORGP
46	AI_0	AI_0	K_P	K_P	RS5
47	AI_2	AI_2	RS2	RS2	RS2
48	MUMAX	MUMAX	SHAL_N	SHAL_N	SHAL_N
49	RHOQ	RHOQ	PRF	PRF	PRF
50	K_N	K_N	SPEXP	SPEXP	SPEXP
51	K_P	K_P	SPCON	SPCON	SPCON
52	RS1	RS1	CH_COV1	CH_COV1	CH_COV1
53	RS2	RS2	CH_COV2	CH_COV2	CH_COV2
54	RS5	RS5	SMTMP	SMTMP	SMTMP
55	BC4	BC4	SFTMP	SFTMP	SFTMP

SWAT Phosphorus output at low and high flows

SWAT 2009 version 451 and 477

Most of the data presented in this section have been reported in conferences, seminars, and meetings. The discussion about SWAT phosphorus output during low and high flows was presented at and was part of the proceedings of the 2011 ASABE Annual International Meeting in St. Louisville, KY, in August 7-10, 2011. The article of the proceedings is attached as Appendix 1, and for brevity it will not be discussed here again.

SWAT 2009 version 488

Table 4 shows the results of un-calibrated SWAT simulations for all of the 4 study watersheds. The different sizes and "flashiness" of the watersheds seems to have affected the water yield. For smaller watersheds (Rock Creek and Honey Creek), at least 71% of the flows occurred during the upper 10 percentile of the flows. Sixty-four percent of the flows in the Sandusky occurred during high flows; while around 40% in the Maumee occurred during the high flows. More than 77% of the sediment yield occurred in the Maumee during high flows with up to more than 90% in Rock Creek and Honey Creek. In all the watersheds, more than 80% of the total phosphorus was exported during the high flows. This is not surprising since the sediment-attached phosphorus constitutes more than 62% of total P in the Maumee and as high as 87% of total P in Rock Creek.

In Rock Creek, the export of different phosphorus forms was comparable with or without the in-stream processing modeled. The dissolved phosphorus was around 10% of the total P. This is most likely due to the low water residence time (more "flashy") before Rock Creek joins the Sandusky River. However, for the three other watersheds without in-stream processing, the dissolved P ranged between 7- 9% of the total P. With in-stream processing, the dissolved P ranged from 15% (Honey Creek) to 38% (Maumee). It is noteworthy that in version 488, the total P exports were comparable with or without in-stream processing. In the earlier SWAT versions, the total P values were at least 10% higher when there is no in-stream processing than when there is in-stream processing (see Table 2 of the attached article in Appendix 1). This lower value of total P could be due to the assimilation of phosphorus by the algae in the stream. Furthermore, in earlier SWAT versions, when there was in-stream processing, the dissolved P values were more than 70% of the total P. These values are quite unrealistic. NCWQR data shows that dissolved P exports are 8 to 25 % of the total P.

Table 4. Annual average simulated flow volume, sediment yield, and phosphorus forms at different flow regimes for water years 2007 to 2009.[1]

SWAT Setup	Flow[2] Regime	Volume (million m3)	Sediment (1000 tons)	Ppar (tons)	Pdis (tons)	Ptot (tons)
			Rock Creek			
IWQO[2]	Low	11.1 (29.1)	1.8 (3.4)	1.6 (3)	0.2 (.5)	1.9 (3.5)
	High	27.1 (70.9)	51.7 (96.6)	46.9 (87.3)	5 (9.2)	51.9 (96.5)
	All	38.2 (100)	53.5 (100)	48.6 (90.3)	5.2 (9.7)	53.8 (100)

IWQ1[3]	Low	11.1(29.1)	1.8 (3.4)	1.6 (3)	0.2 (.5)	1.9 (3.5)
	High	27.1(70.9)	51.7 (96.6)	46.9 (87.3)	5.0 (9.2)	51.9 (96.5)
	All	38.2(100)	53.5 (100)	48.6 (90.3)	5.2 (9.7)	53.8 (100)
			Honey Creek			
IWQO	Low	37.1(25)	11.3 (5.8)	14.9 (5.9)	1.6 (.6)	16.4 (6.5)
	High	112 (75)	184 (94.2)	218 (85.8)	19.6 (7.7)	237 (93.5)
	All	149 (100)	195 (100)	232.6 (91.7)	21.1 (8.3)	254 (100)
IWQ1	Low	37.1 (25)	11.3 (5.8)	12.8 (5.2)	3.3 (1.4)	16.1 (6.6)
	High	112 (75)	184 (94.2)	194 (79.1)	35.2 (14.4)	229 (93.4)
	All	149 (100)	195 (100)	206 (84.3)	38.5 (15.7)	245.1 (100)
			Sandusky			
IWQO	Low	531 (36)	104 (11.7)	323 (15.5)	31.1 (1.5)	354 (16.9)
	High	944 (64)	786 (88.3)	1607 (77)	127 (6.1)	1735 (83.1)
	All	1475 (100)	890 (100)	1930 (92.4)	158 (7.6)	2088 (100)
IWQ1	Low	531 (36)	104 (11.7)	204 (10.2)	132 (6.6)	336 (16.8)
	High	944 (64)	786 (88.3)	1193 (59.9)	465 (23.3)	1658 (83.2)
	All	1475 (100)	890 (100)	1397 (70.1)	596 (29.9)	1993 (100)
			Maumee[3]			
IWQO	Low	4044 (60.7)	337.0 (22.6)	1207 (17.2)	129.2 (1.9)	1336 (19.1)
	High	2615 (39.3)	1152 (77.4)	5150 (73.6)	512.1 (7.3)	5662 (80.9)
	All	6660 (100)	1489 (100)	6356 (90.8)	641.2 (9.2)	6997 (100)
IWQ1	Low	4044 (60.7)	337.0 (22.6)	612.9 (9.2)	623.5 (9.4)	1236 (18.6)
	High	2615 (39.3)	1152 (77.4)	3511 (52.8)	1904 (28.6)	5415 (81.4)
	All	6660 (100)	1489 (100)	4124 (62.0)	2528 (38.0)	6651 (100)

[1] Values in parenthesis are percentages of variables (e.g., Flow volume, Sediments, etc.) at all flows. Phosphorus forms percentages are of *Ptot* at all flows.

[2] High flows were calculated as the upper 10 percentile of the flows and part of the rising limb of the hydrograph to a day after the peak flow. The low flows were the rest of the flows.

[3] For the Maumee, values are the annual average from water year 2008 to 2011.

Calibration and validation results

SWAT performed well in simulating the daily flow, sediment, *Ptot*, *Pdis*, and NO_2+NO_3 yields. The daily NSE values for different SWAT output variables and settings are shown in Table 5. Van Liew et. al. (2005) suggested that simulations results were good if NSE > 0.75, satisfactory if $0.36 \leq \text{NSE} \leq 0.75$, and unsatisfactory if less than 0.36. The wide variation in the NSE values for sediments and nutrients shows the uncertainty in the modeling process. There was a good daily flow simulation for Rock Creek, Honey Creek, and the Maumee and acceptable NSE values in the Sandusky. Graphs of observed vs. simulated values during calibration are presented in Appendix 3. The observed values were within the range of the simulation results; further showing a good fit between the observed and simulated values. It is noteworthy that SWAT simulated well the occurrence of storm events and the peaks of all the variables. However, the dissolved phosphorus was generally over-predicted in most of the simulations.

This overestimation may have been caused by higher phosphorus application rates (50-110 kg-P_2O_5/ha) in the model than what was actually applied in the fields.

It was also observed that at calibration, tradeoffs seem to exist in optimizing simulated flow, dissolved P, and sediments with the observed data, especially when the SWAT simulates in-stream processing. A higher NSE for sediments, total P, and flow resulted in a lower NSE for dissolved P and vice versa. This could be due to SWAT's structure and the observed data. In SWAT, most of the sediments (and particulate P) were exported in the upper 10 percentile of the flow. Thus, increasing the fit for high flows will increase the fit for sediments and particulate P but will decrease the NSE for dissolved P. This condition must have also contributed to the wide range of NSE, thus the negative values.

Table 5. Daily Nash-Sutcliffe values during calibration.[1]

Variable		Flow	Sediments	*Ptot*	*Pdis*	NO_2+NO_3
			Rock Creek			
IWQO[2]	min	0.72	0.41	-2.27	-3.11	-0.53
	max	0.84	0.64	0.69	0.79	0.51
IWQ1[3]	min	0.78	-0.55	0.44	-6.45	-0.06
	max	0.84	0.52	0.73	0.73	0.56
			Honey Creek			
IWQO	min	0.79	-0.35	0.48	-3.35	-0.02
	max	0.84	0.52	0.72	0.75	0.55
IWQ1	min	0.79	0.43	0.57	-6.01	-0.72
	max	0.84	0.67	0.74	0.80	0.48
			Sandusky			
IWQO	min	0.61	-5.41	0.48	-4.16	-2.15
	max	0.74	0.61	0.69	0.65	0.57
IWQ1	min	0.62	-2.06	-0.14	-6.47	-0.57
	max	0.74	0.61	0.70	0.57	0.56
			Maumee			
IWQO	min	0.71	-6.35	0.49	-9.63	-1.06
	max	0.88	0.82	0.82	0.76	0.60
IWQ1	min	0.75	-4.45	-0.18	-32.87	-0.56
	max	0.88	0.83	0.82	0.56	0.56

[1] Minimum and maximum values of 120 simulations at the 200th iteration.
[2] IWQ0 = without in-stream processing.
[3] IWQ0 = with in-stream processing.

Table 6 shows the daily Nash-Sutcliffe efficiency values during validation. As expected, the efficiency values during validation are lower than during calibration due to the fact that the observed data in the validation period were not included in the calibration process. Nonetheless, the maximum NSE values are all acceptable. There was a much wider range of NSE values for the sediments and nutrients as compared with the NSE during calibration. The crop rotation, tillage, and fertilizer operations in the calibration period could probably be different during the validation period. Validation graphs are presented in Appendix 4.

Table 6. Daily Nash-Sutcliffe values at validation.[1]

Variable		Flow	Sediments	*Ptot*	*Pdis*	NO_2+NO_3
			Rock Creek			
IWQO[2]	min	0.53	0.28	-2.72	-16. 6	-0.40
	max	0.70	0.51	0.59	0.35	0.34
IWQ1[3]	min	0.62	0.26	0.39	-26.7	-0.66
	max	0.69	0.48	0.63	0.40	0.33
			Honey Creek			
IWQO	min	0.73	-1.68	0.15	-8.86	-0.06
	max	0.82	0.40	0.67	0.64	0.52
IWQ1	min	0.72	-2.28	-22.4	-12.87	-0.09
	max	0.82	0.40	0.66	0.60	0.54
			Sandusky			
IWQO	min	0.61	-5.41	0.48	-4.16	-2.15
	max	0.74	0.61	0.69	0.65	0.57
IWQ1	min	0.62	-2.06	-0.14	-6.47	-0.57
	max	0.74	0.61	0.70	0.57	0.56
			Maumee			
IWQO	min	0.56	-7.45	-1.83	-13.65	-1.72
	max	0.82	0.67	0.73	0.74	0.72
IWQ1	min	0.60	-4.59	-313	-7171	-433
	max	0.83	0.65	0.72	0.63	0.69

[1] Minimum and maximum values of 120 simulations at the 200th iteration.
[2] IWQ0 = without in-stream processing.
[3] IWQ1 = with in-stream processing.

Effects of fertilizer application method

Due to limited time and resources, the assessment of the effects of fertilizer application timing (spring vs. fall) was excluded in the study. Only two Rock Creek subbasins (6 and 9) were analyzed for the effects of fertilizer application methods. Subbasin 6 was planted with a corn-beans-corn-beans crop rotation and the fertilizer was either incorporated or injected into the soil (scenario-1a). The field was also chisel-plowed in the fall before corn was planted. Subbasin 9 was planted with no-till beans-wheat-beans-wheat crop rotation and fertilizer was broadcast (scenario-2a). Scenario-1b was the same as scenario-1a but fertilizer was broadcast instead of incorporation/injection. Scenario-2b was the same as scenario-2a but fertilizer was incorporated instead of broadcast.

The sediment yields (Figures 4 and 5) between scenario-1a vs. scenario-1b and between scenario-2a vs. scenario-2b were comparable. This was expected because there was no change in the forcing weather and tillage operations. However, the sediment yield in scenario-1 is much higher than the sediment yield in scenario-2. While there are so many factors that may influence sediment yield, the difference in sediment yield between the two scenarios must be mainly due to the effect of tillage operations in scenario-1.

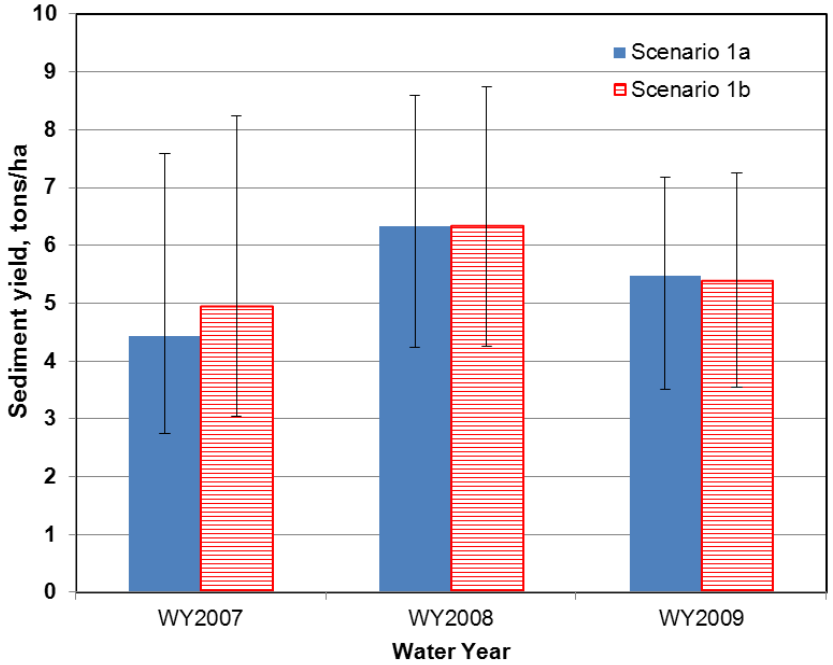

Figure 4. Median annual sediment yield in a corn-beans-corn-beans crop rotation. Error bars indicate the 10th and 90th percentile.

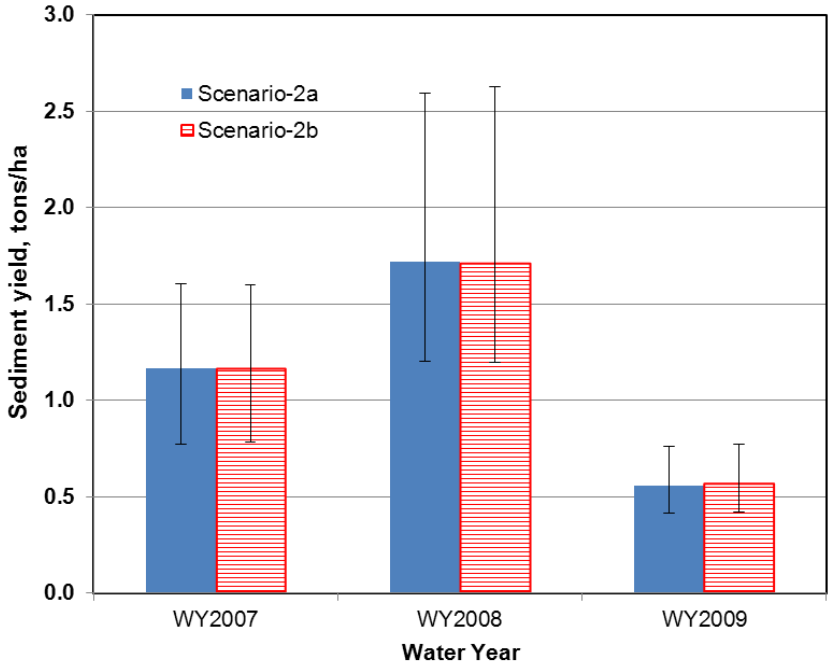

Figure 5. Median annual sediment yield in a beans-wheat-beans-wheat crop rotation. Error bars indicate the 10th and 90th percentile.

The yield of all phosphorus forms (total, dissolved, and sediment-attached mineral P) increased when the fertilizer was broadcast instead of incorporated or injected (Figures 6, 7, and

8). It should be noted that the organic P yield was not included in the analysis. These findings may imply that broadcasted fertilizer can be readily transported with the runoff both in dissolved and soil-attached forms. On the other hand, when the fertilizer was incorporated instead of broadcast, the phosphorus exports decreased (Figures 9, 10, and 11).

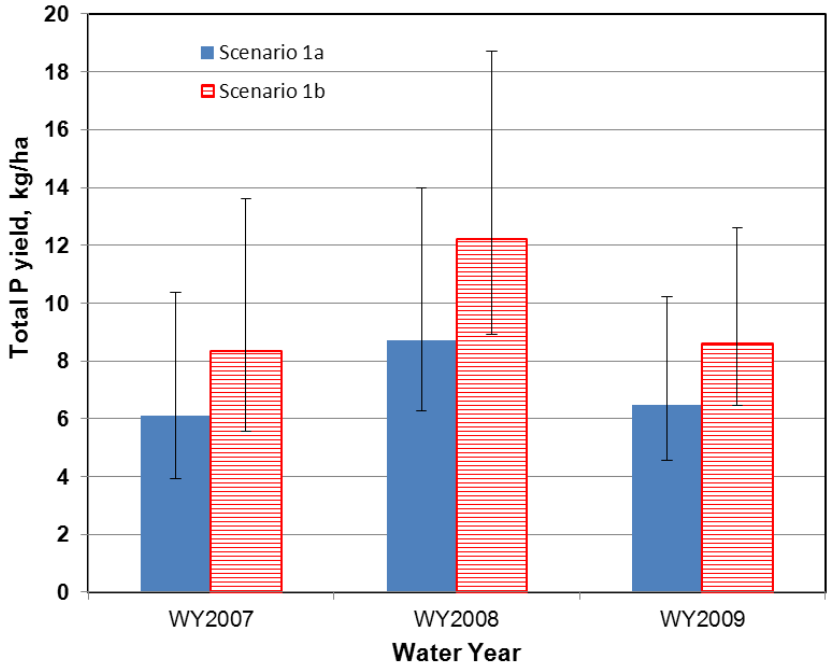

Figure 6. Median annual Total P yield in a corn-beans-corn-beans crop rotation. Error bars indicate the 10th and 90th percentile.

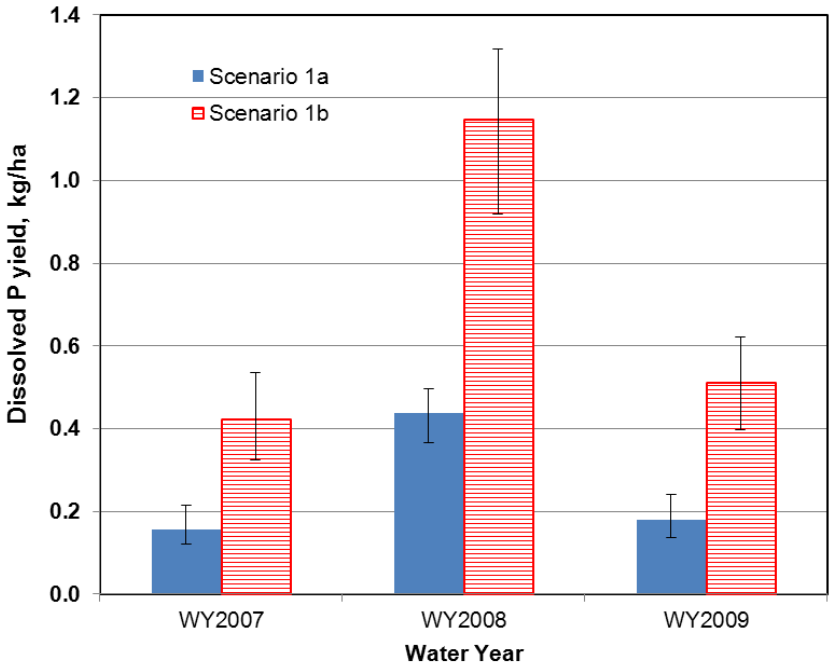

Figure 7. Median annual dissolved P yield in a corn-beans-corn-beans crop rotation. Error bars indicate the 10th and 90th percentile.

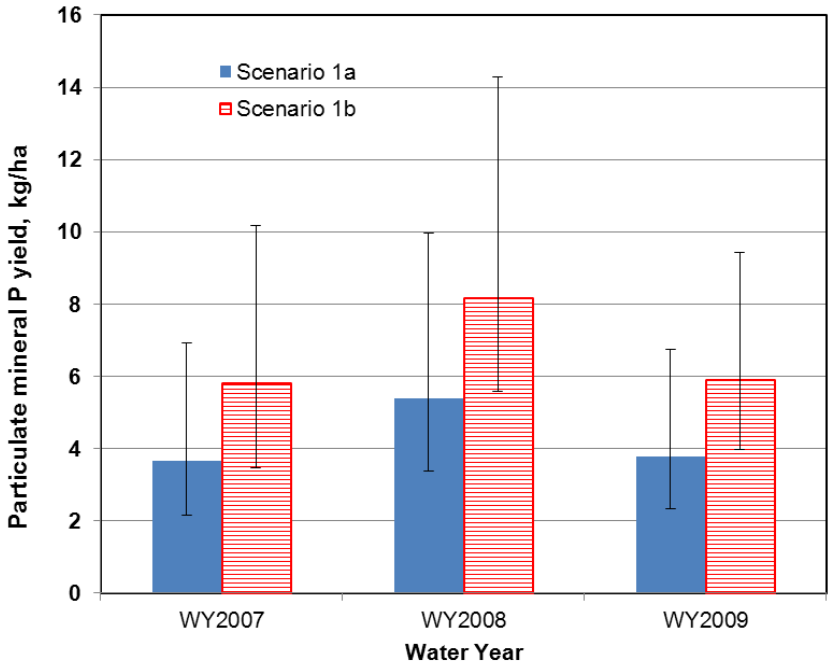

Figure 8. Median annual sediment-attached mineral P yield in a corn-beans-corn-beans crop rotation. Error bars indicate the 10th and 90th percentile.

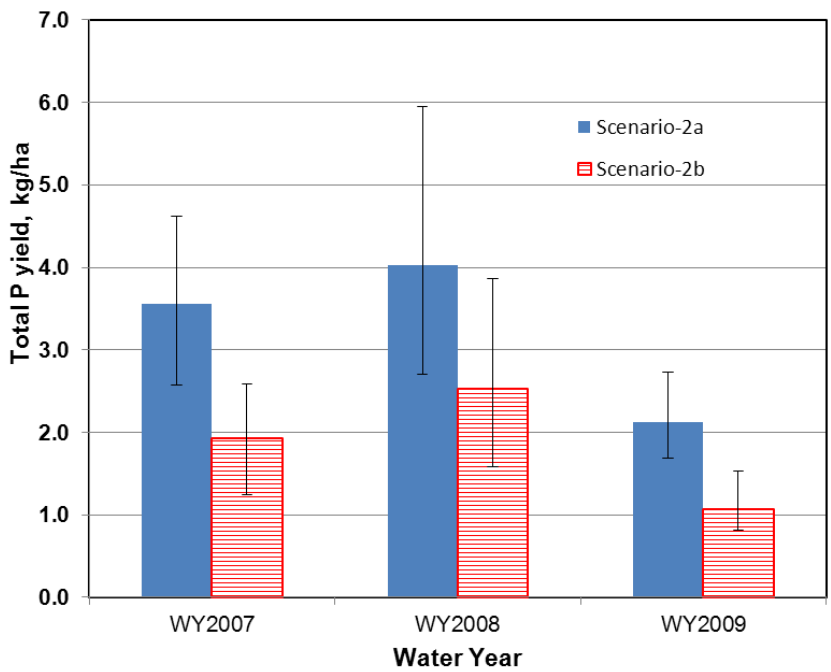

Figure 9. Median annual Total P yield in a beans-wheat-beans-wheat crop rotation. Error bars indicate the 10th and 90th percentile.

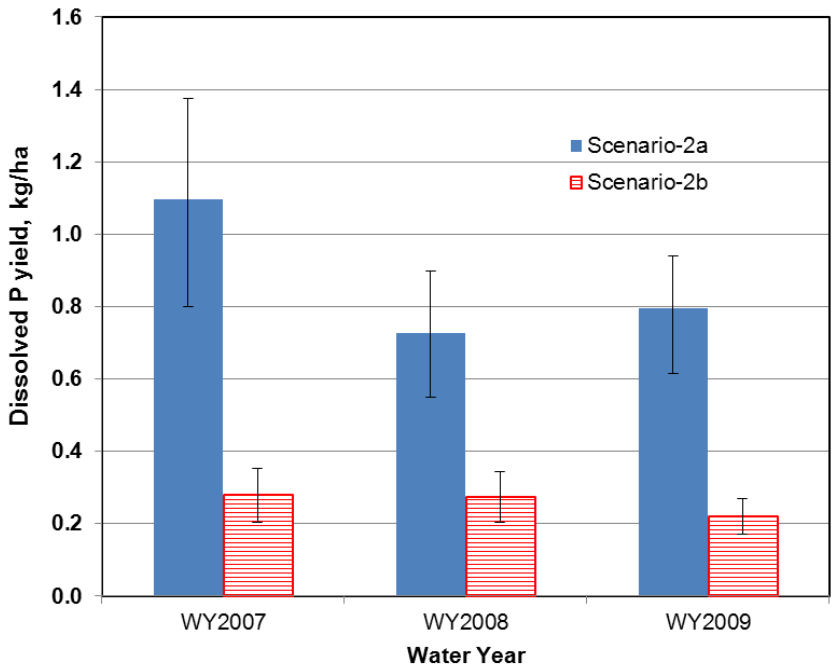

Figure 10. Median annual dissolved P yield in a beans-wheat-beans-wheat crop rotation. Error bars indicate the 10th and 90th percentile.

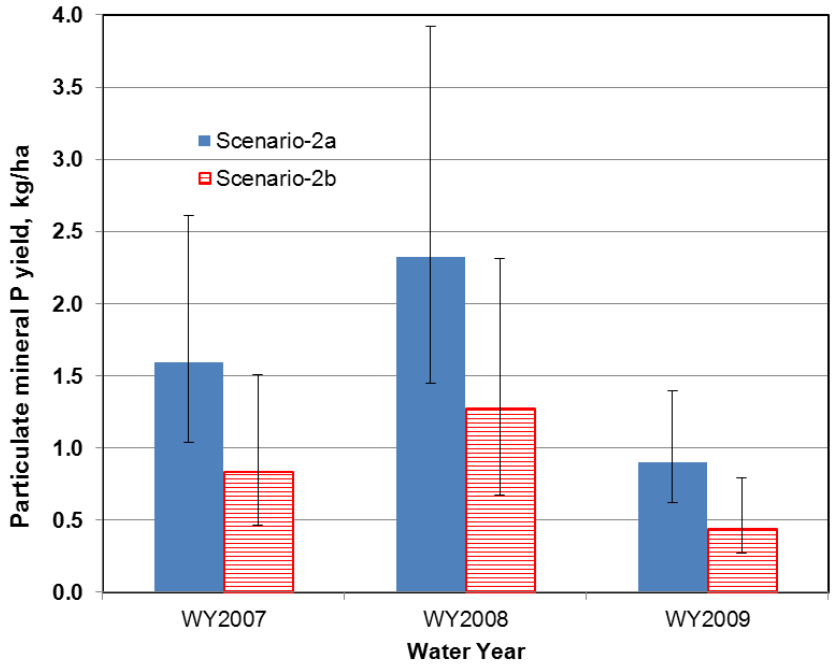

Figure 11. Median annual sediment-attached mineral P yield in a beans-wheat-beans-wheat crop rotation. Error bars indicate the 10th and 90th percentile.

Summary and Conclusions

This study was undertaken to: (1) Add a *Pdis* output variable at the watershed reaches in SWAT, (2) Calibrate and validate the modified SWAT with observed data from the Rock Creek, Honey Creek, Sandusky, and Maumee watersheds, (3) Assess the effect of fertilizer application method (broadcast vs. surface-applied) on nutrient exports from the above watersheds.

Using SWAT2009 versions prior to rev477 (released in April 2011), simulations and statistical analyses showed a lack of difference between the means of *Pmin* and *Pdis* at low flows. This result was not surprising since the sediments and the sediment-attached P from runoff are essentially nil at low flows. At high flows, there was a significant difference between the means of *Pmin* and *Pdis*, with or without in-stream processing. This finding indicates that at high flows, SWAT's original equation for *Pmin* is not applicable to estimate *Pdis*, otherwise the calculation would be inaccurate. However, this inaccuracy was corrected in the newer versions of SWAT2009 but still remains in SWAT2000 and SWAT2005.

SWAT simulated well the flow, sediments, total P, dissolved P and nitrite+nitrate as compared with observed flow. However, tradeoffs exist during the multi-objective calibration of flow, dissolved P, total P, and sediments especially when the SWAT simulates in-stream processing. This tradeoff and the model uncertainties could have resulted in a wider range of NSE. The dissolved phosphorus was generally over-predicted in all the watersheds. This over-prediction was most likely due to the higher phosphorus application rates (50-110 kg-P_2O_5/ha) in the model than what was actually applied in the fields.

SWAT was successfully applied to evaluate the effects of fertilizer application: from broadcast to incorporation and from incorporation to broadcast. Results showed broadcasting the fertilizer instead of incorporating tremendously increased the dissolved P. On the other hand, incorporating the fertilizer instead of broadcasting decreased dissolved P. The results also showed that the applied fertilizer can be transported in both dissolved and particulate form.

Revisions of the SWAT code greatly improved its capacity to simulate flow, sediments, and nutrients exports. This study showed that SWAT has a great potential in the selection and placement of best management practices (BMPs) to reduce dissolved P exports from Lake Erie watersheds. Future studies are recommended using SWAT to further explore all possible BMPs in reducing dissolved P.

References

Baker, D.B., J. Kramer, G. Winston, R. P. Richards, J. Crumrine. 2008. After the storm:Satellite images of Western Lake Erie in relation to tributary loading. Poster paper presented at the National River Rally, May 2-5 2008, Huron, OH.

Confesor, R.B., Whittaker, G., 2007. Automatic calibration of hydrologic models with multi-objective evolutionary algorithm and Pareto optimization. Journal of the American Water Resources Association43, 981–989.

Deb, K., A. Pratap, S. Agarwal, and T. Meyarivan, 2002. A Fast and Elitist Multiobjective Genetic Algorithm: NSGA-II. IEEE Transactions on Evolutionary Computation 6(2):182-197.

Hartig, J.H., M.A. Zarull, J.J.H. Ciborowski, J.E. Gannon, E. Wilke, G. Norwood, and A. Vincent, eds. 2007. State of the Strait: Status and Trends of Key Indicators. Great Lakes Institute for Environmental Research, Occasional Publication No. 5,University of Windsor, Ontario, Canada. ISSN 1715-3980.

Loftus, T. T., D. B. Baker, J.V. Setzler, and J. Crumrine. 2006. Honey Creek Watershed Action Plan. The National Center for Water Quality Research, Heidelberg College, Tiffin, OH 44883..

Makarawicz, J.C. and P. Bertram. 1991. Evidence for the restoration of the Lake Erie ecosystem. Bioscience 41(4): 216-223.

Maringanti, C., I. Chaubey, and J. Popp. 2009. Development of a Multiobjective Optimization Tool for the Selection and Placement of Best Management Practices for Nonpoint Source Pollution Control. Water Resources Research, 45: W06406, doi:10.1029/2008WR007094.

Nash, J.E. and J.E. Suttcliffe, 1970. River Flow Forecasting Through Conceptual Models – Part I: A Discussion of Principles. Journal of Hydrology 10(3):282-290.

Neitsch, S.L., J.G. Arnold, J.R. Kiniry, J.R. Williams. 2005. Soil and Water AssessmentTool Theoretical Documentation Version 2005. Grassland, Soil and WaterResearch Laboratory, United States Department of Agriculture AgriculturalResearch Service (USDA-ARS). 808 East Blackland Road, Temple, Texas.Available at http://swatmodel.tamu.edu (accessed on 17 April 2011).

Nicholls, K.H., D.W. Standen, G.J. Hopkins, and E.C. Carney. 1977. Declines in thenearshore phytoplankton of Lake Erie's western basin since 1971. Journal of GreatLakes Research 3:72-78.

R-Development-Core-Team. 2011. R: A Language and Environment for Statistical Computing. R Foundation for Statistical Computing, Vienna, Austria. http://www.Rproject.org.

U.S. EPA. 1978. The Great Lakes Water Quality Agreement (GLWQA). Available at http://www.epa.gov/glnpo/glwqa/1978/index.html (accessed on 17 April 2011).

Di Luzio, M., R. Srinivasan, and J.G. Arnold, 2001. Arcview Interface for SWAT2000: User's Guide. Agricultural Research Service, USDA, Temple, Texas. http://www.brc.tamus.edu/ swat/downloads/doc/swat2000.pdf, accessed October 2006.

van Griensven, A., A. Francos, and W. Bauwens, 2002. Sensitivity analysis and auto-calibration of an integral dynamic model for river water quality. Water Science and Technology 45(9):325-332.

van Griensven, A., T. Meixner, S. Grunwald, T. Bishop, M. DiLuzio, and R Srinivasan. 2006. A global sensitivity analysis tool for parameters of a multi-variable catchment models. Journal of Hydrology 324:10-23.

Van Liew, M.W., J.G. Arnold, and D.D. Bosch, 2005. Problems and Potential of Autocalibrating a Hydrological Model. Transactions of the ASAE 48(3):1025-1040.

Veith, T.L., M.L. Wolfe, and C. D. Heatwole.2003. Optimization Procedure for Cost Effective BMP Placement at a Watershed Scale.US EPA, 1978.

Appendix 1. ASABE Paper No. 1111060

2950 Niles Road, St. Joseph, MI 49085-9659, USA
269.429.0300 fax 269.429.3852 hq@asabe.org www.asabe.org

An ASABE Meeting Presentation

Paper Number: 1111060

Modeling Dissolved Phosphorus Exports in Lake Erie Watersheds

Remegio B. Confesor Jr., Research Scientist (rconfeso@heidelberg.edu)

NCWQR, Heidelberg University, 310 E. Market St., Tiffin, OH 44883

R. Peter Richards, Senior Research Scientist

NCWQR, Heidelberg University, 310 E. Market St., Tiffin, OH 44883

Jeffrey Arnold , Supervisory Agricultural Engineer

Grassland Soil and Water Research Laboratory, USDA-ARS, 808 East Blackland Rd., Temple, TX 76502.

Gerald Whittaker, Research Hydrologist

NFSPRC-USDA-ARS, 3450 SW Campus Way, Corvallis, OR 97331

Written for presentation at the
2011 ASABE Annual International Meeting
Sponsored by ASABE
Galt House
Louisville, Kentucky
August 7 – 10, 2011

Abstract. Researchers have been exploring the selection and optimal placement of best management practices (BMPs) to reduce nonpoint source pollution from agricultural lands. One vital component in these studies is the use of watershed models, specifically the Soil and Water Assessment Tool (SWAT). However, SWAT output variables in the subwatershed reaches do not include dissolved reactive phosphorus *(Pdr)*, but rather inorganic phosphorus *(Pmin)* and organic phosphorus *(Porg)*. The total phosphorus *(Ptot)* is calculated as the sum of *Pmin* and *Porg*. Pmin includes both dissolved and particulate P and is usually assumed as equal to *Pdr*. Almost all stream water quality monitoring include *Ptot* and *Pdr* but no *Pmin* and *Porg*. The goal of this study was to evaluate SWAT's performance in estimating phosphorus exports in Lake Erie Watersheds.
Our SWAT simulations and statistical analyses showed a lack of difference between the means of *Pmin* and *Pdr* at low flows. This result was not surprising since the sediments and the sediment-attached P from runoff are essentially nil at low flows. In-stream processing is a major factor in determining SWAT's P simulation output. At high flows (> 90th percentile) and in the absence of in-stream processing, *Porg* is at least 71% of *Ptot* while *Pmin* and *Pdr* are less than 18 % and 6.5% of *Ptot*, respectively. When there is in-stream processing, both *Pmin* and *Pdr* exceeded 70% of *Ptot* but *Porg* is less than 4% of *Ptot*. Further studies are needed to improve SWAT's ability to accurately simulate different P forms.

Keywords. SWAT, watershed modeling, Phosphorus, Lake Erie, in-stream processing.

Introduction

The Great Lakes Water Quality Agreement (GLWQA) between the United States and Canada set a target load of 11,000 metric tons/yr of total phosphorus (P) for Lake Erie (US EPA, 1978). The coordinated efforts to control point source pollution resulted in a 60% decrease of total P loading into Lake Erie between the late 1960's and early 1980's (Hartig et al., 2007). As a consequence, algal biomass declined in Lake Erie, especially the blue-green algae *Aphanizomenon flos-aquae* (Nicholls et al., 1977; Makarawicz and Bertram, 1991). However, late-summer algal blooms (e.g., *Microcystis*) have been occurring again with increasing frequency and severity since the mid-1990's (Hartig et al., 2007). This recurrence of harmful algal blooms in Lake Erie is largely attributed to nutrient loading from its tributaries, especially the Maumee and Sandusky watersheds in northwest and north central Ohio. Land use in these watersheds is predominantly agricultural, with unit area nutrient losses comparable to Midwestern croplands and maybe among the highest in the United States (Baker et al., 2008). Northwest Ohio's cropland is less than 20% of Ohio's agricultural land but contributed 50% each of soybean and corn grain and 70% of winter wheat production for the whole state in 2007 (NASS, 2008). The National Center for Water Quality Research (NCWQR) at Heidelberg University in Tiffin, Ohio, has been monitoring daily water quality adjacent to USGS flow gauging stations in the major watersheds draining to Lake Erie for up to 35 years. The NCWQR's data show that sediment and particulate phosphorus runoff to the lake has been reduced and is still decreasing. However, the dissolved P load has been increasing rapidly in all the monitored Lake Erie tributaries since the mid-1990's. Researchers have been exploring the selection and optimal placement of best management practices (BMPs) to reduce nonpoint source pollution from agricultural lands (Veith et al., 2003; Gitau et al., 2004; Maringanti et al., 2009). One vital component in these studies is the use of watershed models, specifically the Soil and Water Assessment Tool (SWAT). However, in SWAT 2005 and prior versions to SWAT 2009 rev477, the output variables in the subwatershed reaches do not include dissolved reactive phosphorus (*Pdr*), but rather mineral phosphorus (*Pmin*) and organic phosphorus (*Porg*). The total phosphorus (*Ptot*) is calculated as the sum of *Pmin* and *Porg*. *Pmin* includes both dissolved and particulate P and is conventionally assumed as equal to *Pdr* by most SWAT modelers. While this assumption is valid during low flows, it is probably incorrect during storm events. Furthermore, *Ptot* and *Pdr* are the P forms usually measured in stream water quality monitoring. The particulate P (*Ppar*) is then calculated as the difference between *Ptot* and *Pdr*. Consequently, the SWAT phosphorus forms in the model output and the observed values from stream monitoring cannot be compared, with the exception of *Ptot*.

To appropriately use SWAT in studying the increased *Pdr* exports from the Lake Erie watersheds, SWAT must be adjusted to correctly simulate dissolved phosphorus. The main goal of this study was to evaluate SWAT's performance in estimating phosphorus exports in Lake Erie Watersheds. The specific objectives are: (1) evaluate and compare SWAT's *Pdr, Pmin, and Ptot* simulation outputs and (2) assess SWAT's phosphorus simulation outputs with (IWQ =1) and without (IWQ = 0) in-stream processing.

Methods

The Project Area

The project area is located in northwest Ohio and includes the Sandusky River (drainage area = 3,239 km^2 at 41°18' 28"N and 83°09' 32" W) and Rock Creek (drainage area = 90 km^2 at 41° 06' 49" N and 83°10' 06" W) subwatershed (Figure 1). These areas are characterized by a humid continental climate (four distinct seasons) and a relatively flat terrain. Daily average temperatures at Tiffin, OH near the confluence of Rock Creek and the Sandusky River, ranged from -8.6°C to -0.1°C in January and 17°C to 29°C in July for the period 1971-2000 (Loftus et al., 2006). Precipitation is distributed throughout the year, and from 1971 to 2000 average annual precipitation was 941.8 mm. Occasional droughts, blizzards, and tornadoes also occur. Agricultural practices in these two watersheds are similar and are typical of agricultural production in Northwest Ohio. The most common agricultural crops are corn, soybeans, and wheat. Four- to five-year crop rotations are sometimes followed with fallow fields usually planted to alfalfa. No-till, strip-till, and mulch-till are used for most (about 90%) soybean and wheat areas. About 80% of corn acreage is chisel plowed; the soil is not inverted but less than 30% of plant residue cover is left on the ground surface.

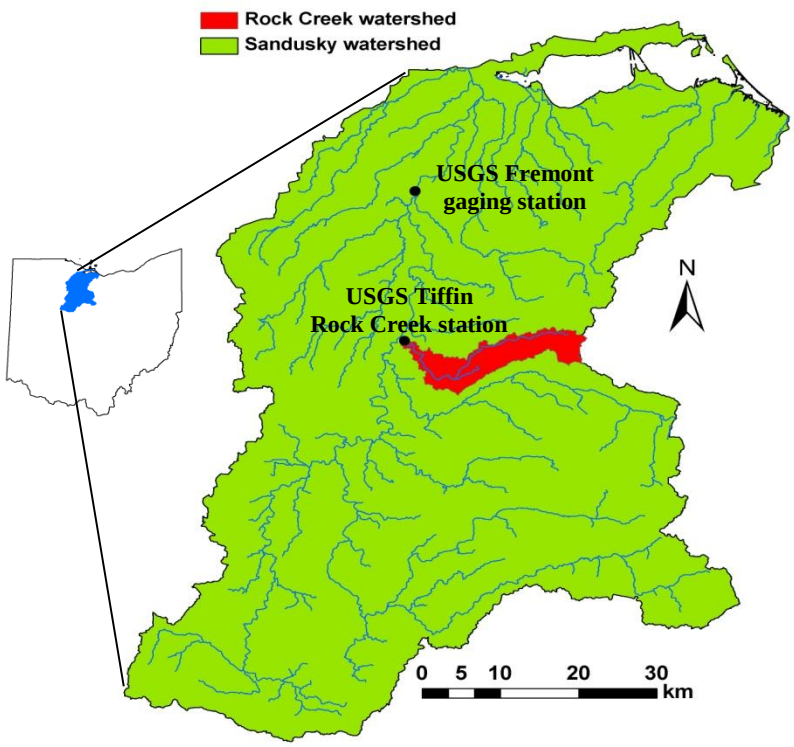

Figure 1. The Sandusky and Rock Creek watersheds in Ohio, USA.

SWAT setup

SWAT was developed by the United States Department of Agriculture - Agricultural Research Service (USDA-ARS) "to predict the impact of land management practices on water, sediment and agricultural chemical yields in large complex watersheds with varying soils, land use and management conditions over a long period of time" (Neitsch et al., 2005). SWAT is physically based, uses readily available inputs, is computationally efficient, and is a continuous model that operates on a daily time step. In SWAT, the entire watershed can be divided into sub-basins and each sub-basin is further divided into unique combinations of land use and soil properties called hydrologic response units (HRUs). A Geographic Information Systems (GIS) interface is used to input and designate land use, soil, weather, groundwater, water use, management, pond and stream water quality data, and the simulation period (Di Luzio et al., 2001). GIS input files include a digital elevation model (DEM), land use/land cover and soil properties layers, and a weather database.

We acquired the 10-m digital elevation models (DEM), soil data (Soil Survey Geographic (SSURGO) Database), daily rainfall and minimum/maximum temperature, and other geographic information system (GIS) layers from the websites of federal agencies (USGS, USDA, NOAA, etc.). These data were used in ArcSWAT (SWAT2005 version 2.3.4 and SWAT2009 version 93.5) to setup SWAT. For brevity, we only report the methods and results with SWAT2009. The Sandusky watershed was delineated with 373 subwatersheds ranging from 100 to 2000 hectares and a total of 719 HRUs. The thresholds for determining the HRUs were 20% landuse/crop cover, 33 % soil type, and 33% slope. The thresholds indicate that landuses/crop cover that are less 20% of the subwatershed area, soil types that are less than 33% of the landuse area within the subwatershed, and slopes that are less than 33% of the soil type area, are all excluded. The remaining combinations of crop cover, soil types, and slopes are the HRUs and their areas are adjusted to reflect the original subwatershed area. The Rock Creek watershed was delineated with 168 subwatersheds (approximately 10 to 100 ha) and a total of 471 HRUs. We used higher thresholds (25% landuse/crop cover, 25 % soil type, and 40% slope) to obtain these HRUs, otherwise, the thresholds used for Sandusky watershed would result in smaller areas and much higher number of watersheds in the Rock Creek watershed. Crop rotation for each HRU in both the Sandusky and Rock Creek watersheds was established using the crop cover GIS layers for 2006-2009 with corn, wheat, and soybean as the three dominant crop types. Agricultural management includes:

1. Corn crop: soil is tilled and fertilizer (11-52-00, 130 kg/ha) is applied in fall. In early spring, the soil is tilled again and anhydrous ammonia (100 kg/ha) is applied right before seeding. Anhydrous ammonia (100 kg/ha) is applied again 1 month after seeding.
2. Wheat crop: no tillage, fertilizer applied in fall (18-46-00, 100 kg/ha) before seeding and in early spring (11-52-00, 160 kg/ha).
3. Soybean crop: no tillage, fertilizer (00-15-00, 112 kg/ha) applied before seeding in early spring.

SWAT modification

The SWAT FORTRAN source codes are available from http://swatmodel.tamu.edu/software/swat-model. In this study, we added an output variable to SWAT2005 and SWAT2009 (rev451) that accounted for the dissolved and inorganic form of

phosphorus. The equations in subroutine virtual (FORTRAN file *virtual.f*) that summarize *Porg* and *Pmin* for subbasins with multiple HRUs are:

varoute(5,ihout) = (sub_yorgp(sb) + sub_sedps(sb)) * sub_ha (1)

varoute(7,ihout) = (sub_solp(sb) + sub_gwsolp(sb) + sub_sedpa(sb)) * sub_ha (2)

sub_gwsolp(sb) = sub_gwsolp(sb) + minpgw(j) * hru_dafr(j) (3)

where,

varoute(5,:) = *Porg* = organic phosphorus routed out of the reach on a day (kg P)
varoute(7,:) = *Pmin* = mineral phosphorus routed out of the reach on a day (kg P)
sub_yorgp(:) = organic P in surface runoff on day in subbasin (kg P/ha)
sub_sedpa(:) = amount of active mineral P attached to sediment removed in surface runoff on day in subbasin (kg P/ha)
sub_sedps(:) = amount of stable mineral P attached to sediment removed in surface runoff on day in subbasin (kg P/ha)
sub_solp(:) = soluble P in surface runoff on day in subbasin (kg P/ha)
sub_gwsolp(:)= soluble P loading to reach in groundwater in subbasin (kg P/ha)
minpgw(:) = soluble P loading to reach in groundwater (kg P/ha)
hru_dafr = fraction of watershed area in HRU
ihout = hydrograph storage location number for subbasin
j = hru number
sb = subbasin number
sub_ha = area of subbasin in hectares

It can be seen in equation (2) that *Pmin* is composed of soluble (or dissolved) P and sediment-attached mineral P. The appropriate equation for *Ppar* to denote total particulate P and *Pdr* to denote soluble P, assuming that the dissolved organic P is negligible compared to *Ppar*, should be:

Ppar = varoute(5,ihout) = (sub_yorgp(sb) + sub_sedps(sb) + sub_sedpa(sb)) * sub_ha (4)

Pdr = varoute(7,ihout) = (sub_solp(sb) + sub_gwsolp(sb)) * sub_ha (5)

Instead of modifying equations (1) and (2) into equations (4) and (5) we added another allocatable variable varoute(29,:) through the equation:

varoute(29,ihout) = (sub_solp(sb) + sub_gwsolp(sb)) * sub_ha (6)

Equation (6) was added in order to compare *Pmin* and *Pdr* without changing SWAT's original equations. It is noteworthy that equations (4) and (5) replaced equations (1) and (2) in SWAT2009 rev477 released in April 25, 2011. However, equations (1) and (2) still remain unchanged in SWAT2005.

SWAT Phosphorus forms

Uncalibrated SWAT simulations were done with and without in-stream processing routing methods. The phosphorus forms (*Pmin* and *Pdr*) were classified during high flows (≥ 90th percentile of the daily discharges) and low flows (≤ 33rd and ≤ 10th percentile of the daily discharges and receding for at least 2 days for Rock Creek and Sandusky, respectively). The means of *Pmin* and *Pdr* are compared using the Mann-Whitney non-parametric test package in R (R-Development-Core-Team, 2011) with the null hypothesis that the mean of *Pdr* is equal to the mean of *Pmin*.

Results and Discussion

SWAT Phosphorus forms output at low flows

Table 1 shows the p-values of the nonparametric Mann-Whitney test to compare the means of *Pdr* and *Pmin*. At low flows there was no difference between the means of *Pmin* and *Pdr*. This result was not surprising since the sediments and the sediment-attached P from runoff are essentially nil at low flows. Furthermore, the predominant P forms in low flow conditions are most probably the dissolved groundwater P and the release of mineral P as a result of in-stream processing.

Table 1. P-values with null hypothesis mean(*Pdr*) = mean(*Pmin*).

Flow conditions	Rock Creek		Sandusky	
	IWQ0	IWQ1	IWQ0	IWQ1
High Flows	0.0047	0.518	2.20E-16	0.019
Low Flows	0.4879	0.6803	0.1422	0.5885

The lack of difference between means of *Pmin* and *Pdr* at low flows is also shown by the comparable values of *Pmin* and *Pdr* (Figures 2, 3, 4, and 5) regardless of watershed and routing method. Thus, a single regression line was created for both *Pmin* and *Pdr* against *Ptot*. There seems to be a linear relation between *Pmin* (or *Pdr*) and *Ptot*. However, this relationship occurred in Rock Creek only at very low (< 0.04 kg/day) *Ptot* loads when there was in-stream processing (Figure 3). Otherwise, *Pmin* and *Pdr* are almost nil beyond *Ptot* loads of 0.04 kg/day in Rock Creek at low flows.

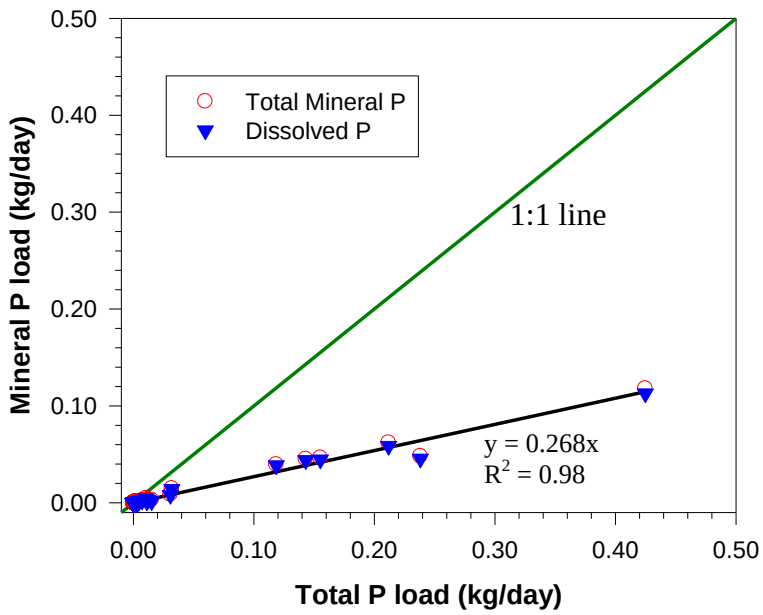

Figure 2. Mineral P and Total P loads at Rock Creek watershed without in-stream processing at low flows.

In Sandusky watershed, the slope of the line when there was no in-stream processing are far smaller than the slope of the line when there is in-stream processing (Figures 4 and 5). The slope

of the fitted lines represents *Pmin* (or *Pdr*) as a fraction of *Ptot*. This observation indicates that SWAT produces more inorganic P when there is in-stream processing than when the nutrients are routed without in-stream processing. There maybe several factors that caused the difference in the P loads of Rock Creek and Sandusky when there is in-stream processing. Probably, the amount of flow and P loads (and concentration) is lower in Rock Creek such that in-stream processing (i.e., assimilation of inorganic P by organisms) is pronounced.

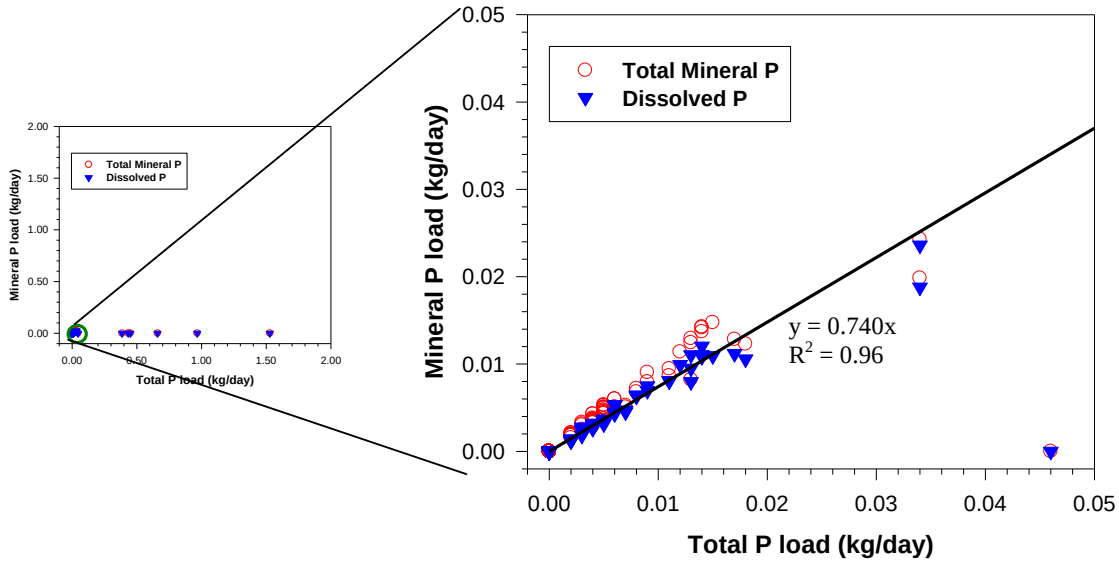

Figure 3. Mineral P and Total P loads at Rock Creek watershed with in-stream processing at low flows.

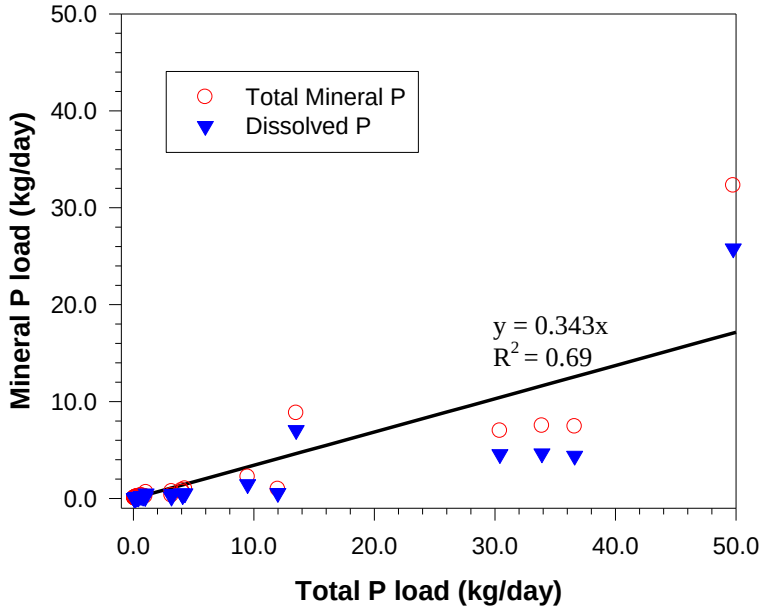

Figure 4. Mineral P and Total P loads at Sandusky watershed without in-stream processing at low flows.

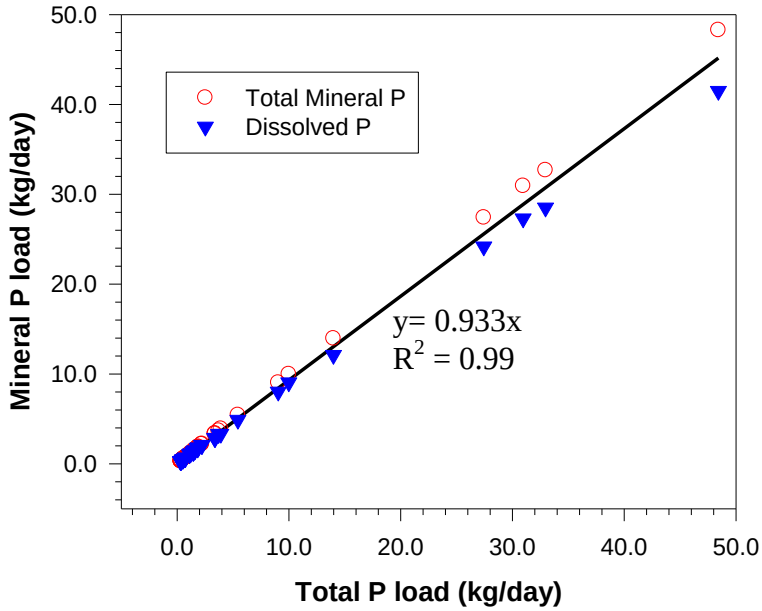

Figure 5. Mineral P and Total P loads at Sandusky watershed with in-stream processing at low flows.

SWAT Phosphorus forms output at high flows

As seen from Table 1, there was a significant difference between *Pmin* and *Pdr* at high flows, with or without in-stream processing. Flows during storm events are usually characterized by high sediment content from direct runoffs. Thus, during high flows, the equation for *Pmin* (equation 2) is not applicable to estimate *Pdr*. Furthermore, *Ptot* has a higher fraction of *Pmin*

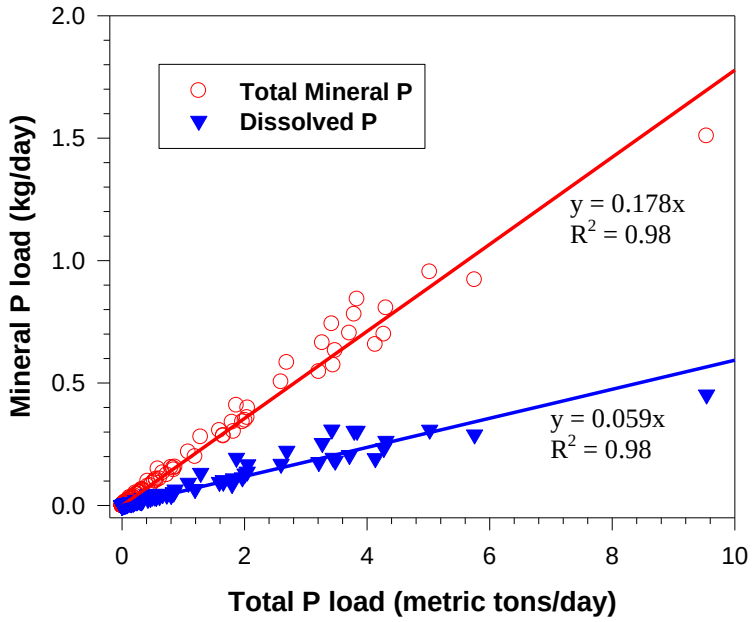

Figure 6. Mineral P and Total P loads at Rock Creek watershed without in-stream processing at high flows.

(0.977 and 0. 987) and *Pdr* (0.816 and 0.835) when there is in-stream processing than without in-stream processing (0.150 and 0.178 for *Pmin*; 0.059 and 0.064 for *Pdr*) (see Figures 6, 7, 8, and 9).

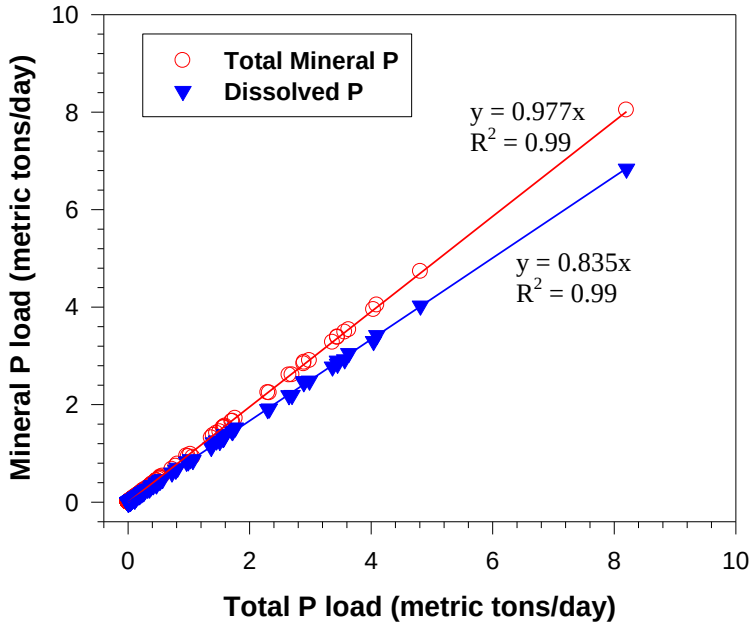

Figure 7. Mineral P and Total P loads at Rock Creek watershed with in-stream processing at high flows.

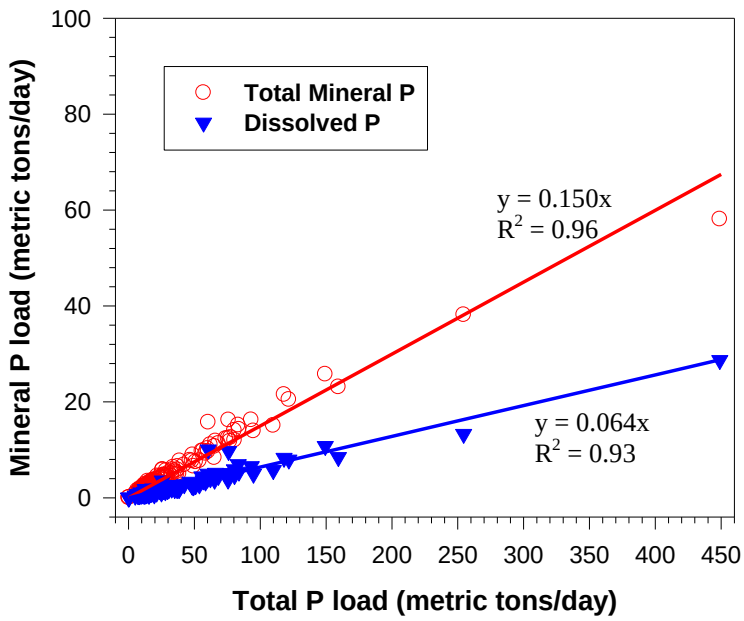

Figure 8. Mineral P and Total P loads at Sandusky watershed without in-stream processing at high flows.

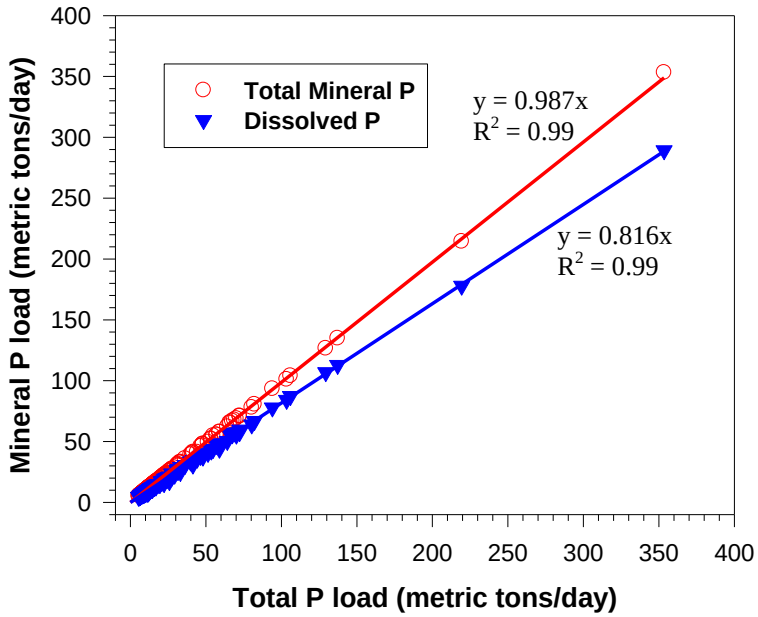

Figure 9. Mineral P and Total P loads at Sandusky watershed with in-stream processing at high flows.

Ptot is composed mostly of *Pmin* and contains more than 80% *Pdr*, indicating that *Ptot* is dominated by inorganic P and at dissolved form. However, one would expect the dominance of particulate P during high flows. Thus, SWAT phosphorus simulation maybe suspect when there is in-stream processing. Without in-stream processing, the reverse occurs where there is high Porg but low *Pmin* and *Pdr.* This condition probably closely depicts the real conditions, since Porg is mostly composed of sediment-attached but stable P (Equation 1).

The above results are also seen in Table 2, where the flow, sediment, and the different forms of load at high flows are summarized. At flows greater than 90th percentile and in the absence of in-stream processing, *Porg* is at least 71% of *Ptot* while *Pmin* and *Pdr* are less than 18 % and 6.5% of *Ptot*, respectively for both Rock Creek and Sandusky. When there is in-stream processing, both *Pmin* and *Pdr* exceeded 70% of *Ptot* but *Porg* is less than 4% of *Ptot*. It is also noteworthy that 99% of the Ptot in Rock Creek and 85% of Ptot in Sandusky were exported in the upper 10th percentile flows. The table also shows that almost all of the sediment exports occurred in Rock Creek (99%) and Sandusky (92%) in flows greater than 90th percentile.

Table 2. Flow volume, sediment yield, and phosphorus forms at high flows and over all flows during the simulation period 2006-2009.[1]

Flow Classification	Flow Volume (million m^3)	Sediments (1000 tons)	*Porg* (tons)	*Pmin* (tons)	*Pdr* (tons)	*Ptot* (tons)
Rock Creek, without in-stream processing (IWQ=0)						
90%ile flow	48.0(83.3)	126.7(99.3)	85.0(81.0)	19.2(18.3)	6.7(6.4)	104.2(99.2)
All Flow	57.7(100)	127.7(100)	85.6(81.5)	19.4(18.5)	6.8(6.5)	105.0(100)
Rock Creek, with in-stream processing (IWQ=1)						
90%ile flow	48.0(83.3)	126.7(99.3)	3.4(3.6)	88.7(94.9)	76.5(81.8)	92.1(98.5)
All Flow	57.7(100)	127.7(100)	4.4(4.7)	89.1(95.3)	76.9(82.2)	93.5(100)

	Sandusky, without in-stream processing (IWQ=0)					
90%ile flow	2626.0(66.7)	2242.8(92.5)	4468.0(71.5)	870.4(13.9)	358.2(5.7)	5338.4(85.5)
All Flow	3938.5(100)	2424.4(100)	5214.4(83.5)	1032.4(16.5)	430.0(6.9)	6246.9(100)
	Sandusky, without in-stream processing (IWQ=1)					
90%ile flow	2620.2(66.5)	2241.6(92.5)	74.6(1.4)	4411.0(84.3)	3658.3(69.9)	4485.6(85.7)
All Flow	3938.5(100)	2424.4(100)	94.1(1.8)	5139.9(98.2)	4267.5(81.5)	5234.0(100)

[1] Values in parenthesis are percentages of variables (e.g., Flow Volume, Sediments, etc.) at all flows. Phosphorus forms percentages are of the Ptot at all flows.

Summary and Conclusions

This study was undertaken to: (1) evaluate and compare SWAT's *Pdr, Pmin, and Ptot* simulation outputs and (2) assess SWAT's phosphorus simulation outputs with (IWQ =1) and without (IWQ = 0) in-stream processing in the Lake Erie watersheds. Our SWAT simulations and statistical analyses showed a lack of difference between the means of *Pmin* and *Pdr* at low flows. This result was not surprising since the sediments and the sediment-attached P from runoff are essentially nil at low flows. At high flows, there was a significant difference between the means of *Pmin* and *Pdr*, with or without in-stream processing. This finding indicates that at high flows, SWAT's original equation for *Pmin* is not applicable to estimate *Pdr*, otherwise the calculation would be inaccurate.

In-stream processing is a major factor in determining SWAT's P simulation output. At high flows (> 90th percentile) and in the absence of in-stream processing, *Porg* is the dominant P form (>71% of *Ptot)*. When there is in-stream processing, the dominant P forms are *Pmin* and *Pdr* (> 70% of Ptot). The high *Pdr* ratio when there is in-stream processing, rather than just the particulate P makes the SWAT simulation questionable. Further studies are needed to improve SWAT's ability to accurately simulate different P forms.

Acknowledgements

This study was funded by the Lake Erie Commission through the Lake Erie Protection Fund (LEPF) Grant No. SG 397-10.

References

Baker, D.B., J. Kramer, G. Winston, R. P. Richards, J. Crumrine. 2008. After the storm: Satellite images of Western Lake Erie in relation to tributary loading. Poster paper presented at the National River Rally, May 2-5 2008, Huron, OH.

Gitau, M. W., T. L. Veith, W. J. Gburek. 2004. Farm–Level Optimization of Bmp Placement for Cost–Effective Pollution Reduction. Transactions of the ASABE. Vol. 47(6): 1923-1931.

Hartig, J.H., M.A. Zarull, J.J.H. Ciborowski, J.E. Gannon, E. Wilke, G. Norwood, and A. Vincent, eds. 2007. State of the Strait: Status and Trends of Key Indicators. Great Lakes Institute for Environmental Research, Occasional Publication No. 5, University of Windsor, Ontario, Canada. ISSN 1715-3980.

Loftus, T. T., D. B. Baker, J.V. Setzler, and J. Crumrine. 2006. Honey Creek Watershed Action Plan. The National Center for Water Quality Research, Heidelberg College, Tiffin, OH 44883..

Makarawicz, J.C. and P. Bertram. 1991. Evidence for the restoration of the Lake Erie ecosystem. Bioscience 41(4): 216-223.

Maringanti, C., I. Chaubey, and J. Popp. 2009. Development of a Multiobjective Optimization Tool for the Selection and Placement of Best Management Practices for Nonpoint Source Pollution Control. Water Resources Research, 45: W06406, doi:10.1029/2008WR007094.

Neitsch, S.L., J.G. Arnold, J.R. Kiniry, J.R. Williams. 2005. Soil and Water Assessment Tool Theoretical Documentation Version 2005. Grassland, Soil and Water Research Laboratory, United States Department of Agriculture Agricultural Research Service (USDA-ARS). 808 East Blackland Road, Temple, Texas. Available at http://swatmodel.tamu.edu (accessed on 17 April 2011).

Nicholls, K.H., D.W. Standen, G.J. Hopkins, and E.C. Carney. 1977. Declines in the nearshore phytoplankton of Lake Erie's western basin since 1971. Journal of Great Lakes Research 3:72-78.

R-Development-Core-Team. 2011. R: A Language and Environment for Statistical Computing. R Foundation for Statistical Computing, Vienna, Austria. http://www.R-project.org.

U.S. EPA. 1978. The Great Lakes Water Quality Agreement (GLWQA). Available at http://www.epa.gov/glnpo/glwqa/1978/index.html (accessed on 17 April 2011).

Veith, T.L., M.L. Wolfe, and C. D. Heatwole.2003. Optimization Procedure for Cost Effective BMP Placement at a Watershed Scale. Journal of the American Water Resources Association 39(6):1331-1343.

Appendix 2. Sensitivity analysis results for Honey Creek, Sandusky, and Maumee

Table A2.1. SWAT sensitivity ranking of 55 parameters for Honey Creek, no in-stream processing.

Rank	FLOW	SED	TOTP	SRP	NO23
1	CN2	CN2	SMFMN	REVAPMN	SOLCRK
2	SOLCRK	CH_N2	TIMP	SMFMN	REVAPMN
3	SOL_AWC	PRF	REVAPMN	SOL_AWC	SMFMN
4	CH_K2	HRUSLP	SOLCRK	TIMP	TIMP
5	SURLAG	SPEXP	GWQMN	GWQMN	GWQMN
6	GWQMN	USLE_K	CANMX	SOLCRK	SOL_AWC
7	ALPHABF	USLE_P	CN2	SURLAG	SURLAG
8	ESCO	USLE_C	PSP	CN2	ESCO
9	REVAPMN	SOLCRK	SOL_AWC	PHOSKD	CH_K1
10	SMFMN	SURLAG	SURLAG	CANMX	ALPHABF
11	TIMP	ESCO	ESCO	ESCO	CANMX
12	CH_N1	SPCON	USLE_P	HRUSLP	CN2
13	GWDELAY	CH_N1	USLE_K	SOL_K	SDNCO
14	CH_N2	SOL_AWC	USLE_C	CH_K2	HRUSLP
15	SLSUBSN	OVN	HRUSLP	SMFMX	SOL_K
16	OVN	ADJ_PKR	SOLSOLP	ALPHABF	CH_N1
17	SMFMX	ALPHABF	SLSUBSN	SLSUBSN	CH_K2
18	GWREVAP	CH_K2	ALPHABF	P_UPDIS	GWDELAY
19	HRUSLP	CH_K1	SOL_K	SOLSOLP	RCN
20	SDNCO	SDNCO	SOL_ORGP	PSP	OVN
21	CANMX	SLSUBSN	GWREVAP	CH_K1	ADJ_PKR
22	SOL_K	GWQMN	CH_K2	ADJ_PKR	SMFMX
23	CH_K1	REVAPMN	GWDELAY	CH_N2	NPERCO
24	ADJ_PKR	CH_COV1	CH_N2	CH_N1	SLSUBSN
25	RCN	CH_COV2	CH_N1	GWSOLP	N_UPDIS
26	N_UPDIS	GWDELAY	CH_K1	GWREVAP	CH_N2
27	USLE_K	TIMP	ADJ_PKR	GWDELAY	GWREVAP
28	USLE_C	CANMX	PHOSKD	OVN	USLE_P
29	NPERCO	SMFMN	P_UPDIS	SDNCO	USLE_K
30	USLE_P	GWREVAP	OVN	PPERCO	USLE_C
31	SOLSOLP	SMFMX	SDNCO	USLE_P	P_UPDIS
32	PSP	NPERCO	SMFMX	USLE_K	SOLSOLP
33	P_UPDIS	N_UPDIS	PPERCO	USLE_C	PSP
34	PHOSKD	RCN	GWSOLP	N_UPDIS	PHOSKD
35	PPERCO	SOLSOLP	NPERCO	SOL_ORGP	PPERCO
36	SOL_ORGP	SOL_K	N_UPDIS	RCN	SOL_ORGP
37	SMTMP	P_UPDIS	RCN	NPERCO	SHAL_N
38	SFTMP	PHOSKD	PRF	PRF	GWSOLP
39	PRF	PSP	SPEXP	SPEXP	PRF
40	SPCON	PPERCO	SPCON	SPCON	SPEXP
41	SPEXP	SOL_ORGP	CH_COV1	CH_COV1	SPCON
42	SHAL_N	SMTMP	CH_COV2	CH_COV2	CH_COV1
43	GWSOLP	SFTMP	SMTMP	SMTMP	CH_COV2
44	CH_COV1	SHAL_N	SFTMP	SFTMP	SMTMP
45	CH_COV2	GWSOLP	SHAL_N	SHAL_N	SFTMP
46	AI_0	AI_0	AI_0	AI_0	AI_0
47	AI_2	AI_2	AI_2	AI_2	AI_2
48	MUMAX	MUMAX	MUMAX	MUMAX	MUMAX
49	RHOQ	RHOQ	RHOQ	RHOQ	RHOQ
50	K_N	K_N	K_N	K_N	K_N
51	K_P	K_P	K_P	K_P	K_P
52	RS1	RS1	RS1	RS1	RS1
53	RS2	RS2	RS2	RS2	RS2
54	RS5	RS5	RS5	RS5	RS5
55	BC4	BC4	BC4	BC4	BC4

Table A2.2. SWAT sensitivity ranking of 55 parameters for Honey Creek WITH in-stream processing.

Rank	FLOW	SED	TOTP	SRP	NO23
1	CN2	CN2	SMFMN	SMFMN	SOLCRK
2	SOLCRK	CH_N2	REVAPMN	REVAPMN	REVAPMN
3	SOL_AWC	PRF	TIMP	TIMP	SMFMN
4	CH_K2	HRUSLP	GWQMN	GWQMN	TIMP
5	SURLAG	SPEXP	SOLCRK	SOLCRK	GWQMN
6	GWQMN	USLE_K	ESCO	ESCO	ESCO
7	ALPHABF	USLE_P	SOL_AWC	SOL_AWC	SOL_AWC
8	ESCO	USLE_C	CN2	SURLAG	SURLAG
9	REVAPMN	SOLCRK	PSP	CN2	ALPHABF
10	SMFMN	SURLAG	SURLAG	PSP	CANMX
11	TIMP	ESCO	USLE_P	USLE_P	CN2
12	CH_N1	SPCON	USLE_K	USLE_K	CH_K1
13	GWDELAY	CH_N1	SOLSOLP	SOLSOLP	SDNCO
14	CH_N2	SOL_AWC	USLE_C	PHOSKD	HRUSLP
15	SLSUBSN	OVN	HRUSLP	SOL_K	SOL_K
16	OVN	ADJ_PKR	SOL_ORGP	USLE_C	CH_K2
17	SMFMX	ALPHABF	ALPHABF	BC4	CH_N1
18	GWREVAP	CH_K2	PHOSKD	HRUSLP	GWDELAY
19	HRUSLP	CH_K1	SOL_K	SLSUBSN	RCN
20	SDNCO	SDNCO	SLSUBSN	ALPHABF	NPERCO
21	CANMX	SLSUBSN	CH_N1	CH_N2	SLSUBSN
22	SOL_K	GWQMN	CH_K2	SOL_ORGP	OVN
23	CH_K1	REVAPMN	ADJ_PKR	GWREVAP	GWREVAP
24	ADJ_PKR	CH_COV1	P_UPDIS	CANMX	ADJ_PKR
25	RCN	CH_COV2	CANMX	CH_K2	SMFMX
26	N_UPDIS	GWDELAY	OVN	P_UPDIS	CH_N2
27	USLE_K	TIMP	SDNCO	GWDELAY	N_UPDIS
28	USLE_C	CANMX	GWREVAP	SMFMX	USLE_P
29	NPERCO	SMFMN	CH_N2	CH_N1	USLE_K
30	USLE_P	GWREVAP	GWDELAY	CH_K1	USLE_C
31	SOLSOLP	SMFMX	RS5	SDNCO	AI_0
32	PSP	NPERCO	SMFMX	ADJ_PKR	RS1
33	P_UPDIS	N_UPDIS	CH_K1	RS5	MUMAX
34	PHOSKD	RCN	BC4	OVN	RHOQ
35	PPERCO	SOLSOLP	PPERCO	AI_0	PHOSKD
36	SOL_ORGP	SOL_K	MUMAX	MUMAX	K_N
37	SMTMP	P_UPDIS	RHOQ	RS1	SOLSOLP
38	SFTMP	PHOSKD	RS1	GWSOLP	PSP
39	PRF	PSP	AI_0	PPERCO	K_P
40	SPCON	PPERCO	GWSOLP	AI_2	BC4
41	SPEXP	SOL_ORGP	AI_2	RHOQ	P_UPDIS
42	SHAL_N	SMTMP	NPERCO	NPERCO	PPERCO
43	GWSOLP	SFTMP	RCN	N_UPDIS	AI_2
44	CH_COV1	SHAL_N	N_UPDIS	RCN	GWSOLP
45	CH_COV2	GWSOLP	K_N	K_N	SOL_ORGP
46	AI_0	AI_0	K_P	K_P	RS5
47	AI_2	AI_2	RS2	RS2	RS2
48	MUMAX	MUMAX	SHAL_N	SHAL_N	SHAL_N
49	RHOQ	RHOQ	PRF	PRF	PRF
50	K_N	K_N	SPEXP	SPEXP	SPEXP
51	K_P	K_P	SPCON	SPCON	SPCON
52	RS1	RS1	CH_COV1	CH_COV1	CH_COV1
53	RS2	RS2	CH_COV2	CH_COV2	CH_COV2
54	RS5	RS5	SMTMP	SMTMP	SMTMP
55	BC4	BC4	SFTMP	SFTMP	SFTMP

Table A2.3. SWAT sensitivity ranking of 55 parameters for Sandusky, no in-stream processing.

Rank	FLOW	SED	TOTP	SRP	NO23
1	CN2	CN2	SOL_AWC	REVAPMN	NPERCO
2	SURLAG	CH_N2	REVAPMN	GWQMN	N_UPDIS
3	SOLCRK	PRF	GWQMN	SOL_AWC	RCN
4	CH_K2	SPCON	SLSUBSN	SURLAG	ADJ_PKR
5	CH_N1	SPEXP	CN2	SLSUBSN	CANMX
6	ESCO	SOLCRK	SOLCRK	ALPHABF	GWREVAP
7	SOL_AWC	SURLAG	SURLAG	TIMP	SDNCO
8	REVAPMN	CH_COV1	TIMP	CN2	CH_K1
9	GWQMN	CH_COV2	ESCO	SOL_K	GWDELAY
10	OVN	ESCO	PSP	ESCO	SMFMX
11	SLSUBSN	CH_N1	CH_N1	SOLCRK	HRUSLP
12	CH_N2	CH_K2	CH_N2	SMFMN	SMFMN
13	ALPHABF	ALPHABF	SMFMN	PHOSKD	OVN
14	HRUSLP	SOL_AWC	OVN	SMFMX	SOL_K
15	GWDELAY	HRUSLP	CH_K2	HRUSLP	TIMP
16	CH_K1	OVN	HRUSLP	CH_K2	ALPHABF
17	TIMP	SLSUBSN	SOL_K	CH_K1	ESCO
18	SDNCO	USLE_K	USLE_P	P_UPDIS	CH_N1
19	SMFMN	CH_K1	USLE_C	GWREVAP	SLSUBSN
20	GWREVAP	USLE_P	USLE_K	SOLSOLP	CH_K2
21	CANMX	USLE_C	CH_K1	CH_N1	P_UPDIS
22	ADJ_PKR	GWQMN	SMFMX	SDNCO	SOLCRK
23	SOL_K	CANMX	GWREVAP	PSP	USLE_P
24	SMFMX	GWDELAY	SOLSOLP	CH_N2	USLE_K
25	RCN	ADJ_PKR	ALPHABF	OVN	USLE_C
26	N_UPDIS	SDNCO	SOL_ORGP	ADJ_PKR	GWQMN
27	NPERCO	REVAPMN	GWDELAY	CANMX	SURLAG
28	USLE_K	GWREVAP	CANMX	GWDELAY	CH_N2
29	USLE_C	TIMP	P_UPDIS	PPERCO	REVAPMN
30	USLE_P	SMFMN	SDNCO	GWSOLP	SOL_AWC
31	P_UPDIS	RCN	PHOSKD	USLE_P	CN2
32	SOLSOLP	SMFMX	ADJ_PKR	USLE_K	SOLSOLP
33	PSP	SOL_K	PPERCO	N_UPDIS	PSP
34	PHOSKD	NPERCO	N_UPDIS	SOL_ORGP	PPERCO
35	PPERCO	N_UPDIS	GWSOLP	USLE_C	PHOSKD
36	SOL_ORGP	SOLSOLP	NPERCO	RCN	SOL_ORGP
37	SMTMP	P_UPDIS	RCN	NPERCO	SHAL_N
38	SFTMP	PSP	PRF	PRF	GWSOLP
39	PRF	PHOSKD	SPCON	SPCON	PRF
40	SPCON	PPERCO	SPEXP	SPEXP	SPCON
41	SPEXP	SOL_ORGP	CH_COV1	CH_COV1	SPEXP
42	SHAL_N	SMTMP	CH_COV2	CH_COV2	CH_COV1
43	GWSOLP	SFTMP	SMTMP	SMTMP	CH_COV2
44	CH_COV1	SHAL_N	SFTMP	SFTMP	SMTMP
45	CH_COV2	GWSOLP	SHAL_N	SHAL_N	SFTMP
46	AI_0	AI_0	AI_0	AI_0	AI_0
47	AI_2	AI_2	AI_2	AI_2	AI_2
48	MUMAX	MUMAX	MUMAX	MUMAX	MUMAX
49	RHOQ	RHOQ	RHOQ	RHOQ	RHOQ
50	K_N	K_N	K_N	K_N	K_N
51	K_P	K_P	K_P	K_P	K_P
52	RS1	RS1	RS1	RS1	RS1
53	RS2	RS2	RS2	RS2	RS2
54	RS5	RS5	RS5	RS5	RS5
55	BC4	BC4	BC4	BC4	BC4

Table A2.4. SWAT sensitivity ranking of 55 parameters for Sandusky WITH in-stream processing.

Rank	FLOW	SED	TOTP	SRP	NO23
1	CN2	CN2	SOL_AWC	SOL_AWC	REVAPMN
2	SURLAG	CH_N2	REVAPMN	REVAPMN	SOL_AWC
3	SOLCRK	PRF	SLSUBSN	SLSUBSN	SOLCRK
4	CH_K2	SPCON	GWQMN	GWQMN	GWQMN
5	CH_N1	SPEXP	SURLAG	SURLAG	ALPHABF
6	ESCO	SOLCRK	TIMP	TIMP	SURLAG
7	SOL_AWC	SURLAG	SOLCRK	SOLCRK	SLSUBSN
8	REVAPMN	CH_COV1	CN2	CN2	CN2
9	GWQMN	CH_COV2	SMFMN	SMFMN	TIMP
10	OVN	ESCO	SOL_K	SOL_K	ESCO
11	SLSUBSN	CH_N1	CH_K1	CH_K1	SOL_K
12	CH_N2	CH_K2	ESCO	ESCO	SMFMX
13	ALPHABF	ALPHABF	HRUSLP	HRUSLP	SMFMN
14	HRUSLP	SOL_AWC	GWREVAP	GWREVAP	HRUSLP
15	GWDELAY	HRUSLP	PSP	PSP	CH_K2
16	CH_K1	OVN	OVN	OVN	CH_K1
17	TIMP	SLSUBSN	SMFMX	SMFMX	RCN
18	SDNCO	USLE_K	CH_N1	CH_N1	GWREVAP
19	SMFMN	CH_K1	CH_K2	CH_K2	CH_N2
20	GWREVAP	USLE_P	GWDELAY	GWDELAY	NPERCO
21	CANMX	USLE_C	PHOSKD	PHOSKD	CH_N1
22	ADJ_PKR	GWQMN	ALPHABF	ALPHABF	SDNCO
23	SOL_K	CANMX	CH_N2	CH_N2	OVN
24	SMFMX	GWDELAY	USLE_P	USLE_P	N_UPDIS
25	RCN	ADJ_PKR	SOLSOLP	SOLSOLP	ADJ_PKR
26	N_UPDIS	SDNCO	USLE_K	USLE_K	USLE_K
27	NPERCO	REVAPMN	USLE_C	USLE_C	USLE_P
28	USLE_K	GWREVAP	ADJ_PKR	ADJ_PKR	USLE_C
29	USLE_C	TIMP	P_UPDIS	P_UPDIS	GWDELAY
30	USLE_P	SMFMN	SOL_ORGP	BC4	CANMX
31	P_UPDIS	RCN	SDNCO	SOL_ORGP	MUMAX
32	SOLSOLP	SMFMX	BC4	SDNCO	AI_0
33	PSP	SOL_K	RS5	CANMX	RS1
34	PHOSKD	NPERCO	CANMX	RS5	RHOQ
35	PPERCO	N_UPDIS	PPERCO	PPERCO	P_UPDIS
36	SOL_ORGP	SOLSOLP	N_UPDIS	GWSOLP	SOLSOLP
37	SMTMP	P_UPDIS	NPERCO	N_UPDIS	K_N
38	SFTMP	PSP	GWSOLP	NPERCO	PHOSKD
39	PRF	PHOSKD	RCN	MUMAX	PPERCO
40	SPCON	PPERCO	MUMAX	AI_0	PSP
41	SPEXP	SOL_ORGP	RHOQ	RCN	K_P
42	SHAL_N	SMTMP	RS1	RS1	SOL_ORGP
43	GWSOLP	SFTMP	AI_0	AI_2	AI_2
44	CH_COV1	SHAL_N	AI_2	RHOQ	GWSOLP
45	CH_COV2	GWSOLP	K_N	K_N	BC4
46	AI_0	AI_0	K_P	K_P	RS5
47	AI_2	AI_2	RS2	RS2	RS2
48	MUMAX	MUMAX	SHAL_N	SHAL_N	SHAL_N
49	RHOQ	RHOQ	PRF	PRF	PRF
50	K_N	K_N	SPCON	SPCON	SPCON
51	K_P	K_P	SPEXP	SPEXP	SPEXP
52	RS1	RS1	CH_COV1	CH_COV1	CH_COV1
53	RS2	RS2	CH_COV2	CH_COV2	CH_COV2
54	RS5	RS5	SMTMP	SMTMP	SMTMP
55	BC4	BC4	SFTMP	SFTMP	SFTMP

Table A2.5. SWAT sensitivity ranking of 55 parameters for Maumee, no in-stream processing.

Rank	FLOW	SED	TOTP	SRP	NO23
1	CN2	CN2	CH_N2	SOL_K	SOL_K
2	GWQMN	GWQMN	SPEXP	REVAPMN	CN2
3	REVAPMN	REVAPMN	PRF	CN2	REVAPMN
4	CH_N2	CH_N2	CN2	SOLCRK	PHOSKD
5	ALPHABF	ALPHABF	SPCON	GWQMN	SOL_AWC
6	ESCO	ESCO	GWQMN	SOL_AWC	GWQMN
7	SURLAG	SURLAG	CH_COV1	PSP	SOLCRK
8	CH_N1	CH_N1	CH_COV2	PHOSKD	HRUSLP
9	CH_K1	CH_K1	REVAPMN	CH_K2	ESCO
10	SOL_AWC	SOL_AWC	ESCO	ESCO	CH_K2
11	GWDELAY	GWDELAY	CH_K1	SURLAG	CH_K1
12	SOLCRK	SOLCRK	SOLCRK	CH_K1	GWREVAP
13	CH_K2	CH_K2	CH_N1	GWREVAP	P_UPDIS
14	GWREVAP	GWREVAP	ALPHABF	CH_N2	CH_N1
15	SLSUBSN	SLSUBSN	CH_K2	CH_N1	SLSUBSN
16	OVN	OVN	SOL_AWC	HRUSLP	SOLSOLP
17	TIMP	TIMP	GWREVAP	SOLSOLP	SMFMN
18	SMFMN	SMFMN	SURLAG	OVN	GWDELAY
19	ADJ_PKR	ADJ_PKR	GWDELAY	USLE_K	SURLAG
20	HRUSLP	HRUSLP	HRUSLP	USLE_P	TIMP
21	SDNCO	SDNCO	USLE_K	ALPHABF	SMFMX
22	SOL_K	SOL_K	USLE_P	P_UPDIS	ALPHABF
23	SMFMX	SMFMX	ADJ_PKR	GWDELAY	PSP
24	CANMX	CANMX	USLE_C	USLE_C	OVN
25	RCN	RCN	TIMP	SLSUBSN	CH_N2
26	NPERCO	NPERCO	OVN	SMFMN	SDNCO
27	N_UPDIS	N_UPDIS	SMFMN	ADJ_PKR	GWSOLP
28	USLE_C	USLE_C	SLSUBSN	SMFMX	CANMX
29	USLE_K	USLE_K	SDNCO	SDNCO	PPERCO
30	P_UPDIS	P_UPDIS	SOL_K	SOL_ORGP	ADJ_PKR
31	USLE_P	USLE_P	CANMX	TIMP	NPERCO
32	SOLSOLP	SOLSOLP	SMFMX	CANMX	RCN
33	PSP	PSP	RCN	PPERCO	USLE_P
34	PHOSKD	PHOSKD	NPERCO	GWSOLP	USLE_K
35	PPERCO	PPERCO	N_UPDIS	RCN	SOL_ORGP
36	SOL_ORGP	SOL_ORGP	P_UPDIS	NPERCO	USLE_C
37	SMTMP	SMTMP	SOLSOLP	N_UPDIS	N_UPDIS
38	SFTMP	SFTMP	PSP	SPEXP	SPEXP
39	PRF	PRF	PPERCO	PRF	PRF
40	SPCON	SPCON	PHOSKD	SPCON	SPCON
41	SPEXP	SPEXP	SOL_ORGP	CH_COV1	CH_COV1
42	SHAL_N	SHAL_N	SMTMP	CH_COV2	CH_COV2
43	GWSOLP	GWSOLP	SFTMP	SMTMP	SMTMP
44	CH_COV1	CH_COV1	SHAL_N	SFTMP	SFTMP
45	CH_COV2	CH_COV2	GWSOLP	SHAL_N	SHAL_N
46	AI_0	AI_0	AI_0	AI_0	AI_0
47	AI_2	AI_2	AI_2	AI_2	AI_2
48	MUMAX	MUMAX	MUMAX	MUMAX	MUMAX
49	RHOQ	RHOQ	RHOQ	RHOQ	RHOQ
50	K_N	K_N	K_N	K_N	K_N
51	K_P	K_P	K_P	K_P	K_P
52	RS1	RS1	RS1	RS1	RS1
53	RS2	RS2	RS2	RS2	RS2
54	RS5	RS5	RS5	RS5	RS5
55	BC4	BC4	BC4	BC4	BC4

Table A2.6. SWAT sensitivity ranking of 55 parameters for Maumee WITH in-stream processing.

Rank	FLOW	SED	TOTP	SRP	NO23
1	CN2	CH_N2	SOL_K	SOL_K	REVAPMN
2	GWQMN	SPEXP	REVAPMN	REVAPMN	SOLCRK
3	REVAPMN	PRF	CN2	CN2	CN2
4	CH_N2	CN2	GWQMN	GWQMN	SOL_K
5	ALPHABF	SPCON	SOLCRK	SOLCRK	GWQMN
6	ESCO	GWQMN	SOL_AWC	SOL_AWC	TIMP
7	SURLAG	CH_COV1	PHOSKD	PHOSKD	SOL_AWC
8	CH_N1	CH_COV2	CH_K2	CH_K2	SURLAG
9	CH_K1	REVAPMN	ESCO	ESCO	ESCO
10	SOL_AWC	ESCO	HRUSLP	TIMP	SLSUBSN
11	GWDELAY	CH_K1	TIMP	HRUSLP	HRUSLP
12	SOLCRK	SOLCRK	GWREVAP	GWREVAP	ALPHABF
13	CH_K2	CH_N1	PSP	PSP	OVN
14	GWREVAP	ALPHABF	CH_K1	CH_K1	SMFMN
15	SLSUBSN	CH_K2	CH_N2	SOLSOLP	GWREVAP
16	OVN	SOL_AWC	SOLSOLP	P_UPDIS	CH_K2
17	TIMP	GWREVAP	P_UPDIS	SURLAG	CH_K1
18	SMFMN	SURLAG	CH_N1	ALPHABF	SDNCO
19	ADJ_PKR	GWDELAY	SURLAG	CH_N1	NPERCO
20	HRUSLP	HRUSLP	ALPHABF	GWDELAY	CH_N1
21	SDNCO	USLE_K	GWDELAY	USLE_P	RCN
22	SOL_K	USLE_P	USLE_P	CH_N2	GWDELAY
23	SMFMX	ADJ_PKR	USLE_K	USLE_K	SMFMX
24	CANMX	USLE_C	SMFMN	SMFMN	CH_N2
25	RCN	TIMP	OVN	SLSUBSN	CANMX
26	NPERCO	OVN	SLSUBSN	OVN	USLE_P
27	N_UPDIS	SMFMN	USLE_C	USLE_C	ADJ_PKR
28	USLE_C	SLSUBSN	SMFMX	SMFMX	USLE_K
29	USLE_K	SDNCO	SDNCO	SDNCO	N_UPDIS
30	P_UPDIS	SOL_K	ADJ_PKR	BC4	USLE_C
31	USLE_P	CANMX	SOL_ORGP	ADJ_PKR	RS1
32	SOLSOLP	SMFMX	RS5	SOL_ORGP	MUMAX
33	PSP	RCN	BC4	RS5	AI_0
34	PHOSKD	NPERCO	PPERCO	GWSOLP	RHOQ
35	PPERCO	N_UPDIS	CANMX	PPERCO	SOLSOLP
36	SOL_ORGP	P_UPDIS	GWSOLP	CANMX	K_P
37	SMTMP	SOLSOLP	RCN	RS1	K_N
38	SFTMP	PSP	RS1	RCN	PSP
39	PRF	PPERCO	NPERCO	MUMAX	PHOSKD
40	SPCON	PHOSKD	RHOQ	NPERCO	PPERCO
41	SPEXP	SOL_ORGP	N_UPDIS	RHOQ	P_UPDIS
42	SHAL_N	SMTMP	MUMAX	AI_0	AI_2
43	GWSOLP	SFTMP	AI_0	N_UPDIS	SOL_ORGP
44	CH_COV1	SHAL_N	AI_2	AI_2	GWSOLP
45	CH_COV2	GWSOLP	K_N	K_N	BC4
46	AI_0	AI_0	K_P	K_P	RS2
47	AI_2	AI_2	RS2	RS2	RS5
48	MUMAX	MUMAX	SHAL_N	SHAL_N	SHAL_N
49	RHOQ	RHOQ	SPEXP	SPEXP	SPEXP
50	K_N	K_N	PRF	PRF	PRF
51	K_P	K_P	SPCON	SPCON	SPCON
52	RS1	RS1	CH_COV1	CH_COV1	CH_COV1
53	RS2	RS2	CH_COV2	CH_COV2	CH_COV2
54	RS5	RS5	SMTMP	SMTMP	SMTMP
55	BC4	BC4	SFTMP	SFTMP	SFTMP

Appendix 3. Calibration graph results

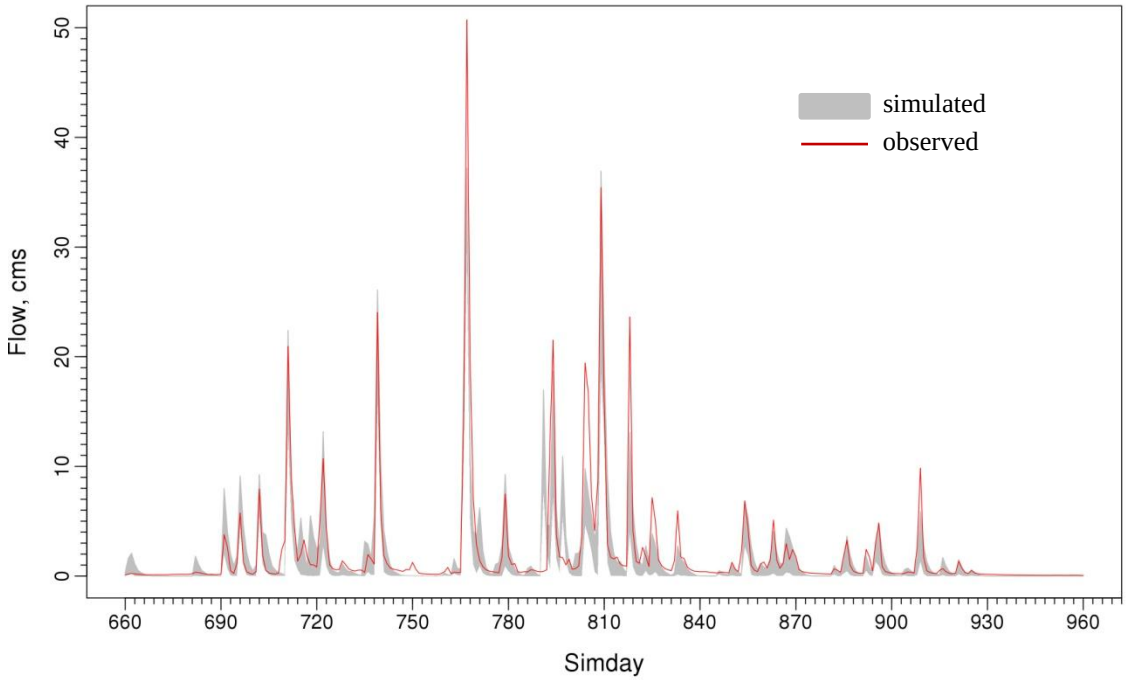

Figure A3.1. Simulated vs. observed flow in Rock Creek without in-stream processing.

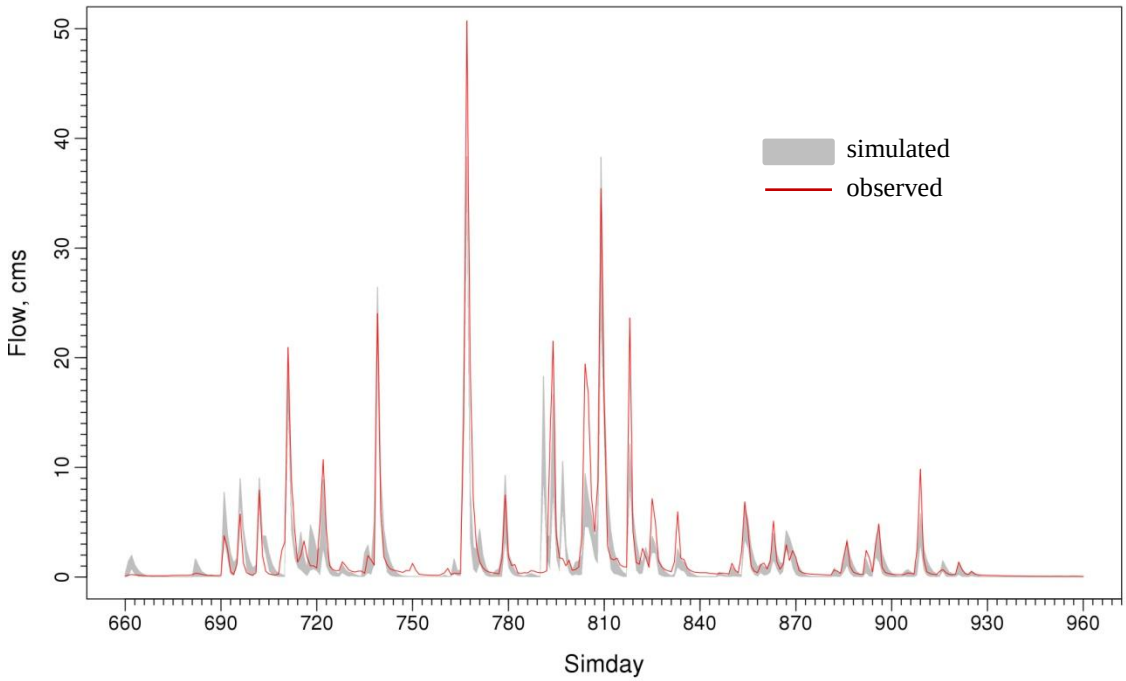

Figure A3.2. Simulated vs. observed flow in Rock Creek with in-stream processing.

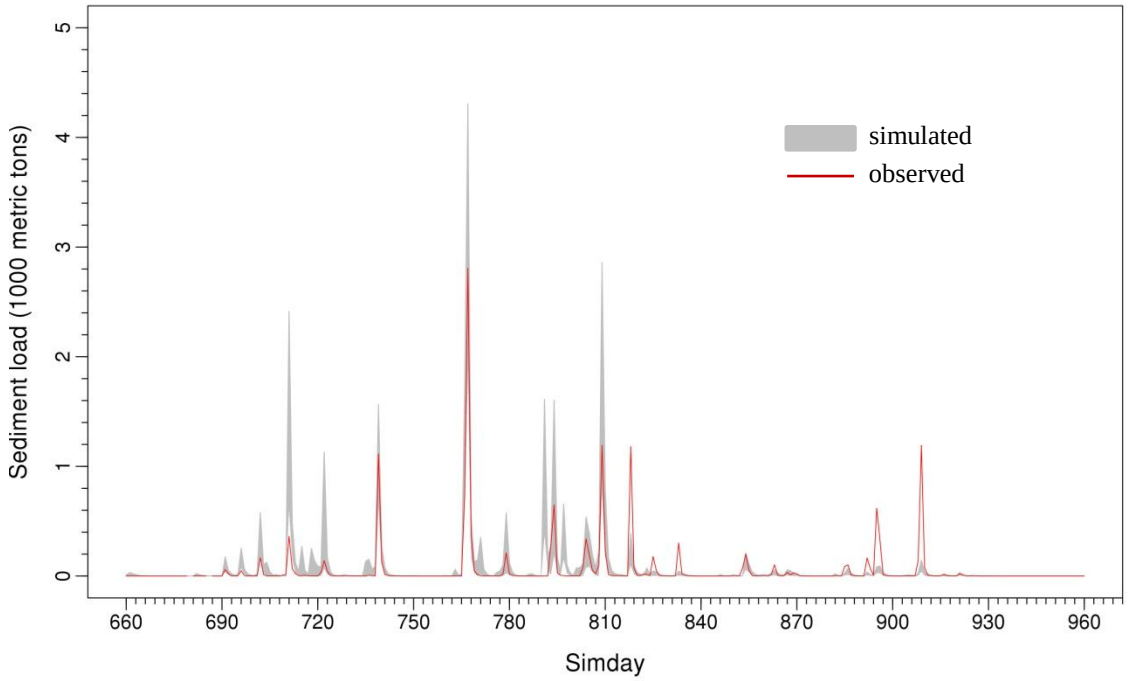

Figure A3.3. Simulated vs. sediment load in Rock Creek without in-stream processing. Simday1 = January 01, 2006.

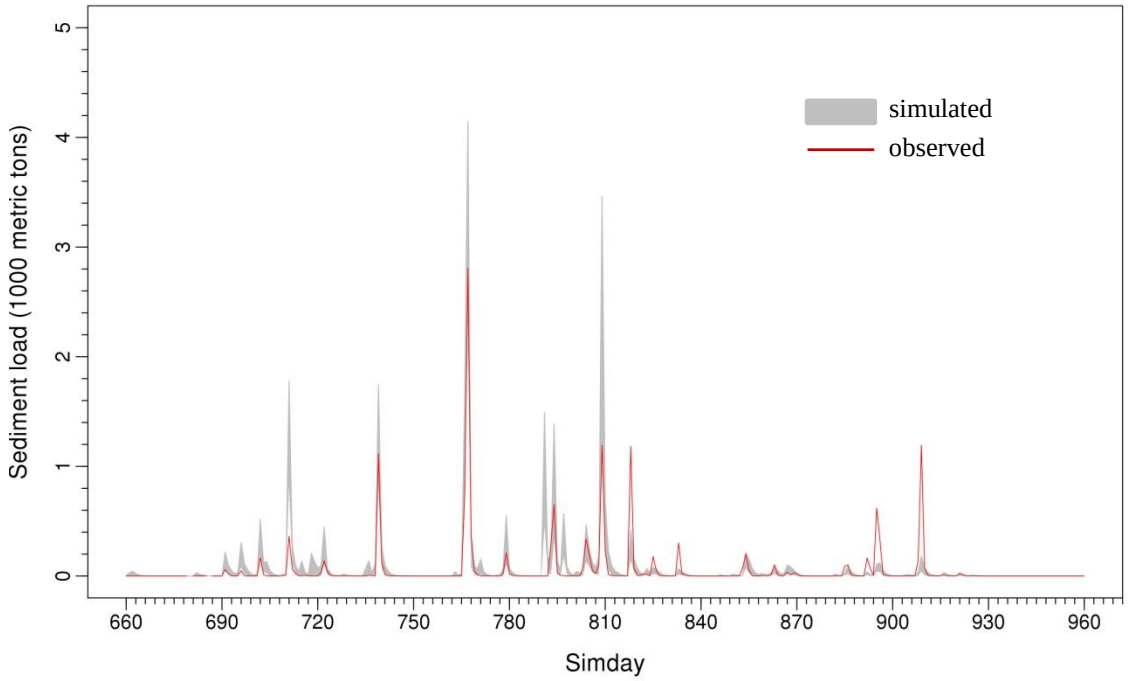

Figure A3.4. Simulated vs. sediment load in Rock Creek with in-stream processing. Simday1 = January 01, 2006.

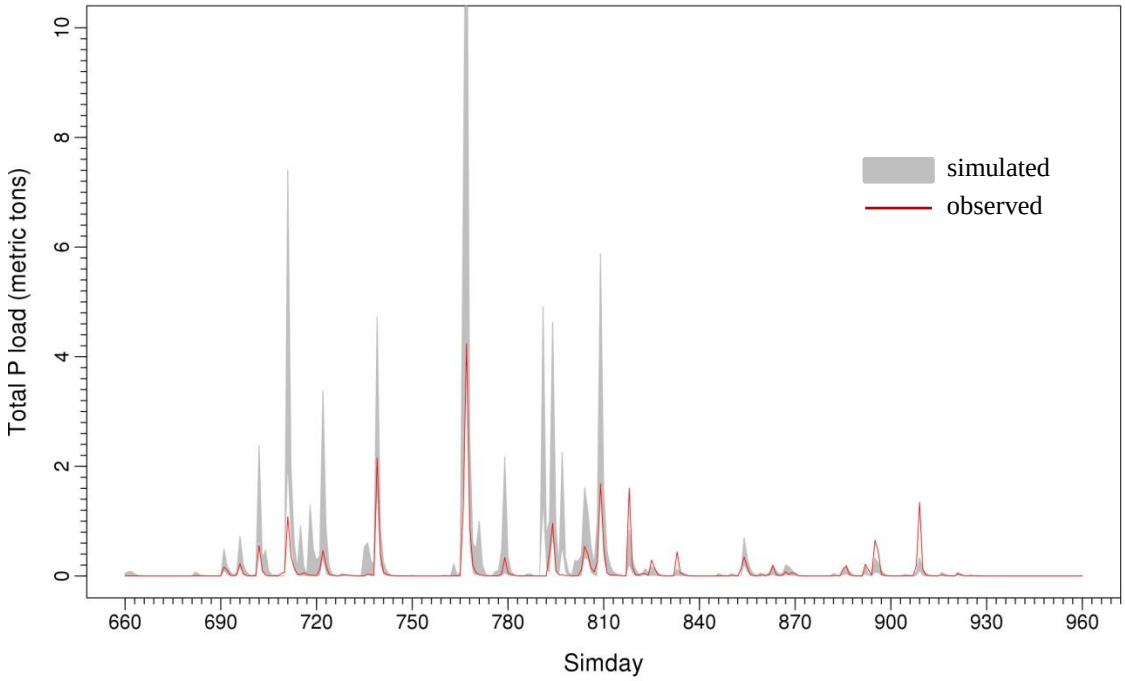

Figure A3.5. Simulated vs. total P load in Rock Creek without in-stream processing. Simday1 = January 01, 2006.

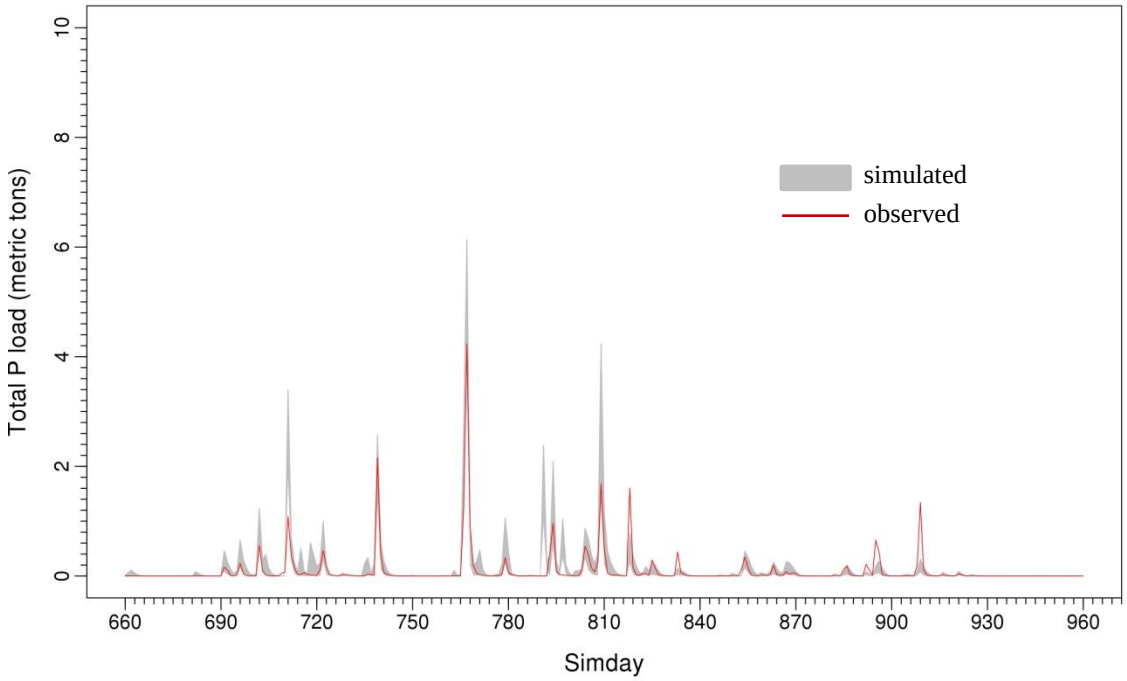

Figure A3.6. Simulated vs. total P load in Rock Creek with in-stream processing. Simday1 = January 01, 2006.

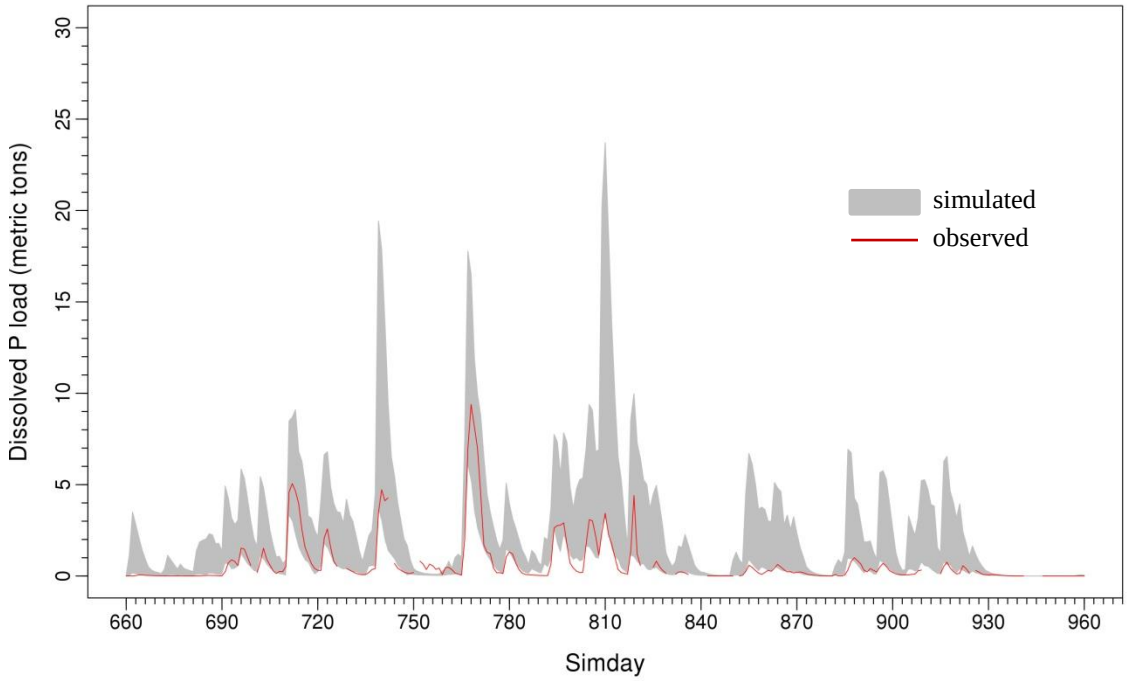

Figure A3.7. Simulated vs. dissolved P load in Rock Creek without in-stream processing. Simday1 = January 01, 2006.

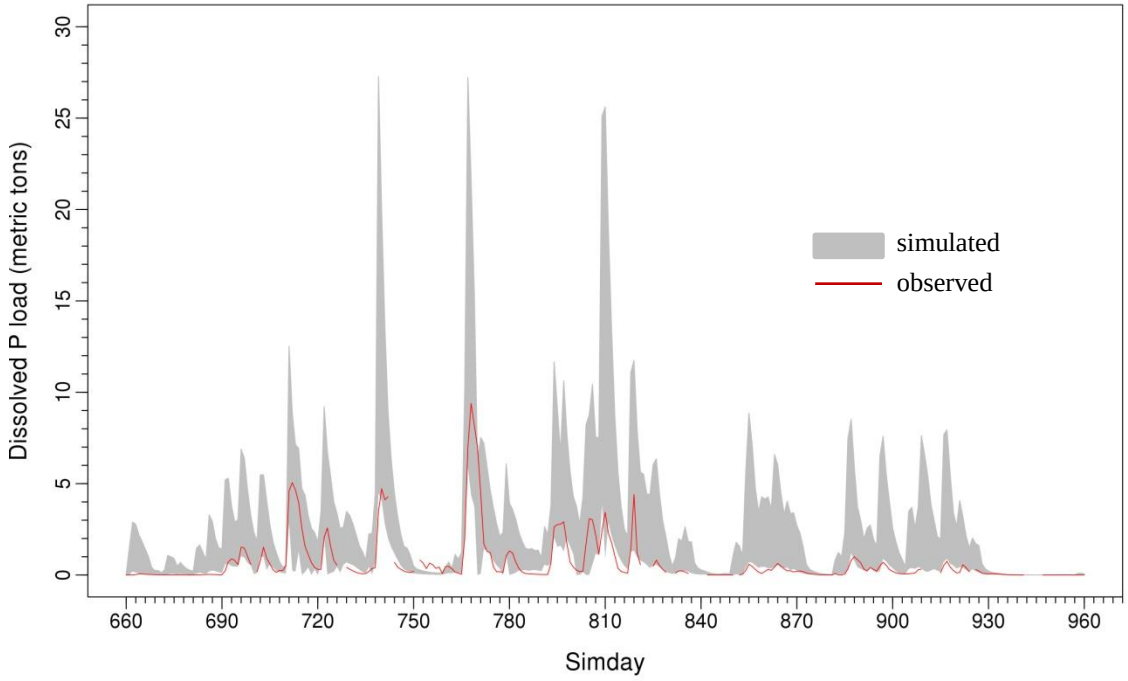

Figure A3.8. Simulated vs. dissolved P load in Rock Creek with in-stream processing. Simday1 = January 01, 2006.

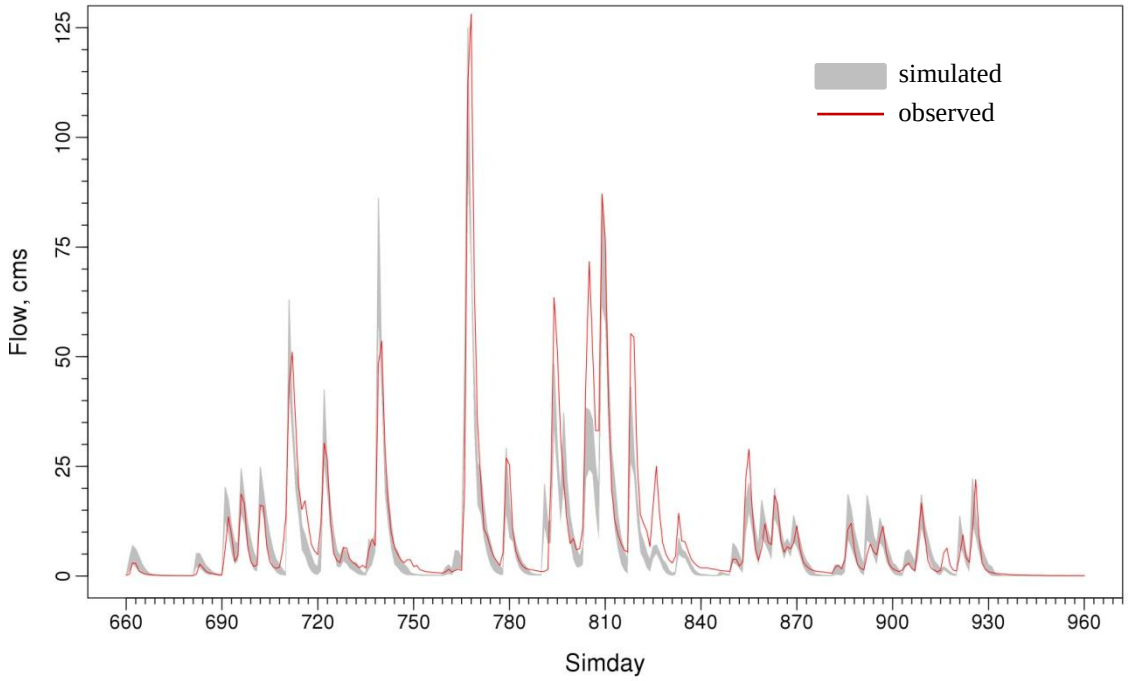

Figure A3.9. Simulated vs. observed flow in Honey Creek without in-stream processing. Simday1 = January 01, 2006.

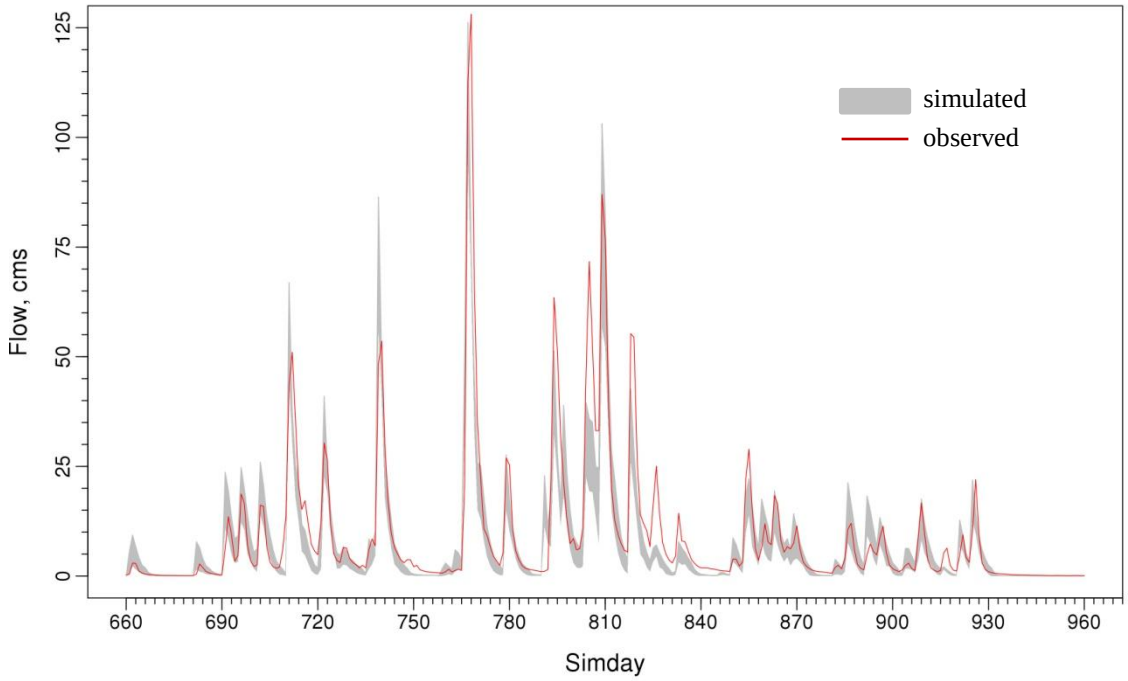

Figure A3.10. Simulated vs. observed flow in Honey Creek with in-stream processing. Simday1 = January 01, 2006.

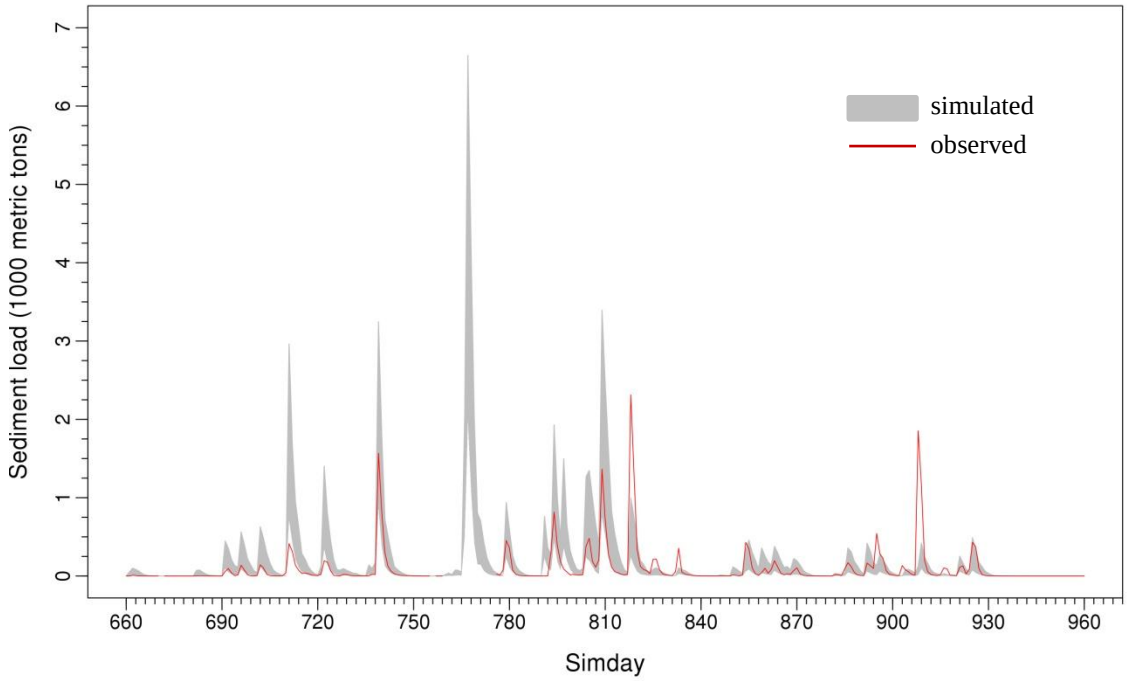

Figure A3.11. Simulated vs. observed sediment load in Honey Creek without in-stream processing. Simday1 = January 01, 2006.

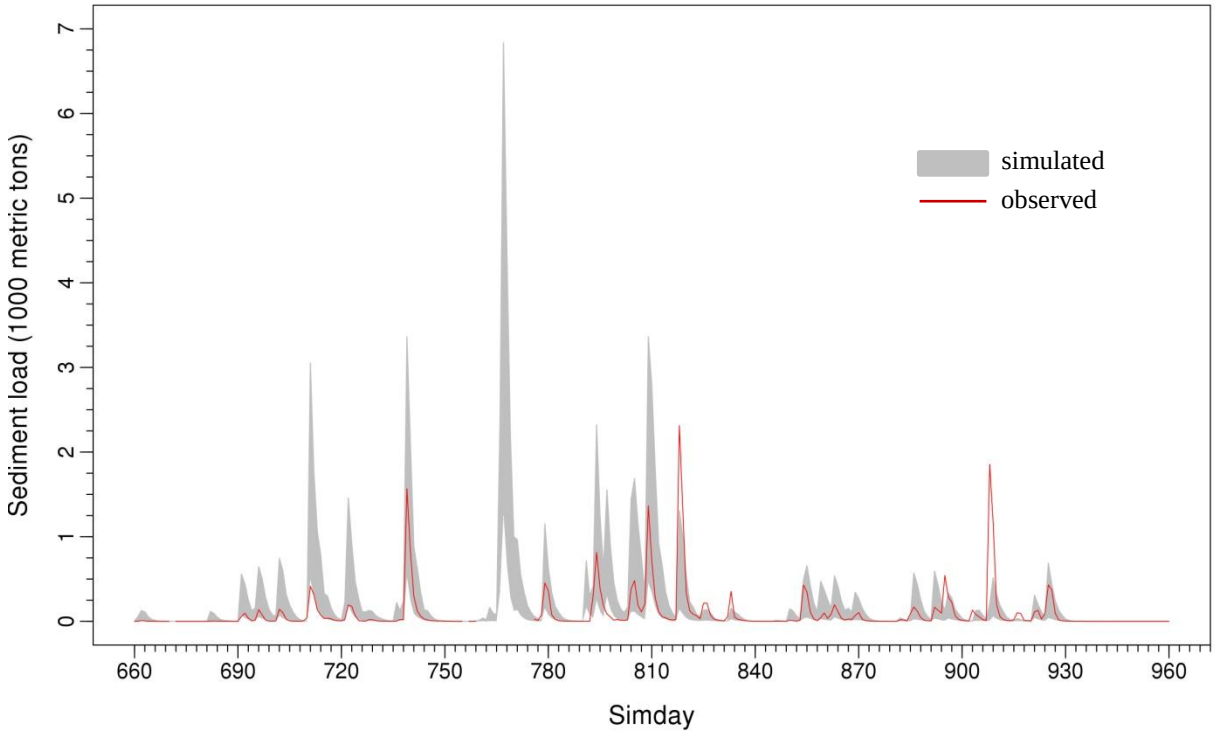

Figure A3.12. Simulated vs. observed sediment load in Honey Creek with in-stream processing. Simday1 = January 01, 2006.

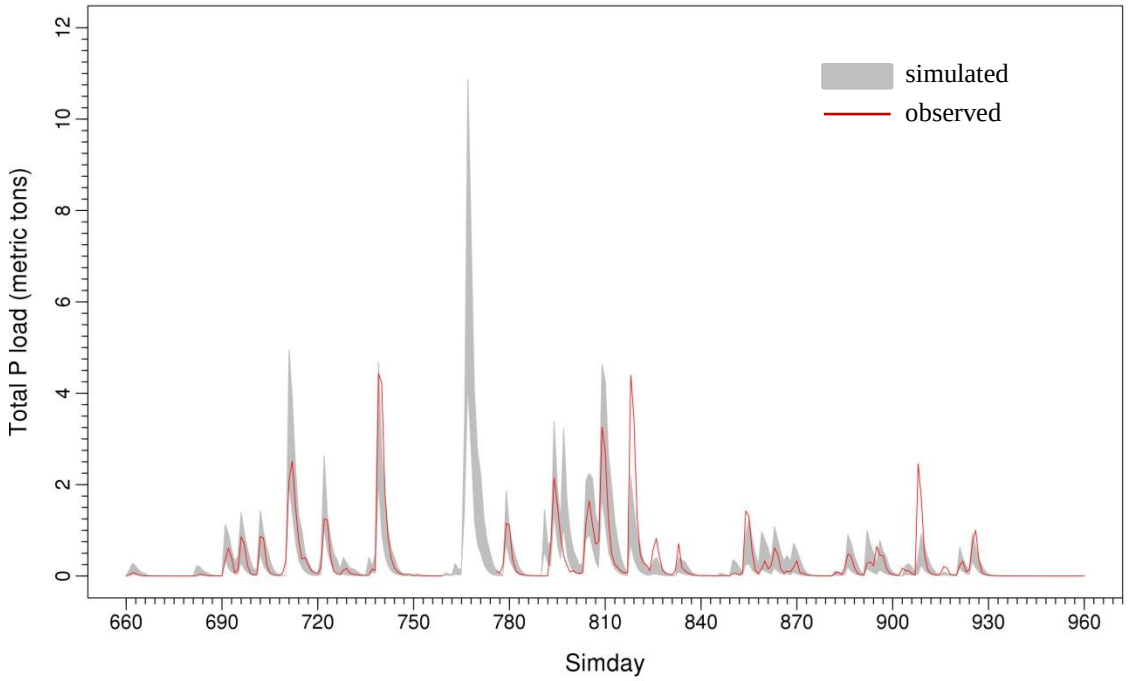

Figure A3.13. Simulated vs. observed total P load in Honey Creek without in-stream processing. Simday1 = January 01, 2006.

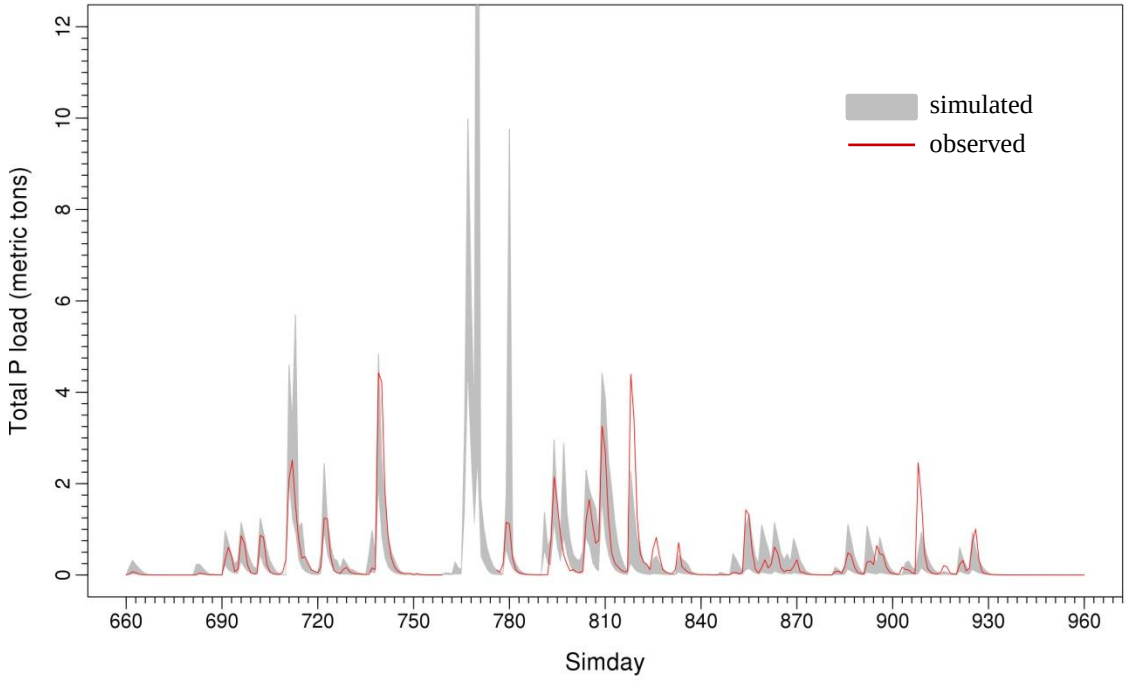

Figure A3.14. Simulated vs. observed total P load in Honey Creek with in-stream processing. Simday1 = January 01, 2006.

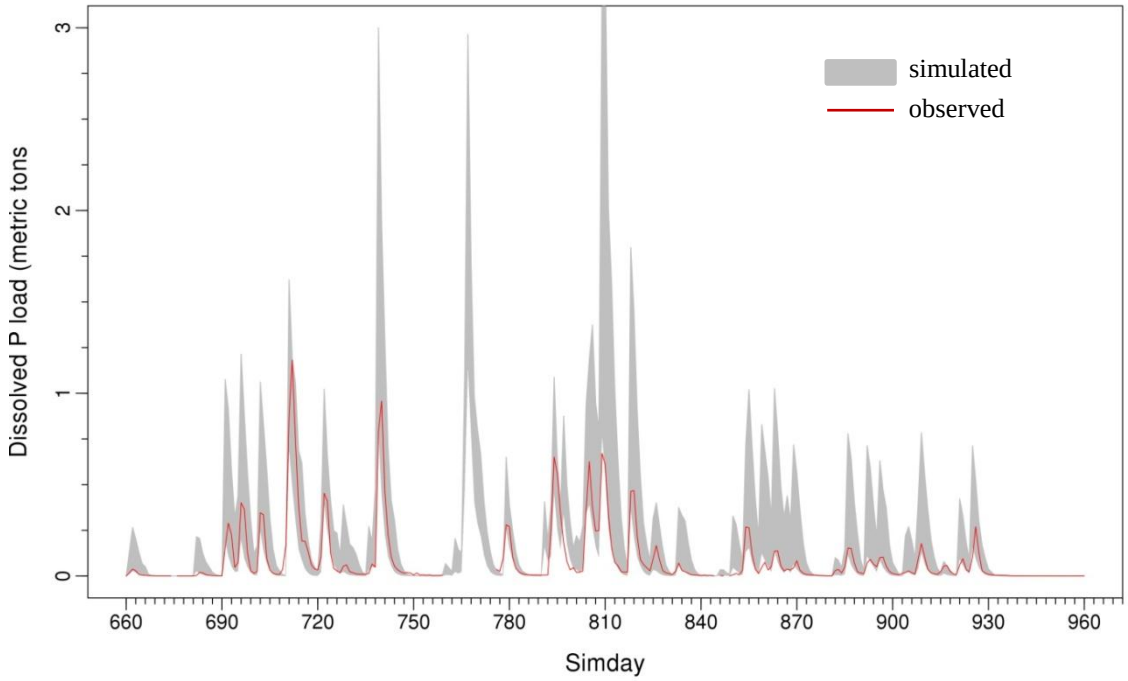

Figure A3.15. Simulated vs. observed dissolved P load in Honey Creek without in-stream processing. Simday1 = January 01, 2006.

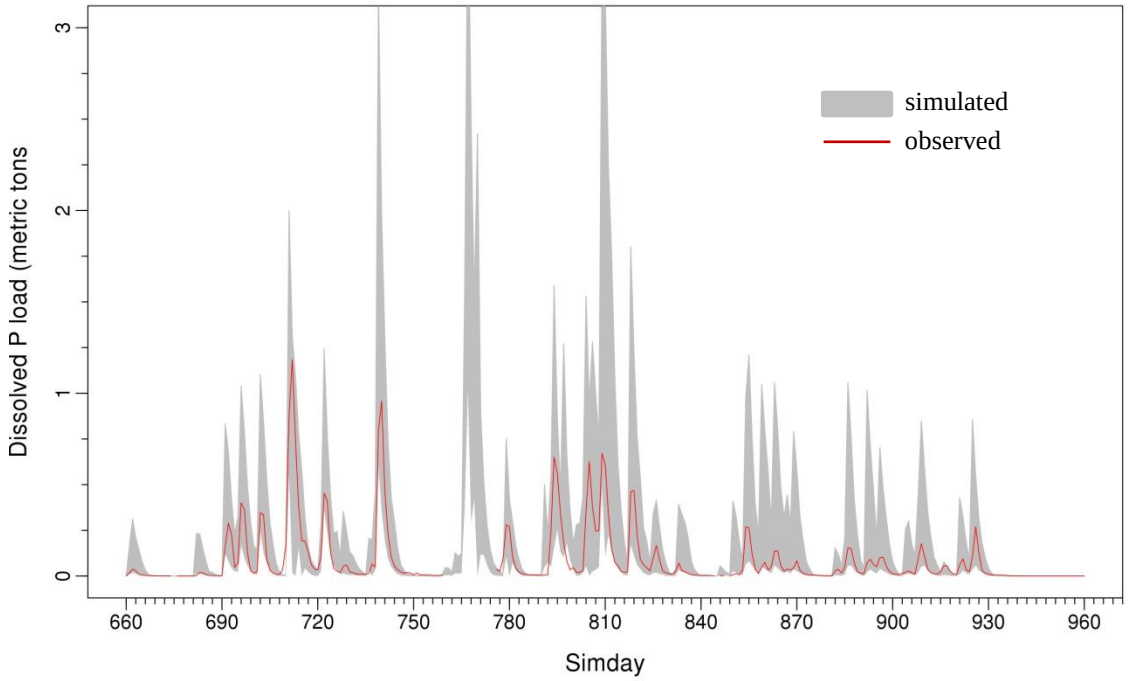

Figure A3.16. Simulated vs. observed dissolved P load in Honey Creek with in-stream processing. Simday1 = January 01, 2006.

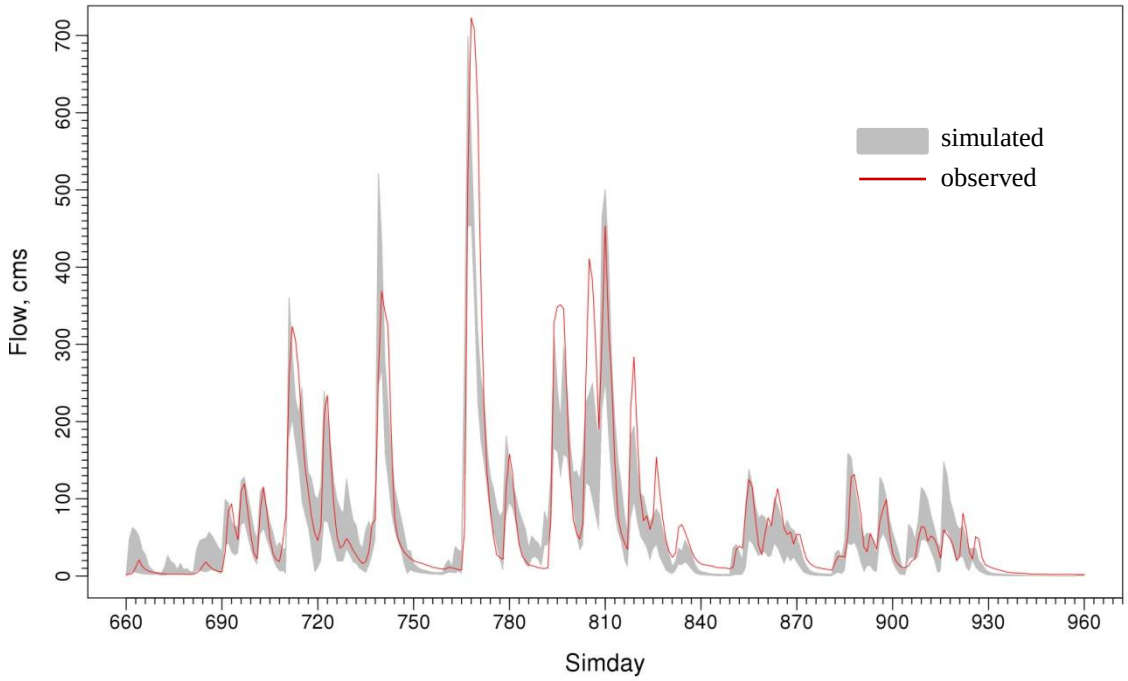

Figure A3.17. Simulated vs. observed flow in Sandusky without in-stream processing. Simday1 = January 01, 2006.

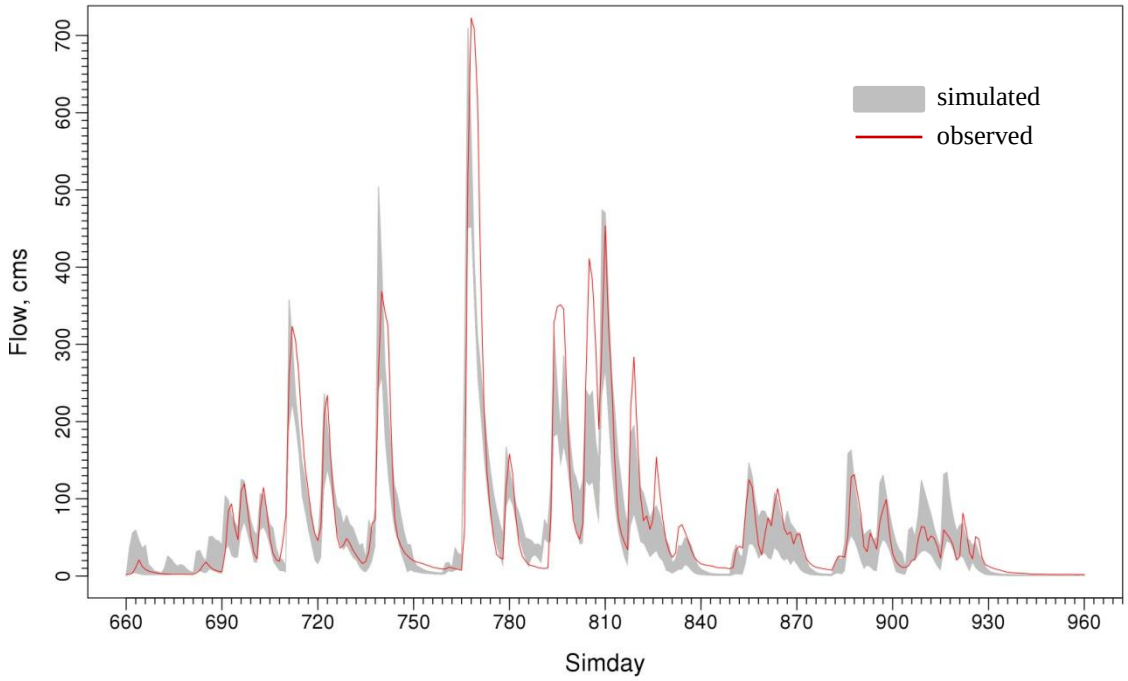

Figure A3.18. Simulated vs. observed flow in Sandusky with in-stream processing. Simday1 = January 01, 2006.

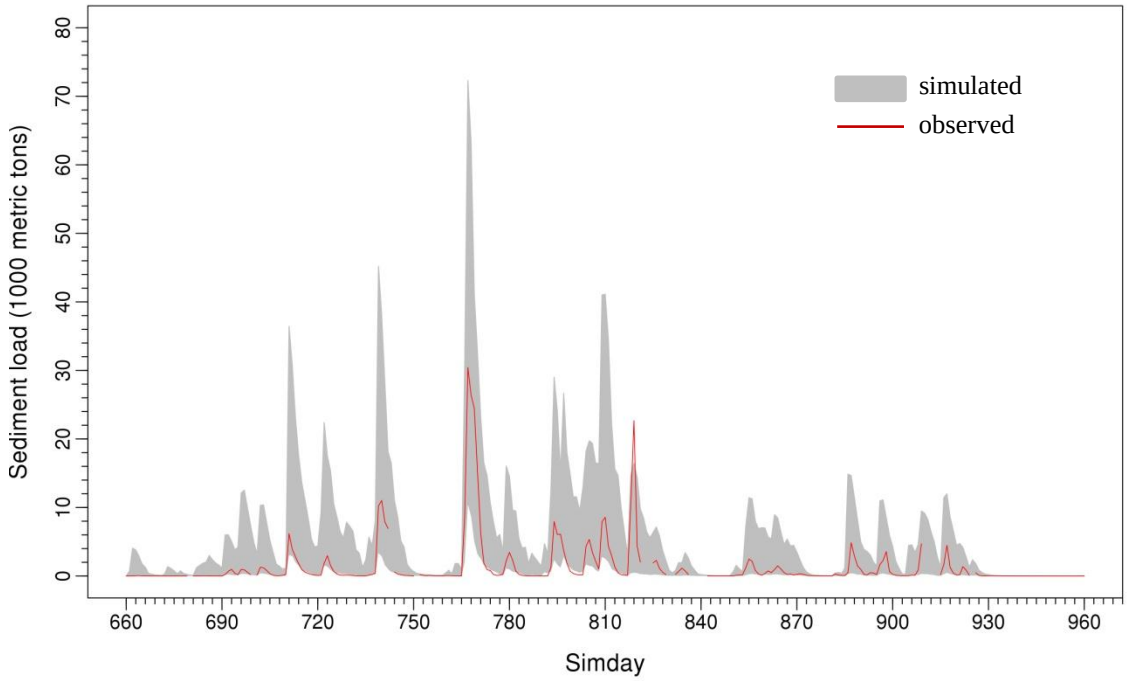

Figure A3.19. Simulated vs. observed sediment load in Sandusky without in-stream processing. Simday1 = January 01, 2006.

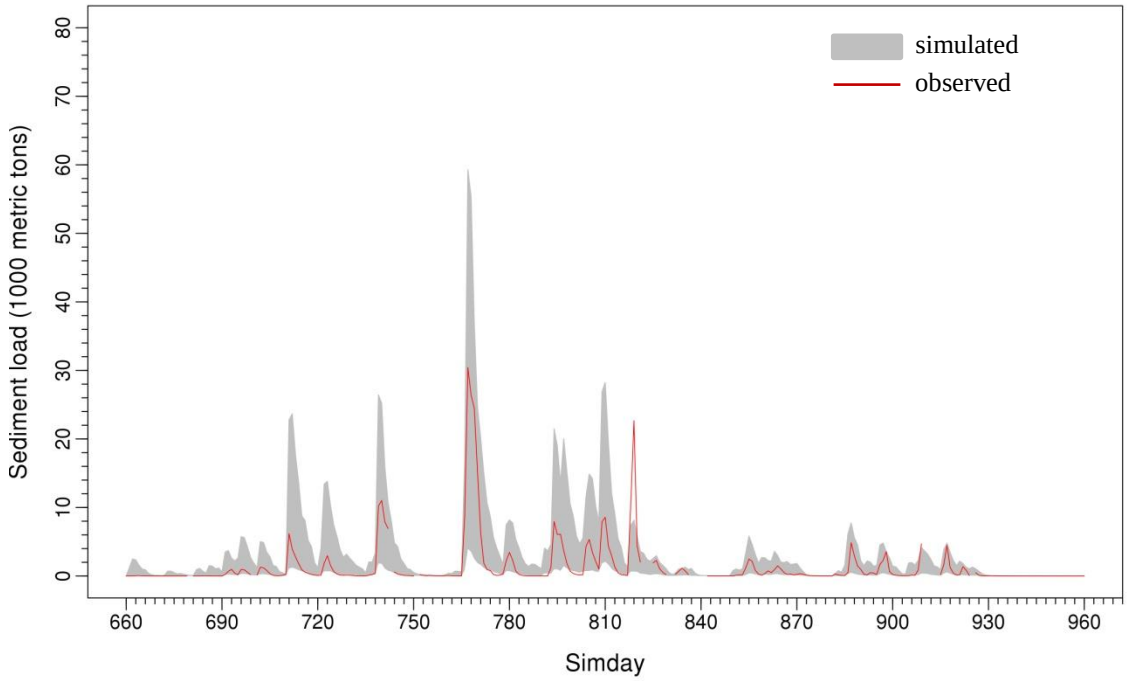

Figure A3.20. Simulated vs. observed sediment load in Sandusky with in-stream processing. Simday1 = January 01, 2006.

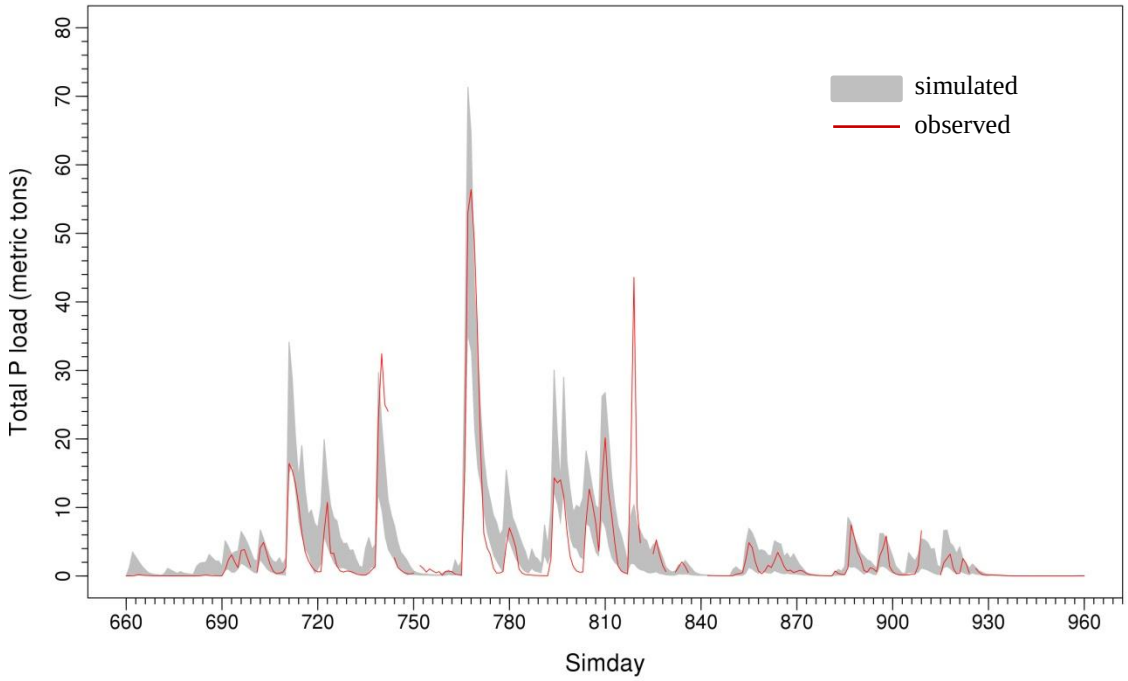

Figure A3.21. Simulated vs. observed total P load in Sandusky without in-stream processing. Simday1 = January 01, 2006.

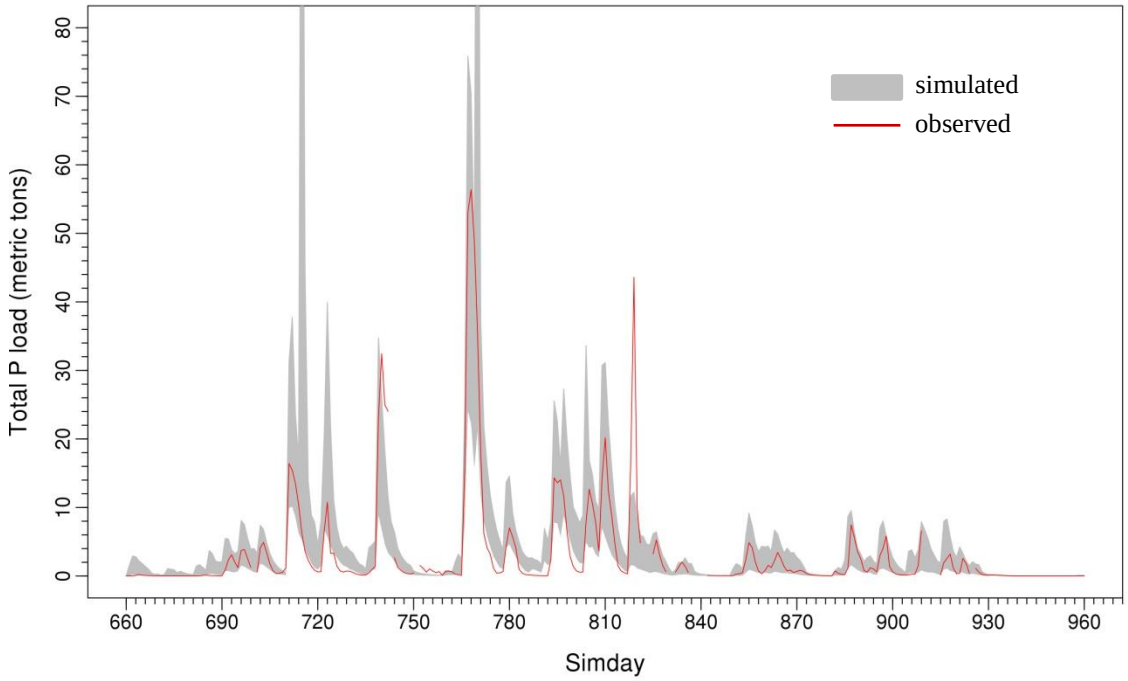

Figure A3.22. Simulated vs. observed total P load in Sandusky with in-stream processing. Simday1 = January 01, 2006.

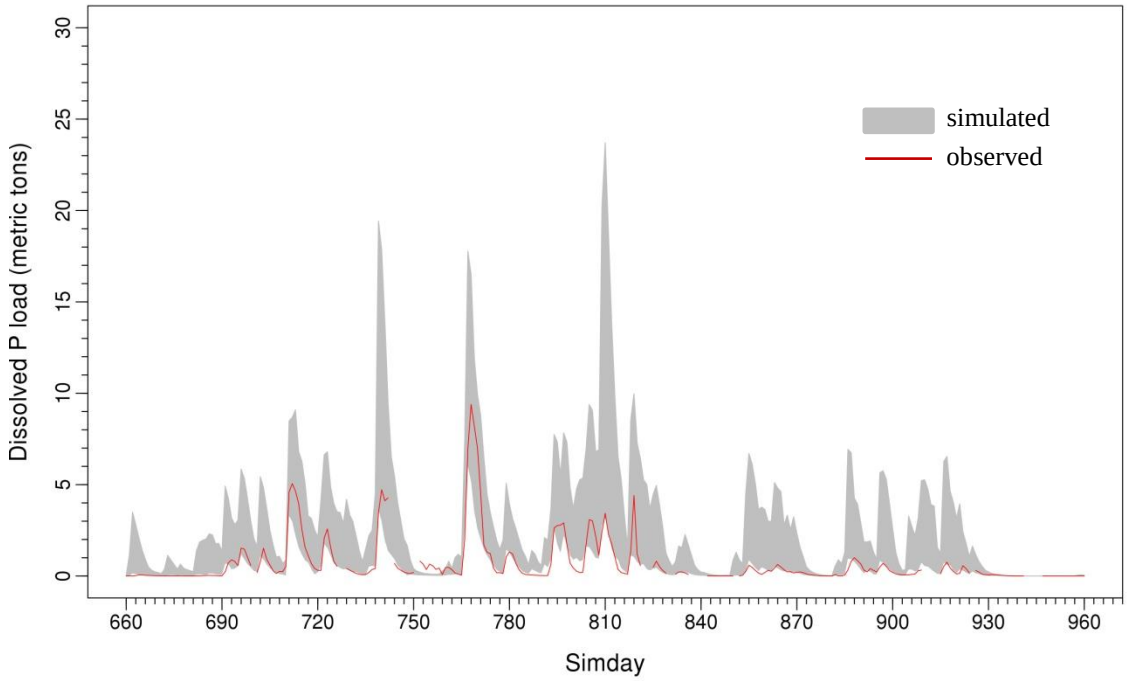

Figure A3.23. Simulated vs. observed dissolved P load in Sandusky without in-stream processing. Simday1 = January 01, 2006.

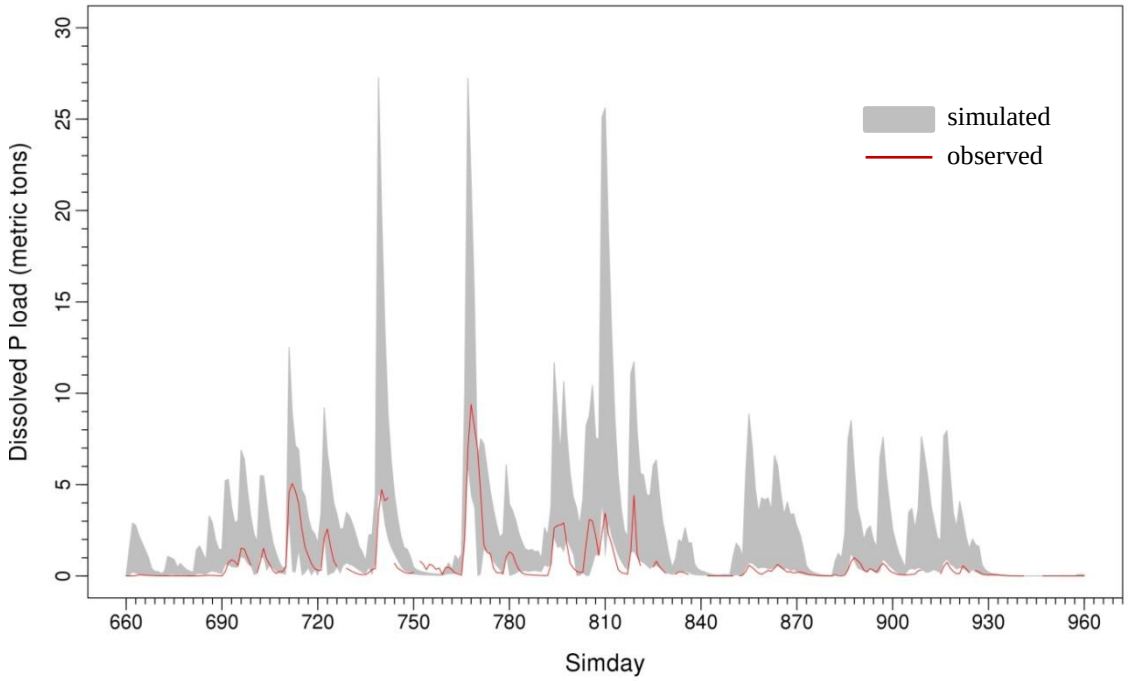

Figure A3.24. Simulated vs. observed dissolved P load in Sandusky with in-stream processing. Simday1 = January 01, 2006.

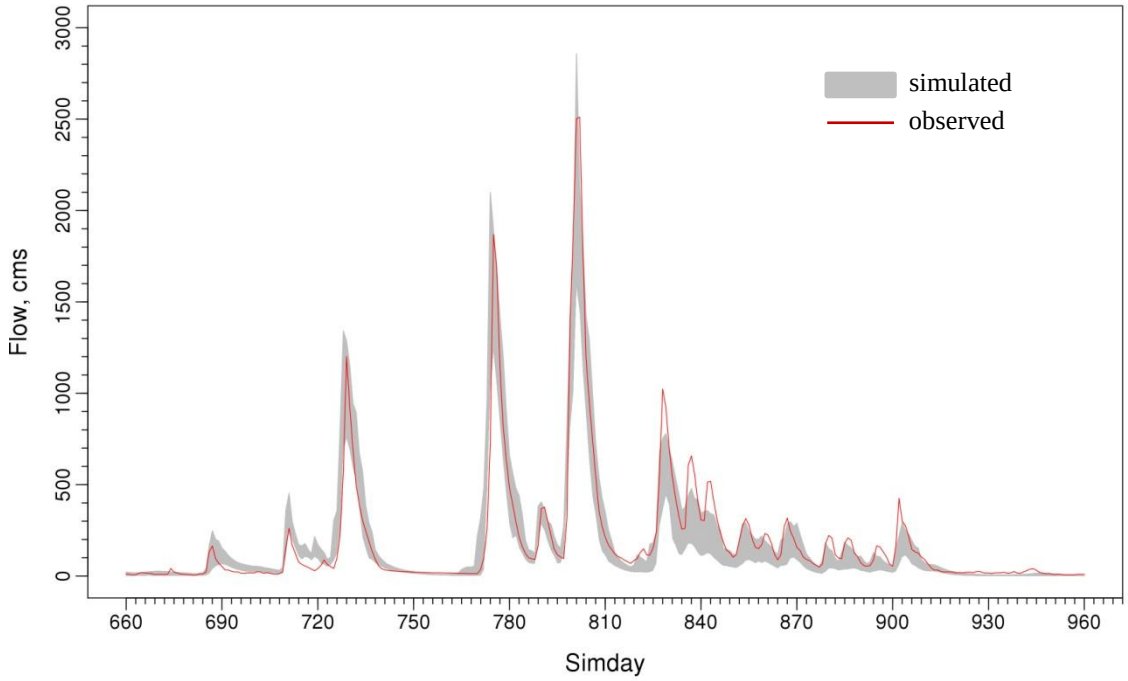

Figure A3.25. Simulated vs. observed flow in Maumee without in-stream processing. Simday1 = January 01, 2006.

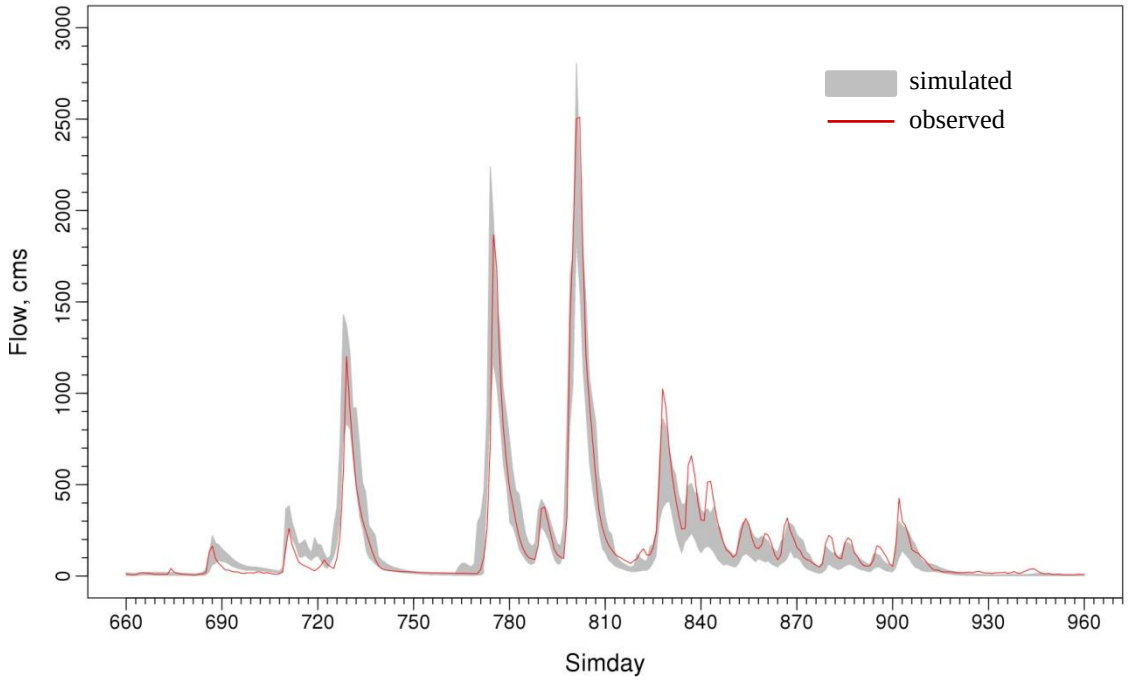

Figure A3.26. Simulated vs. observed flow in Maumee with in-stream processing. Simday1 = January 01, 2006.

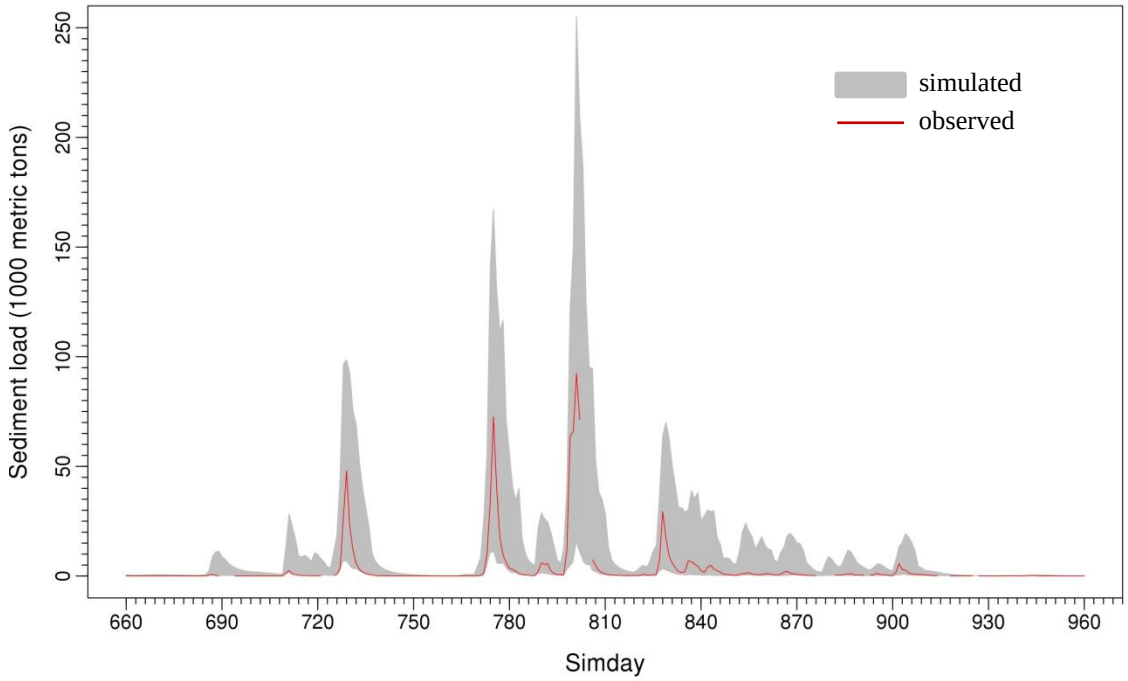

Figure A3.27. Simulated vs. observed sediment load in Maumee without in-stream processing. Simday1 = January 01, 2006.

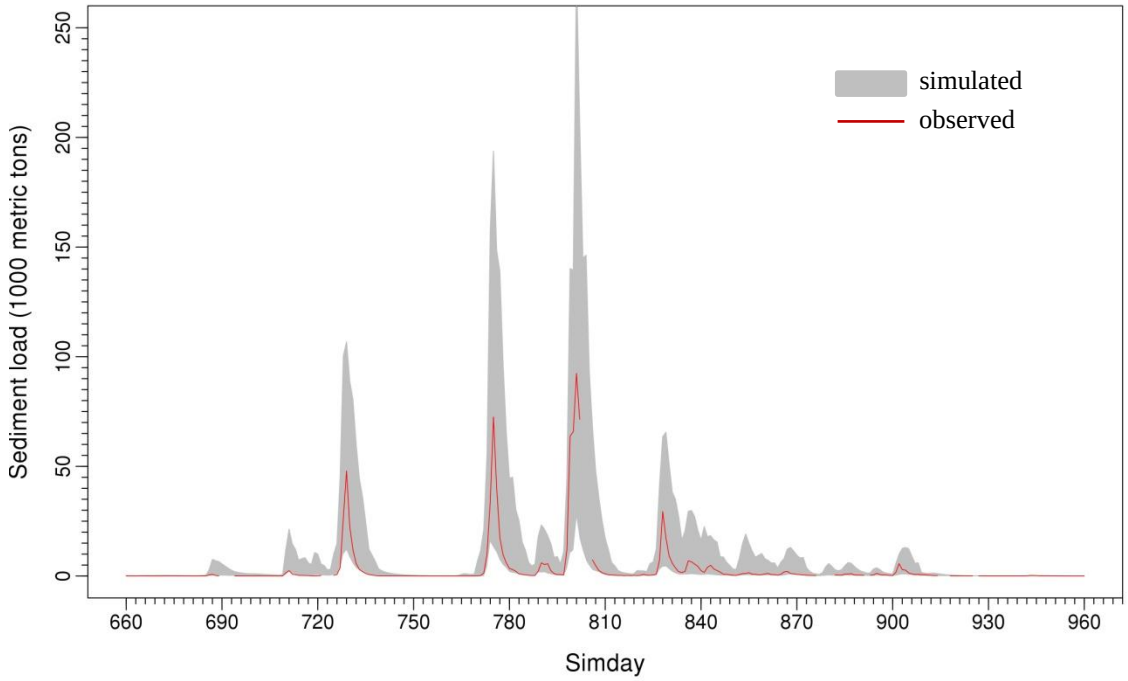

Figure A3.28. Simulated vs. observed sediment load in Maumee with in-stream processing. Simday1 = January 01, 2006.

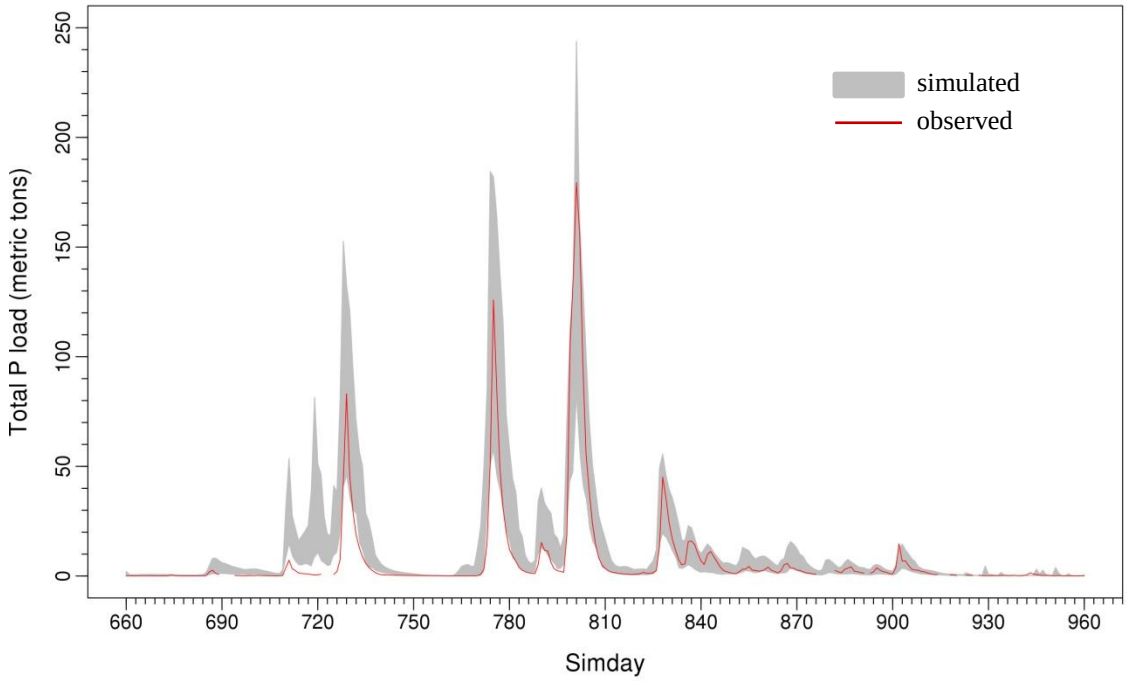

Figure A3.29. Simulated vs. observed total P load in Maumee without in-stream processing. Simday1 = January 01, 2006.

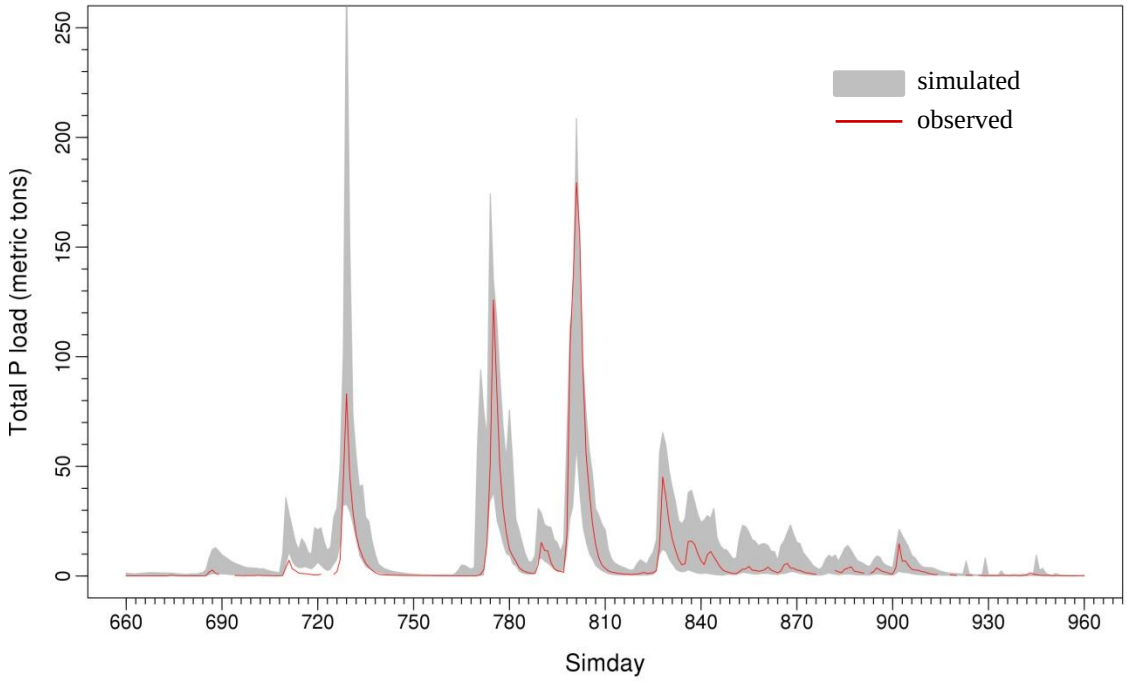

Figure A3.30. Simulated vs. observed total P load in Maumee with in-stream processing. Simday1 = January 01, 2006.

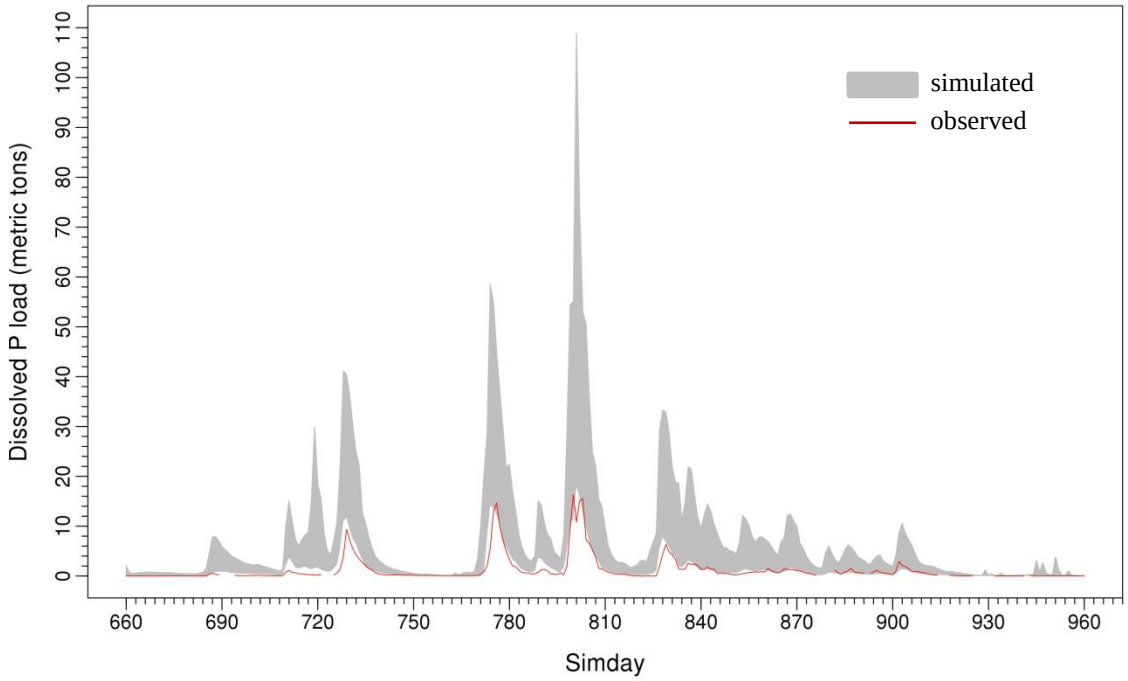

Figure A3.31. Simulated vs. observed dissolved P load in Maumee without in-stream processing. Simday1 = January 01, 2006.

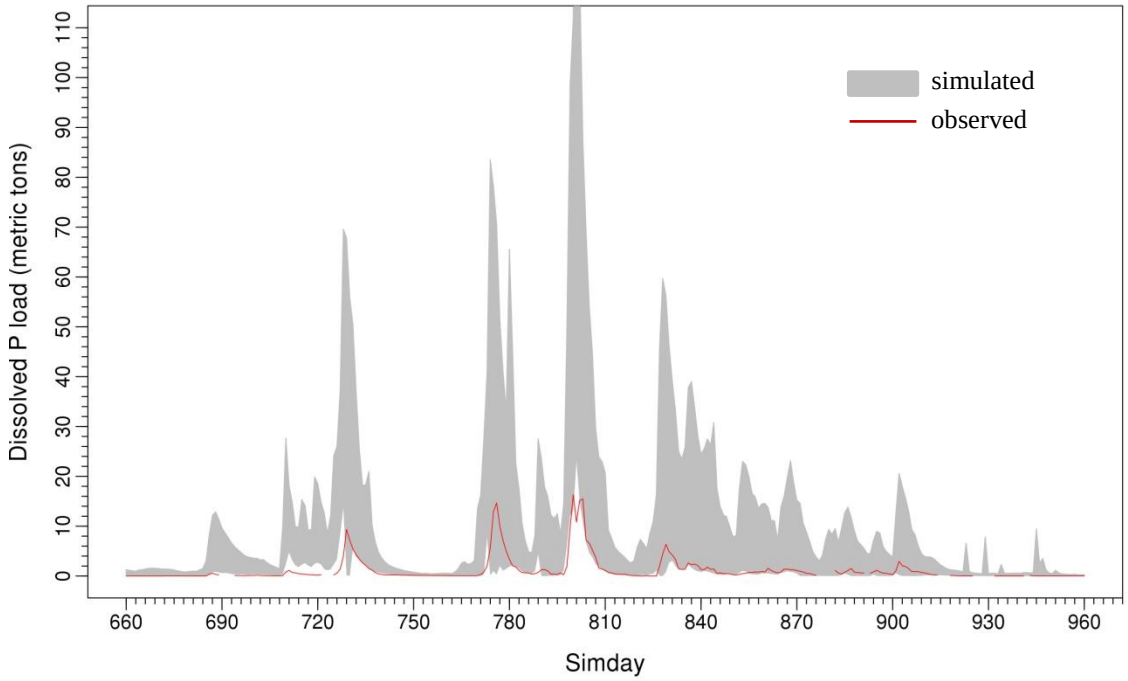

Figure A3.32. Simulated vs. observed dissolved P load in Maumee with in-stream processing. Simday1 = January 01, 2006.

Appendix 4. Validation graph results

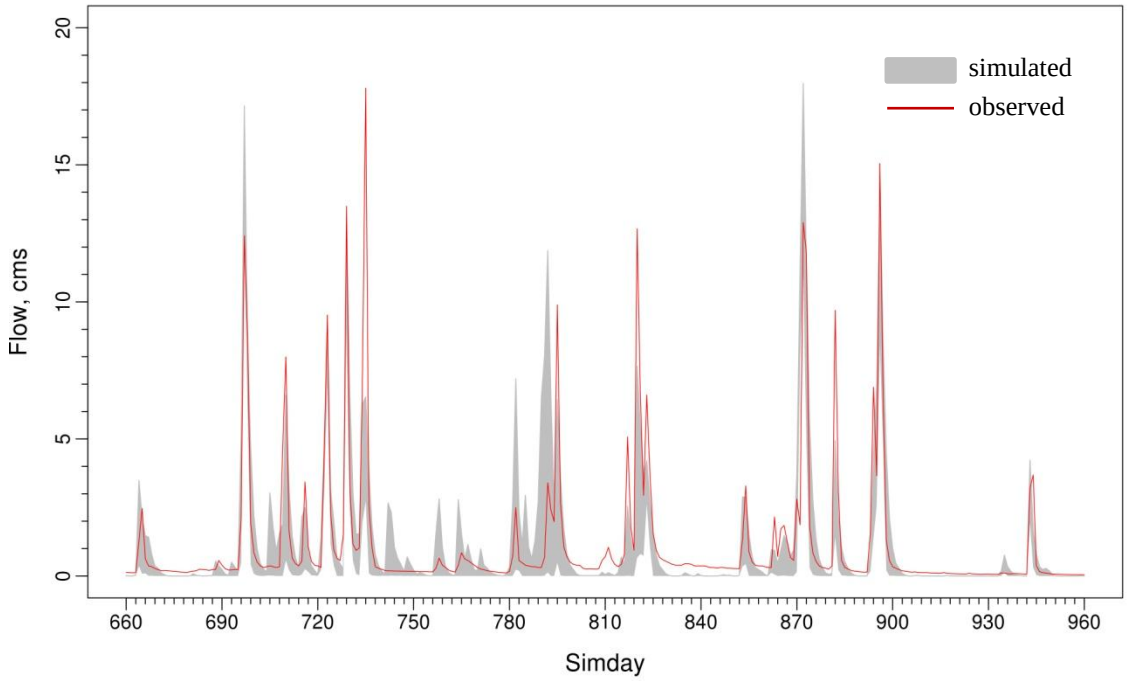

Figure A4.1. Simulated vs. observed flow in Rock Creek without in-stream processing. Simday1 = January 01, 2002.

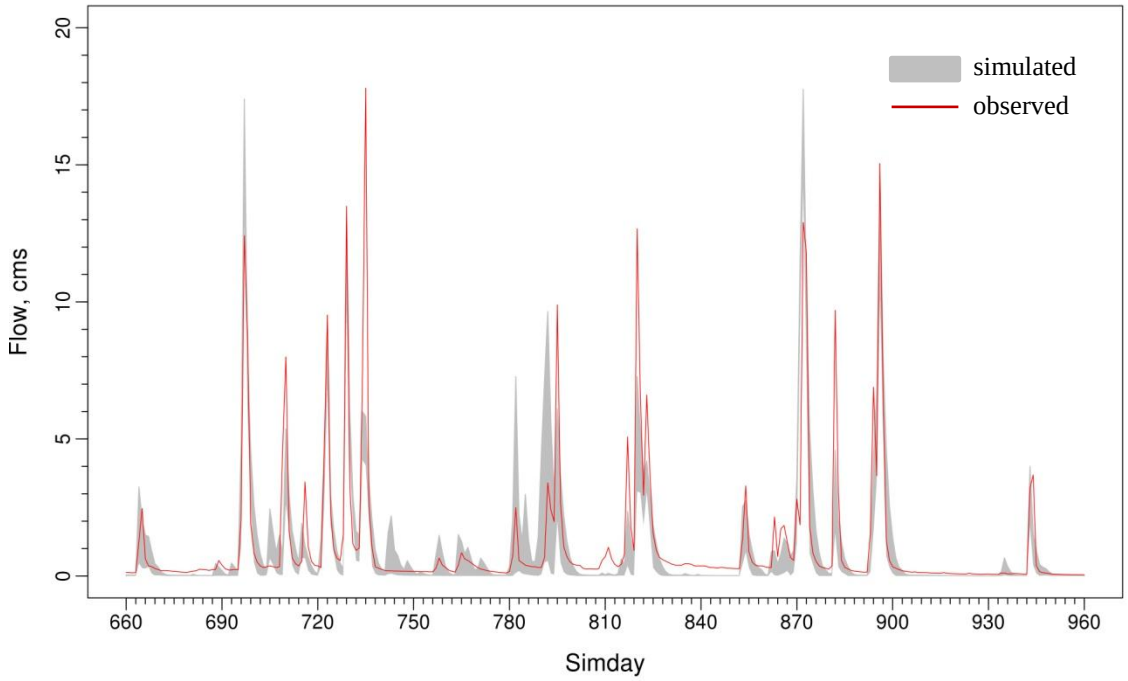

Figure A4.2. Simulated vs. observed flow in Rock Creek with in-stream processing. Simday1 = January 01, 2002.

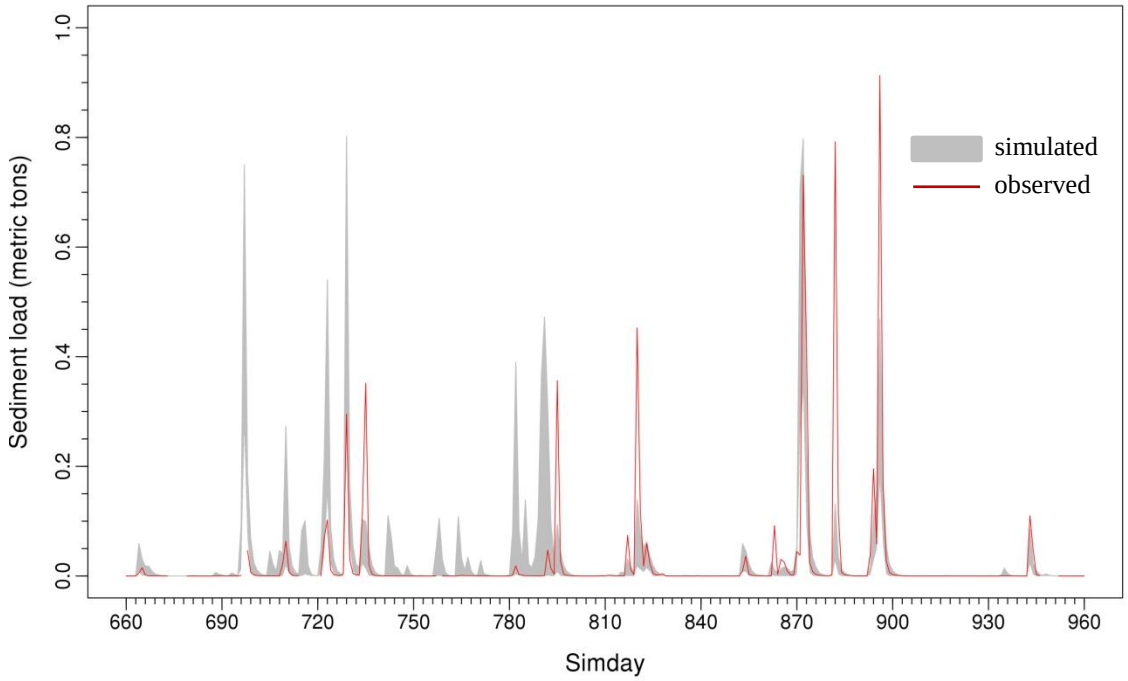

Figure A4.3. Simulated vs. sediment load in Rock Creek without in-stream processing. Simday1 = January 01, 2002.

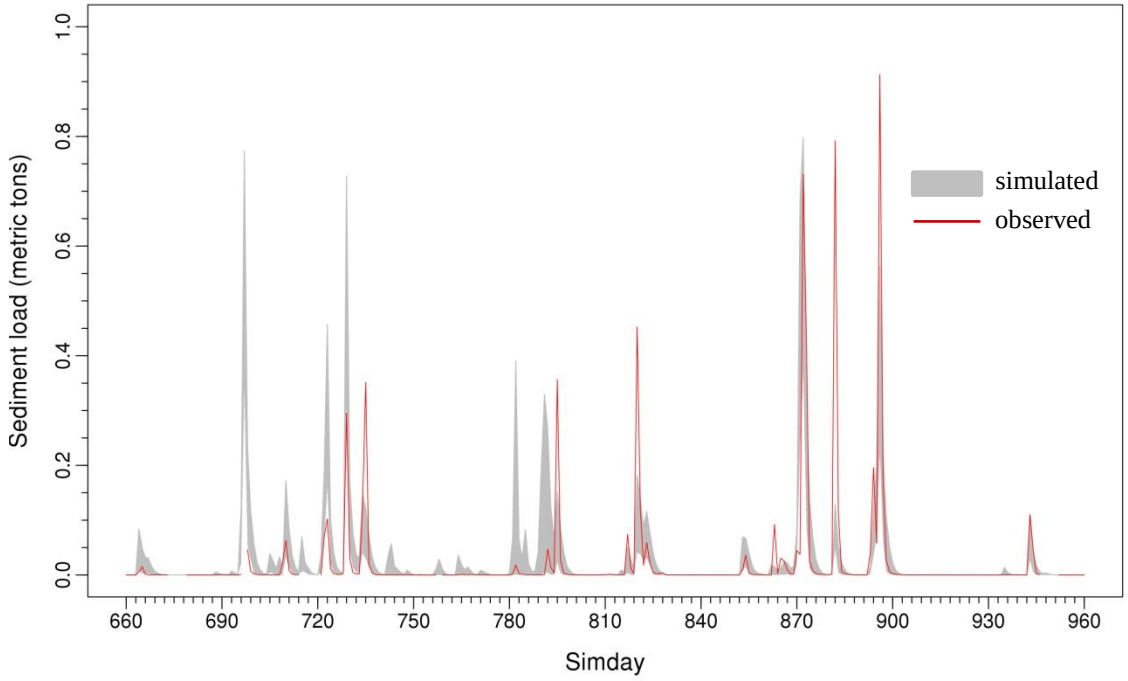

Figure A4.4. Simulated vs. sediment load in Rock Creek with in-stream processing. Simday1 = January 01, 2002.

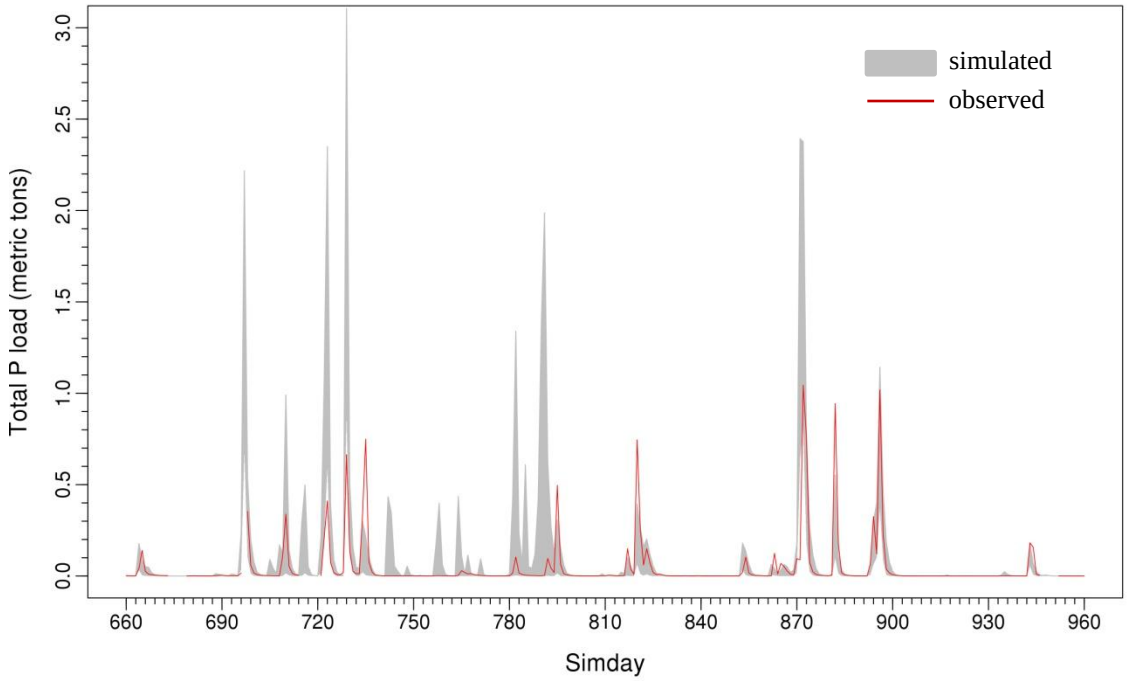

Figure A4.5. Simulated vs. total P load in Rock Creek without in-stream processing. Simday1 = January 01, 2002.

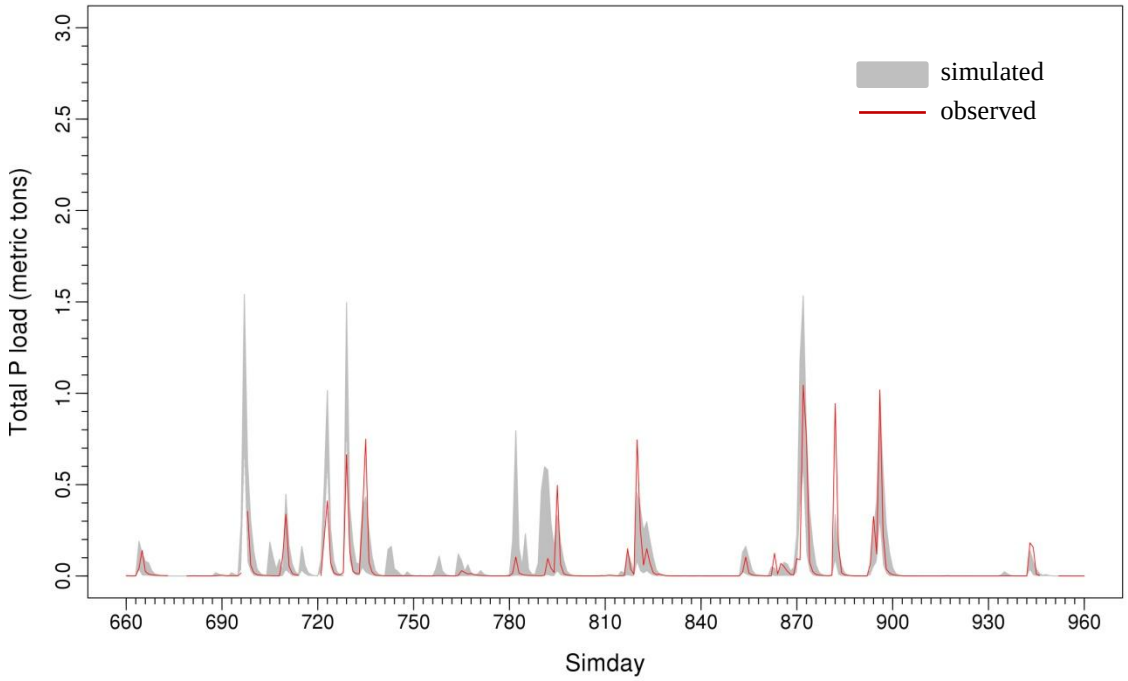

Figure A4.6. Simulated vs. total P load in Rock Creek with in-stream processing. Simday1 = January 01, 2002.

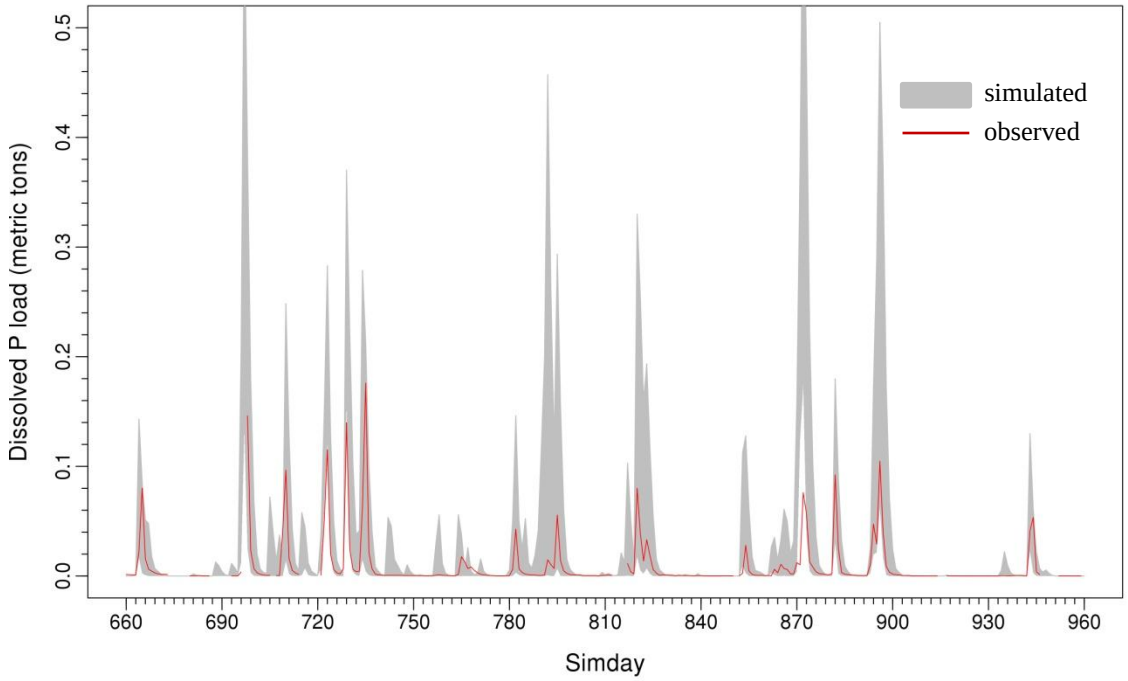

Figure A4.7. Simulated vs. dissolved P load in Rock Creek without in-stream processing. Simday1 = January 01, 2002.

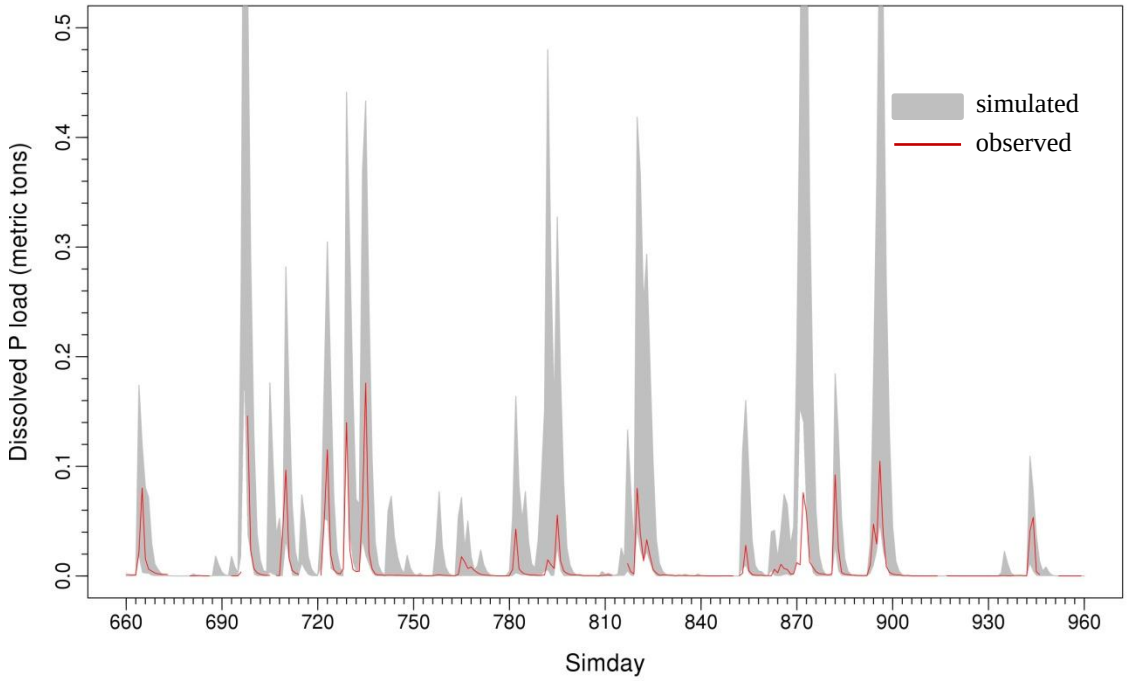

Figure A4.8. Simulated vs. dissolved P load in Rock Creek with in-stream processing. Simday1 = January 01, 2002.

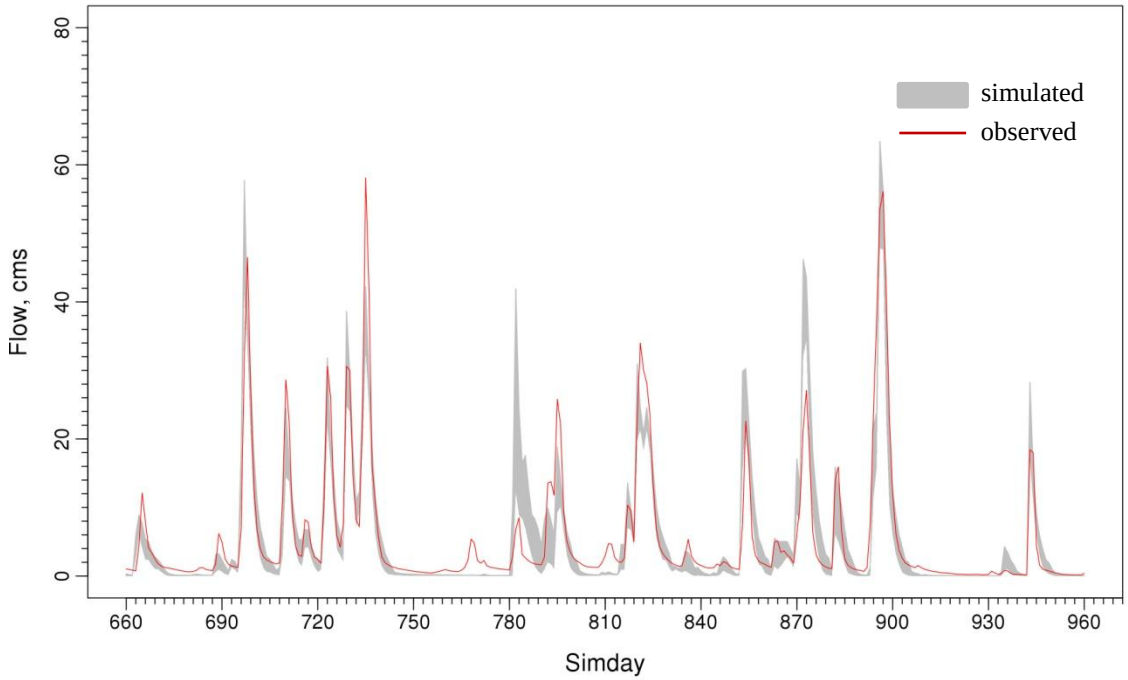

Figure A4.9. Simulated vs. observed flow in Honey Creek without in-stream processing. Simday1 = January 01, 2002.

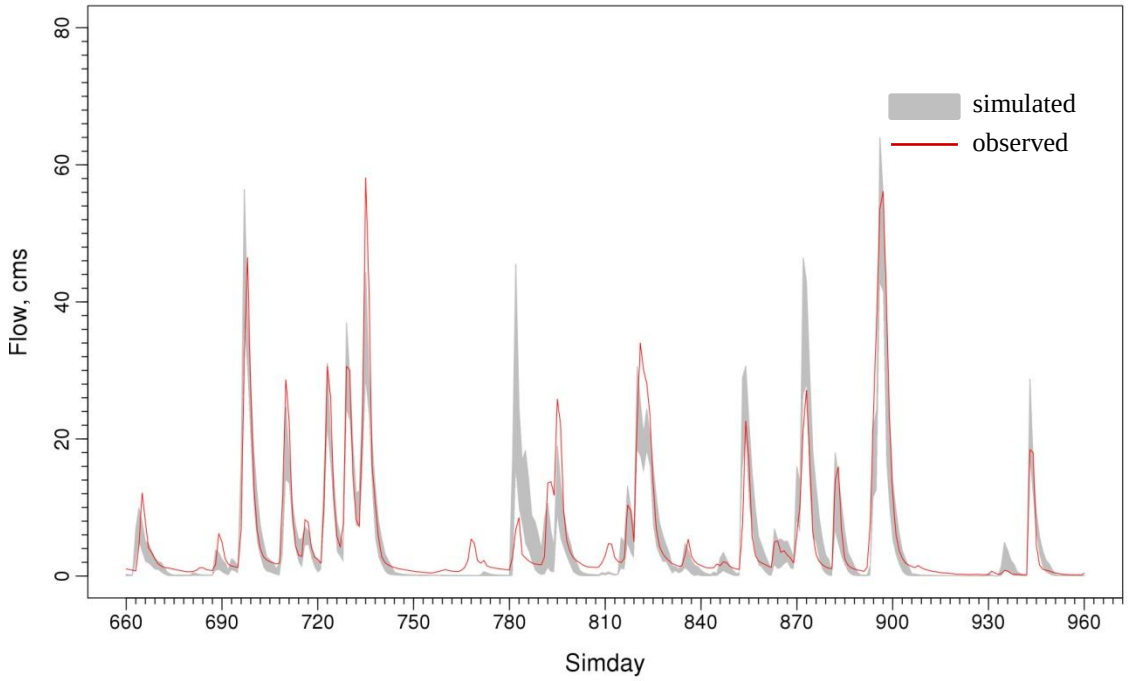

Figure A4.10. Simulated vs. observed flow in Honey Creek with in-stream processing. Simday1 = January 01, 2002.

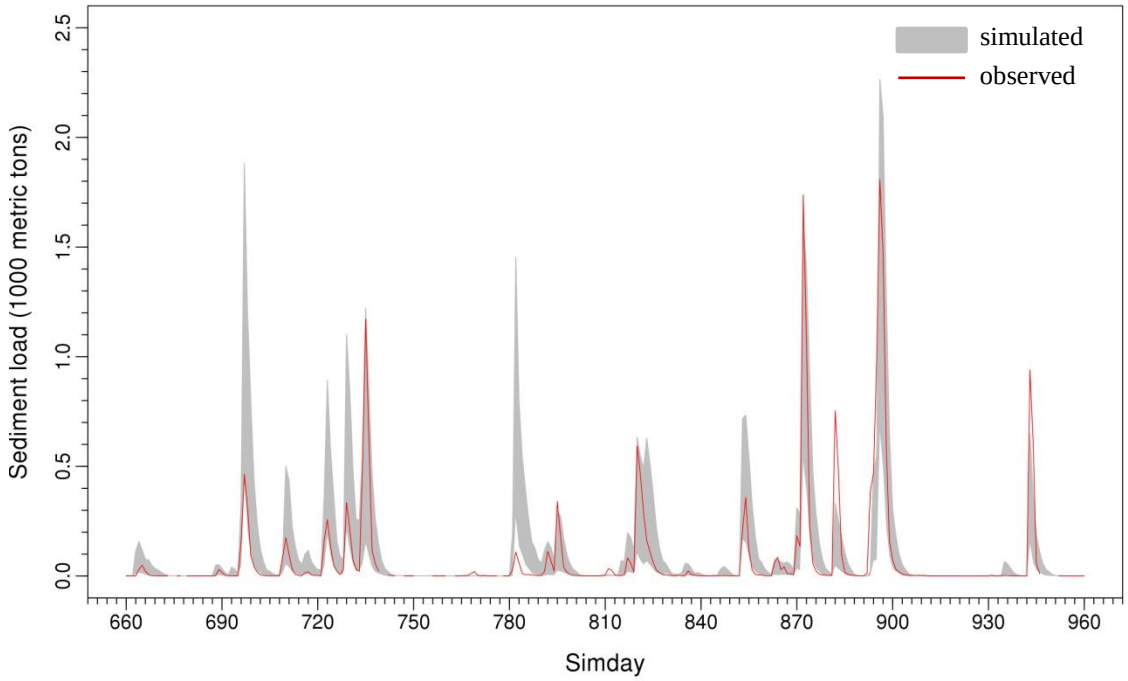

Figure A4.11. Simulated vs. observed sediment load in Honey Creek without in-stream processing. Simday1 = January 01, 2002.

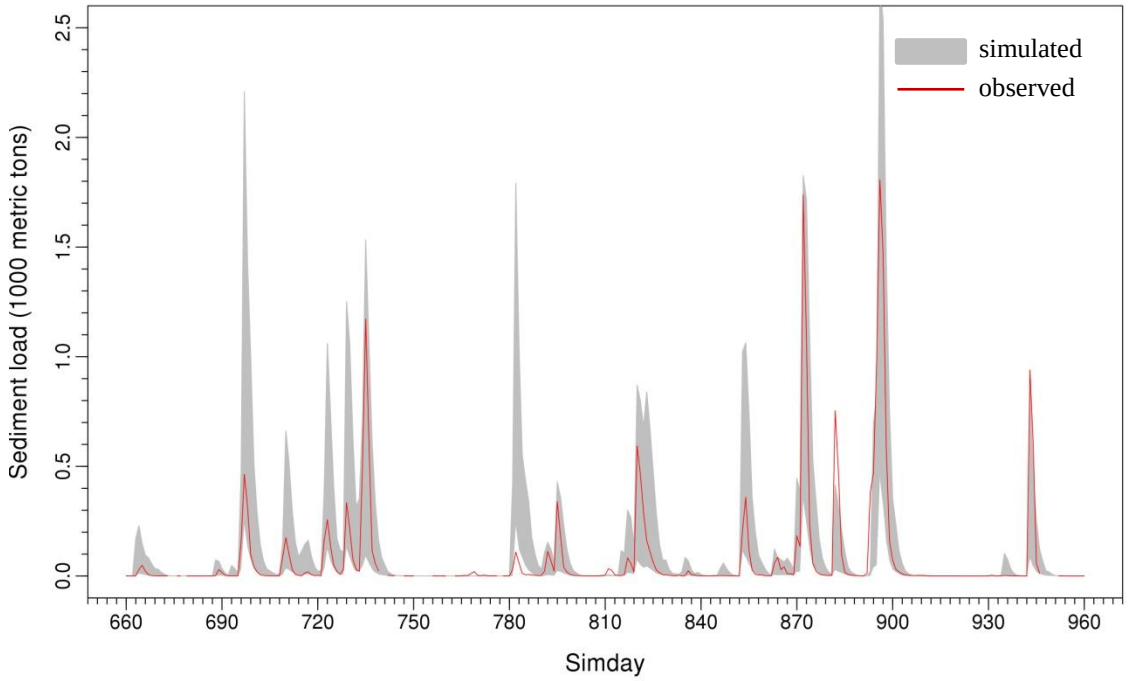

Figure A4.12. Simulated vs. observed sediment load in Honey Creek with in-stream processing. Simday1 = January 01, 2002.

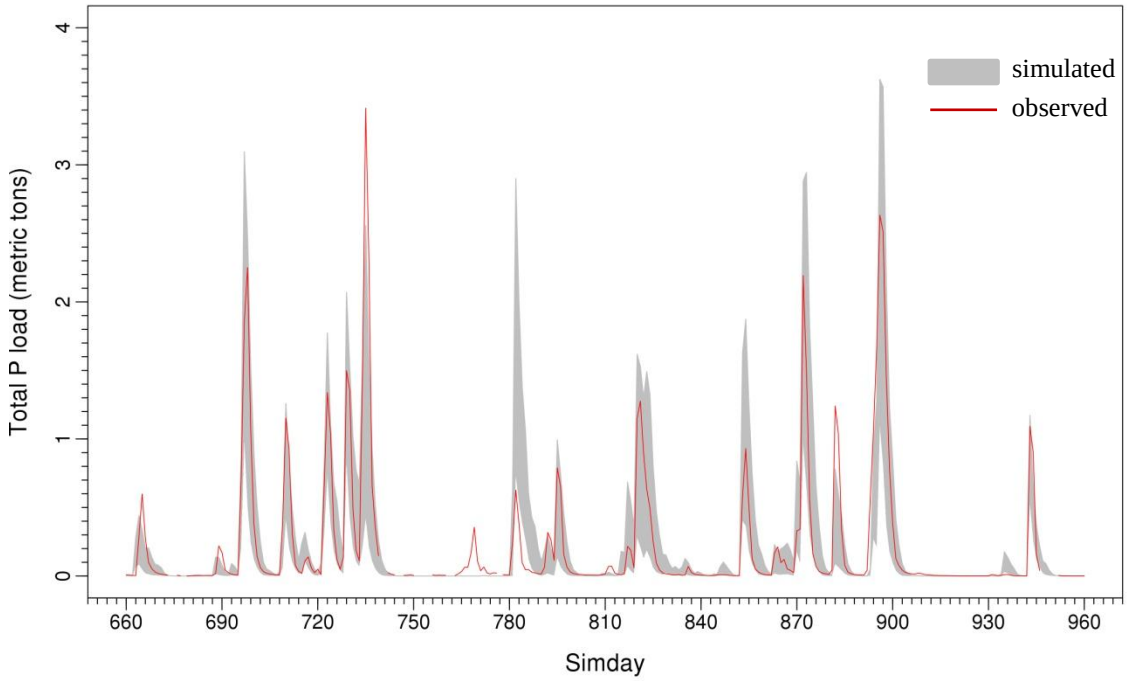

Figure A4.13. Simulated vs. observed total P load in Honey Creek without in-stream processing. Simday1 = January 01, 2002.

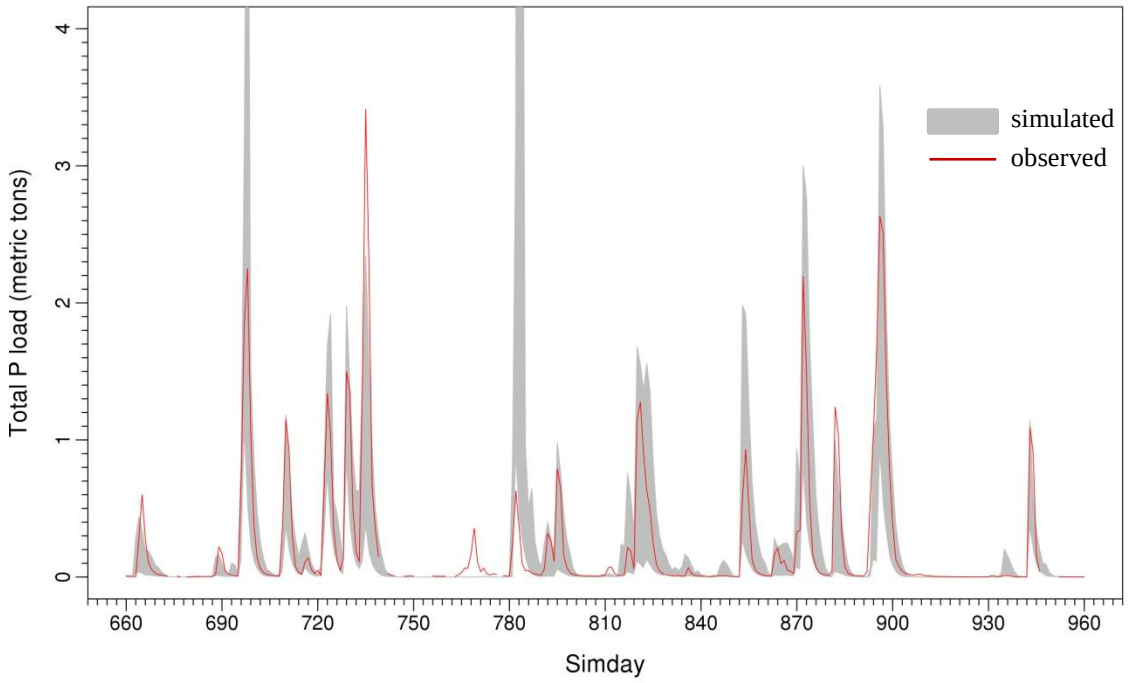

Figure A4.14. Simulated vs. observed total P load in Honey Creek with in-stream processing. Simday1 = January 01, 2002.

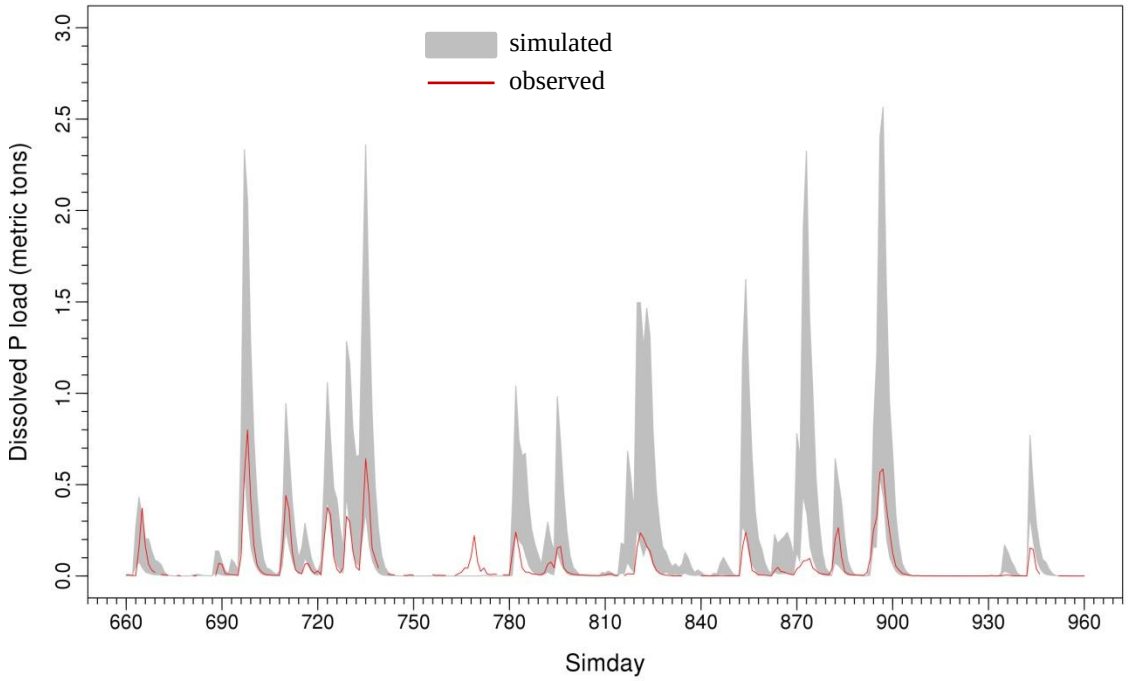

Figure A4.15. Simulated vs. observed dissolved P load in Honey Creek without in-stream processing. Simday1 = January 01, 2002.

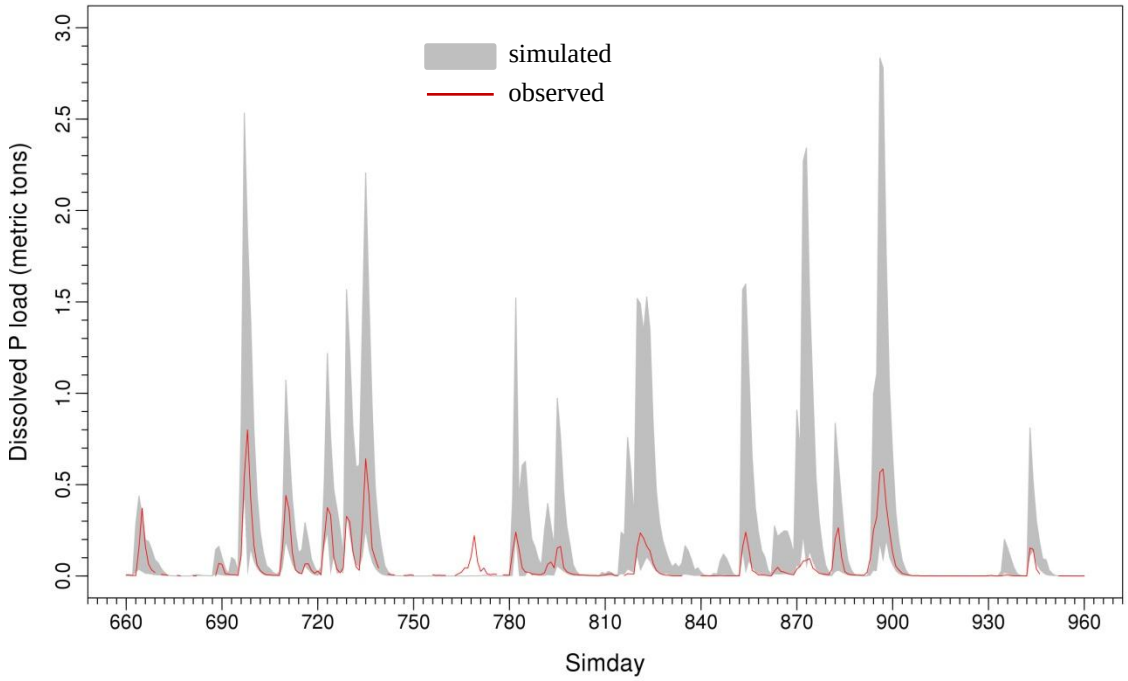

Figure A4.16. Simulated vs. observed dissolved P load in Honey Creek with in-stream processing. Simday1 = January 01, 2002.

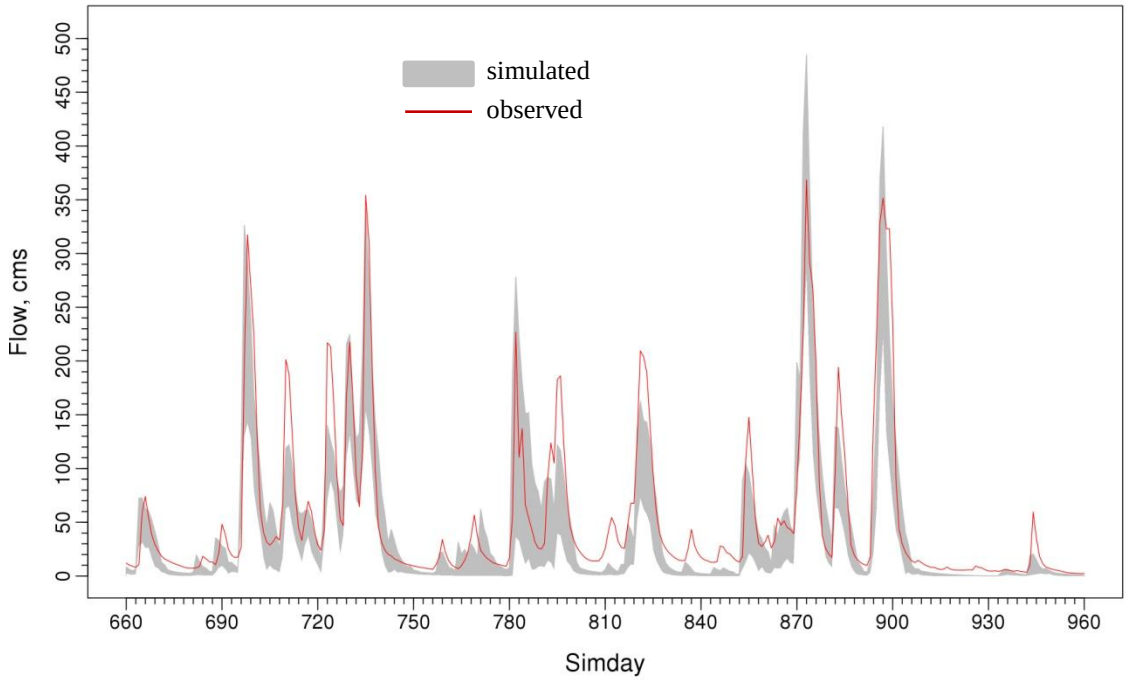

Figure A4.17. Simulated vs. observed flow in Sandusky without in-stream processing. Simday1 = January 01, 2002.

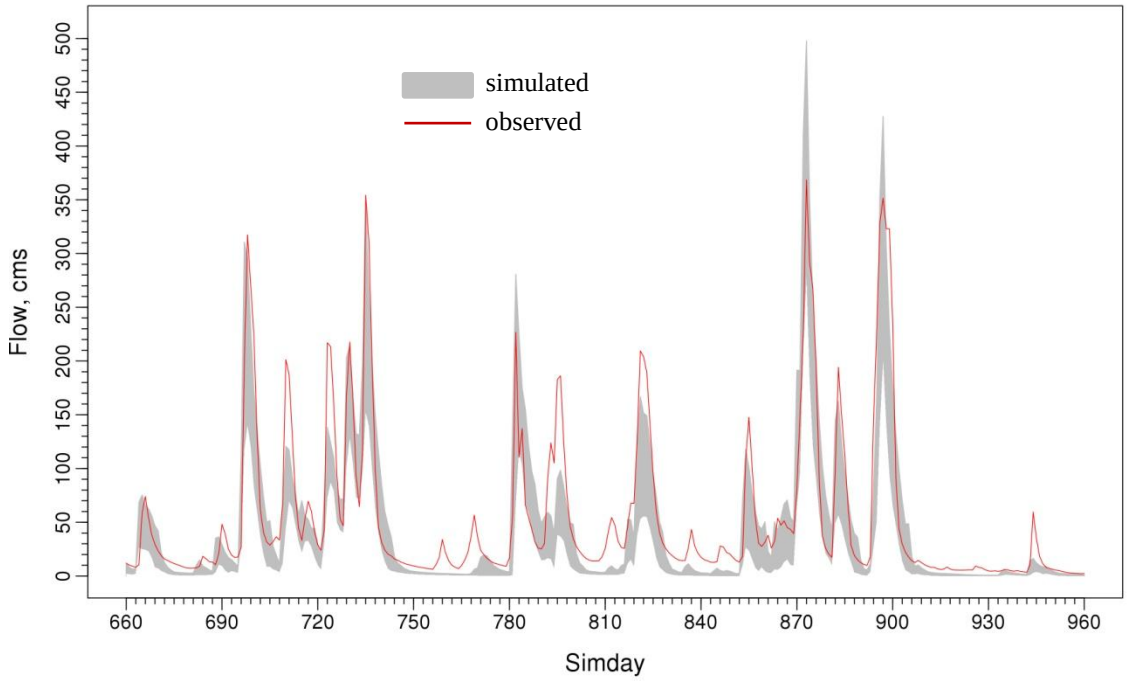

Figure A4.18. Simulated vs. observed flow in Sandusky with in-stream processing. Simday1 = January 01, 2002.

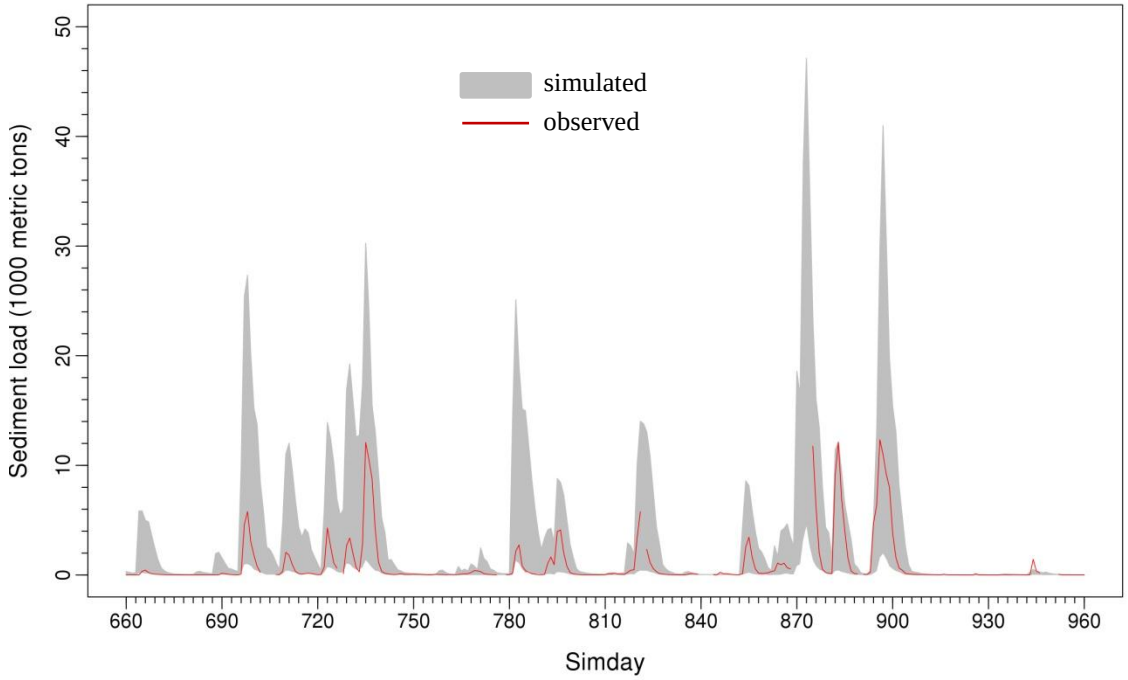

Figure A4.19. Simulated vs. observed sediment load in Sandusky without in-stream processing. Simday1 = January 01, 2002.

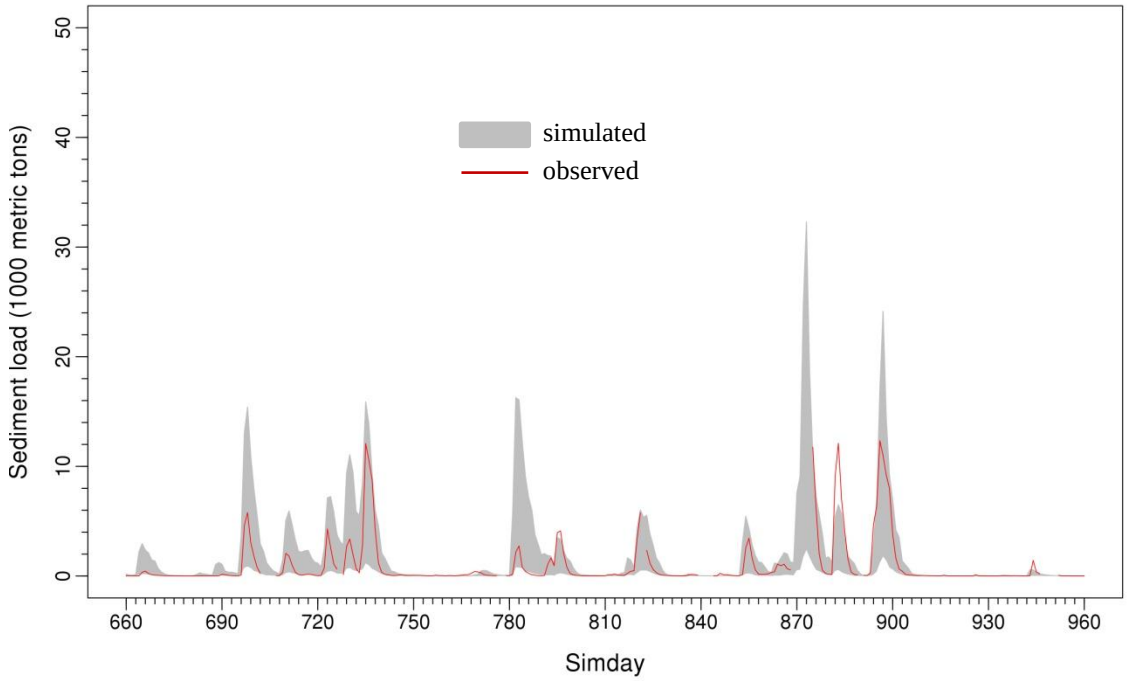

Figure A4.20. Simulated vs. observed sediment load in Sandusky with in-stream processing. Simday1 = January 01, 2002.

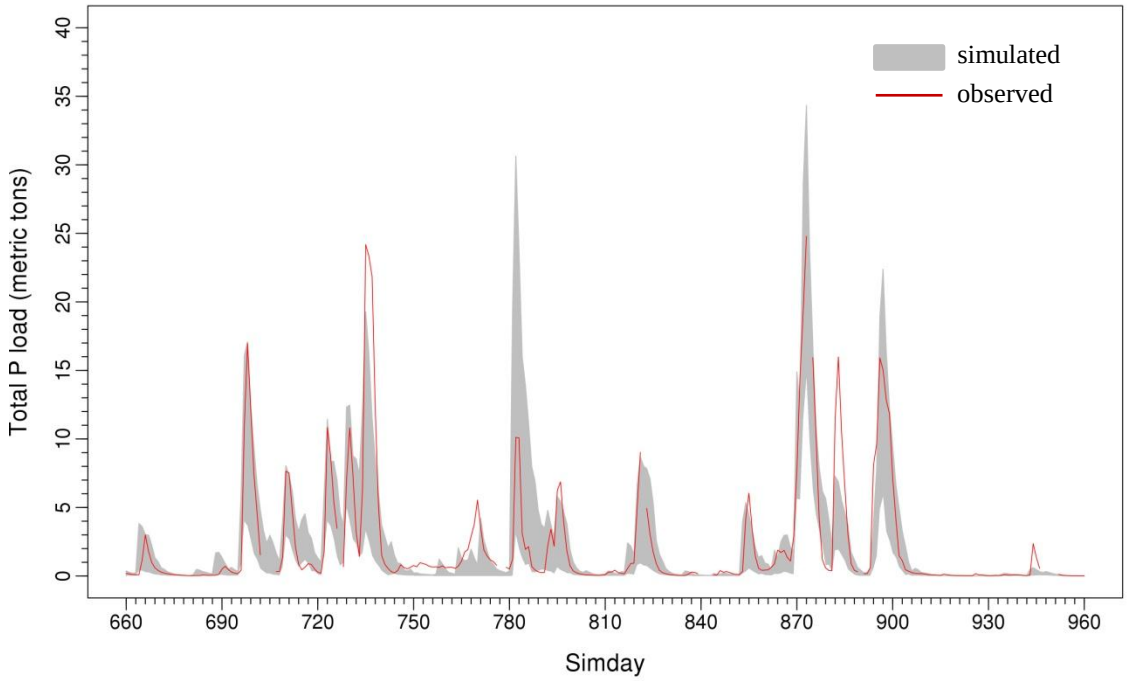

Figure A4.21. Simulated vs. observed total P load in Sandusky without in-stream processing. Simday1 = January 01, 2002.

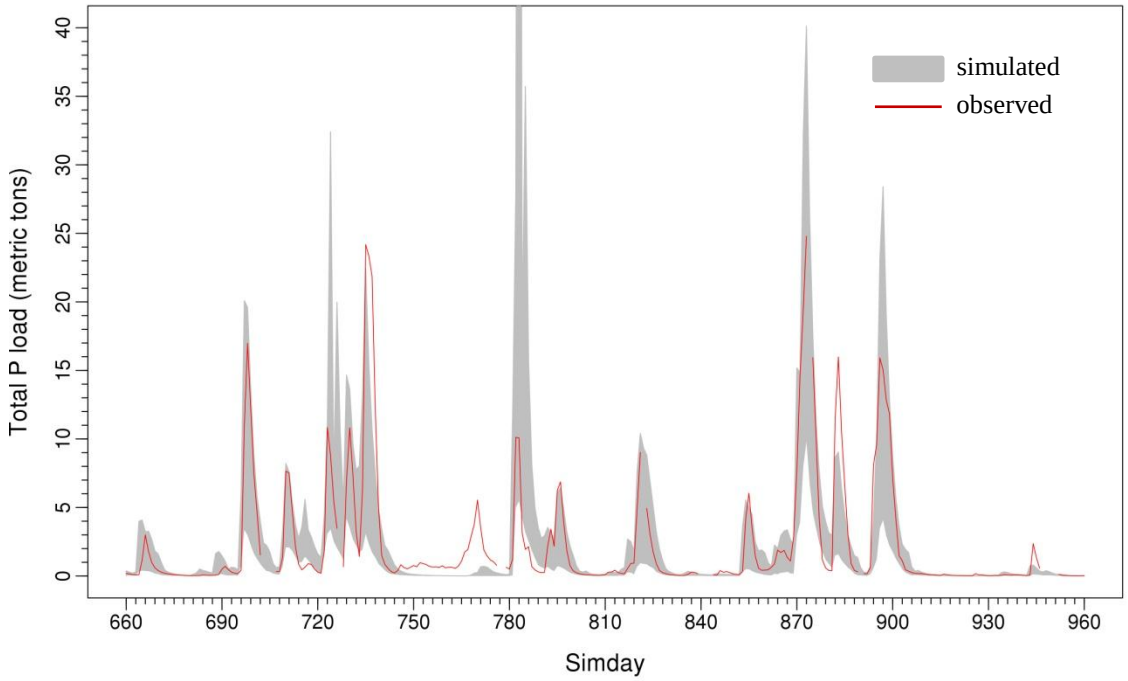

Figure A4.22. Simulated vs. observed total P load in Sandusky with in-stream processing. Simday1 = January 01, 2002.

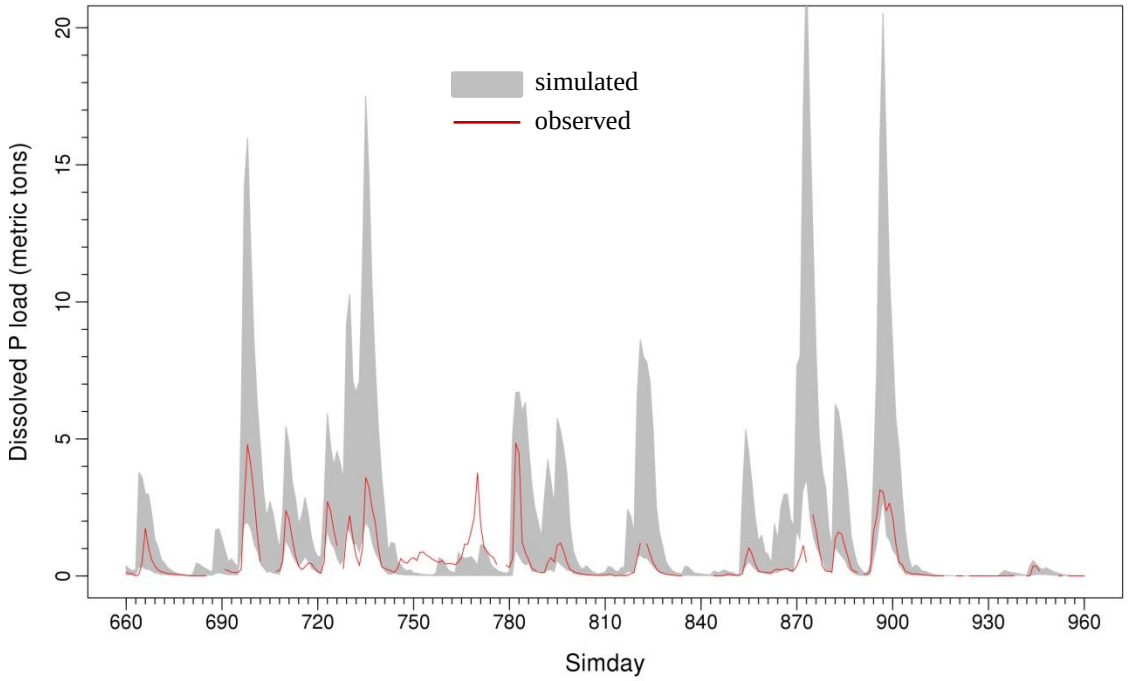

Figure A4.23. Simulated vs. observed dissolved P load in Sandusky without in-stream processing. Simday1 = January 01, 2002.

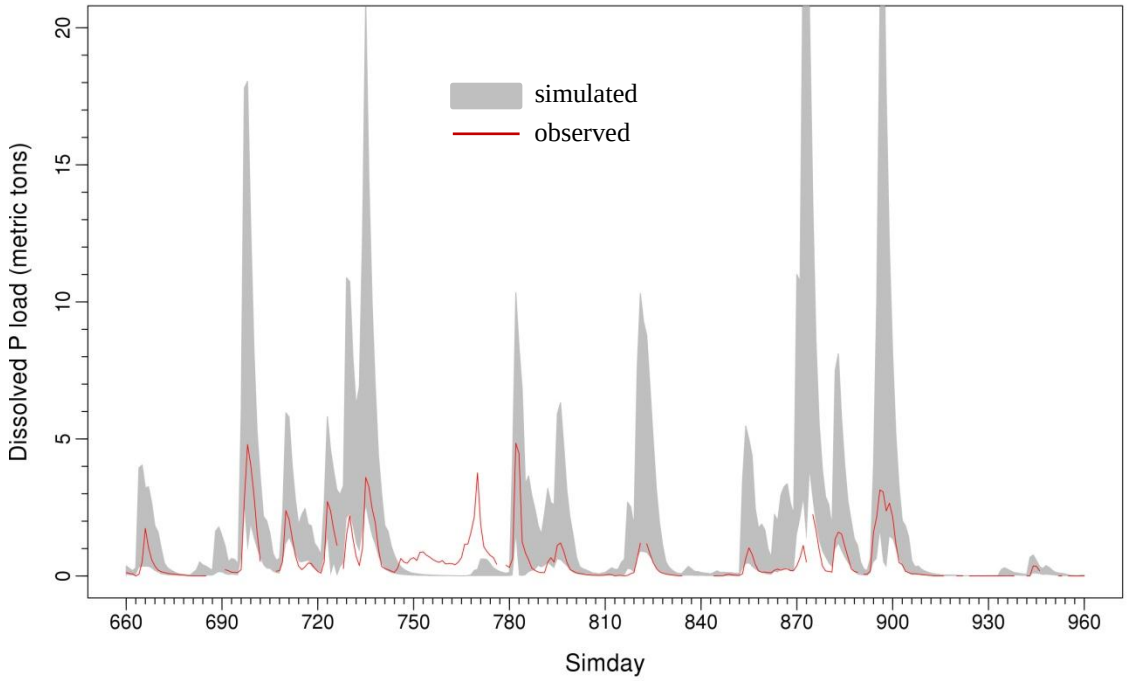

Figure A4.24. Simulated vs. observed dissolved P load in Sandusky with in-stream processing. Simday1 = January 01, 2002.

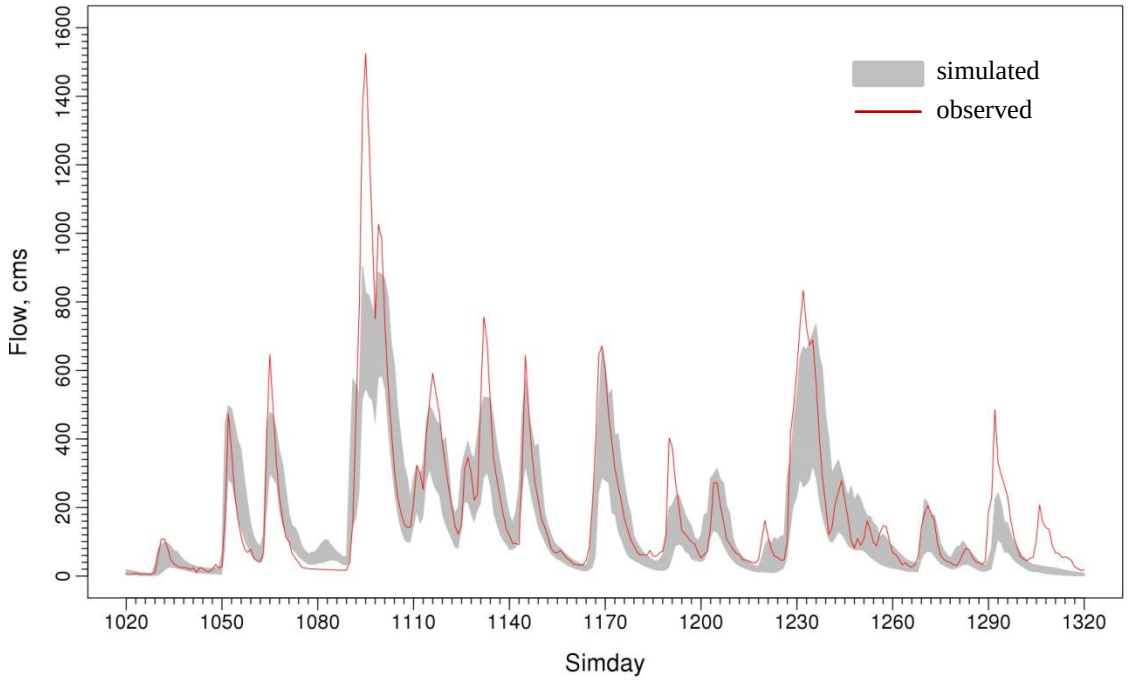

Figure A4.25. Simulated vs. observed flow in Maumee without in-stream processing. Simday1 = January 01, 2002.

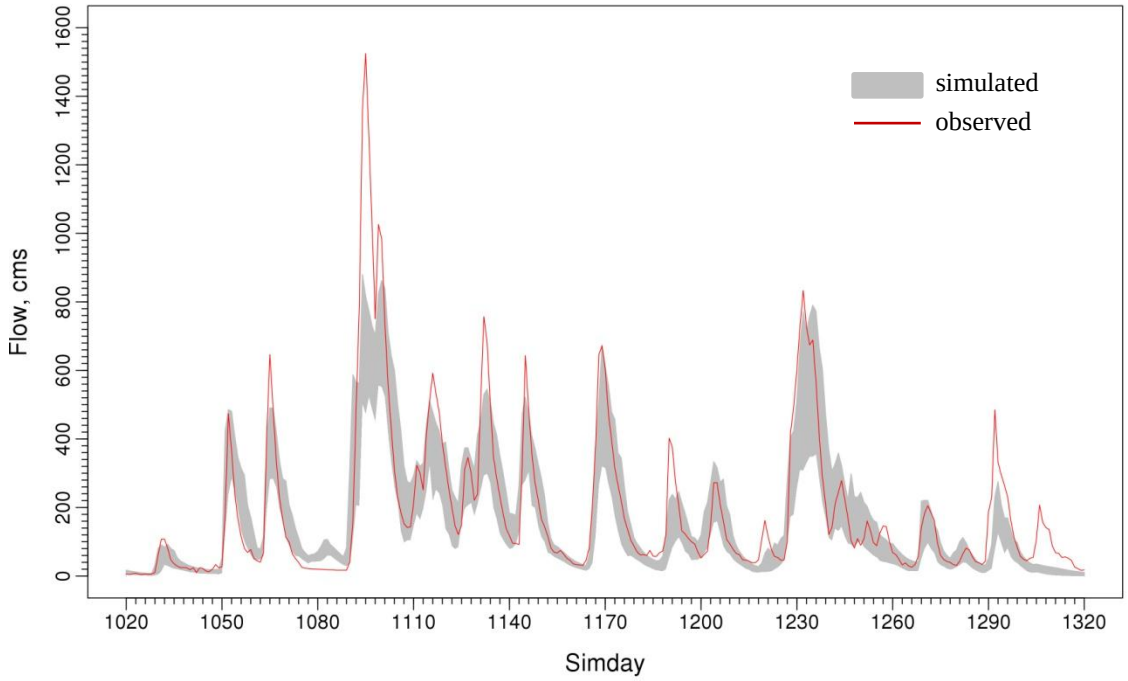

Figure A4.26. Simulated vs. observed flow in Maumee with in-stream processing. Simday1 = January 01, 2002.

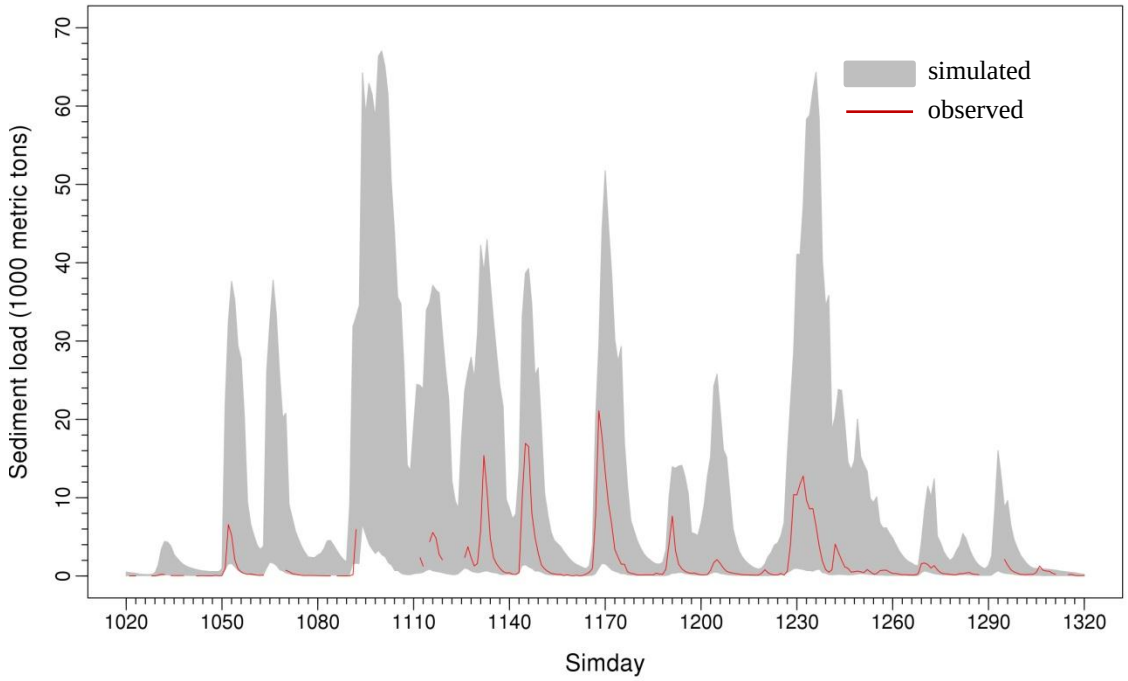

Figure A4.27. Simulated vs. observed sediment load in Maumee without in-stream processing. Simday1 = January 01, 2002.

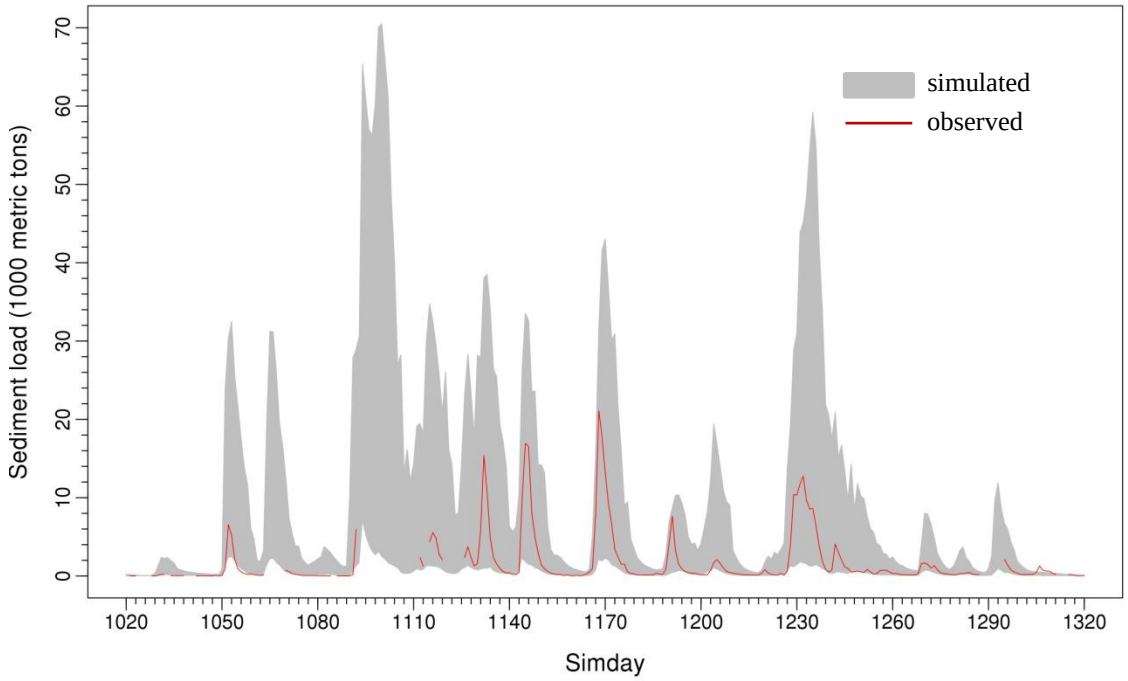

Figure A4.28. Simulated vs. observed sediment load in Maumee with in-stream processing. Simday1 = January 01, 2002.

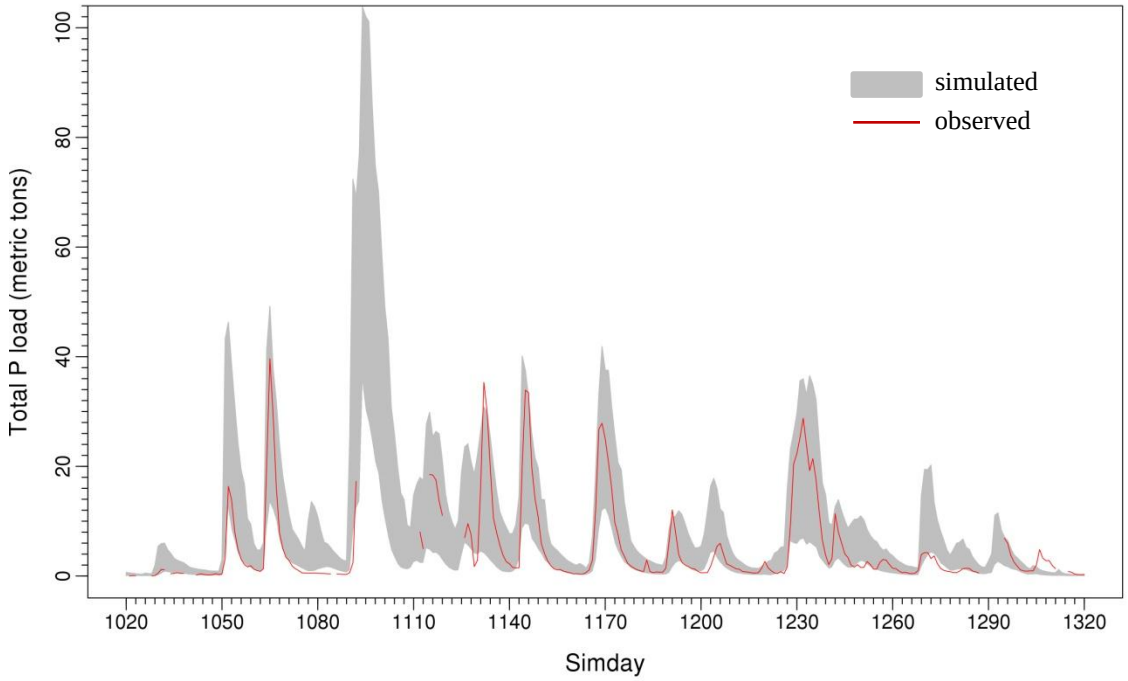

Figure A4.29. Simulated vs. observed total P load in Maumee without in-stream processing. Simday1 = January 01, 2002.

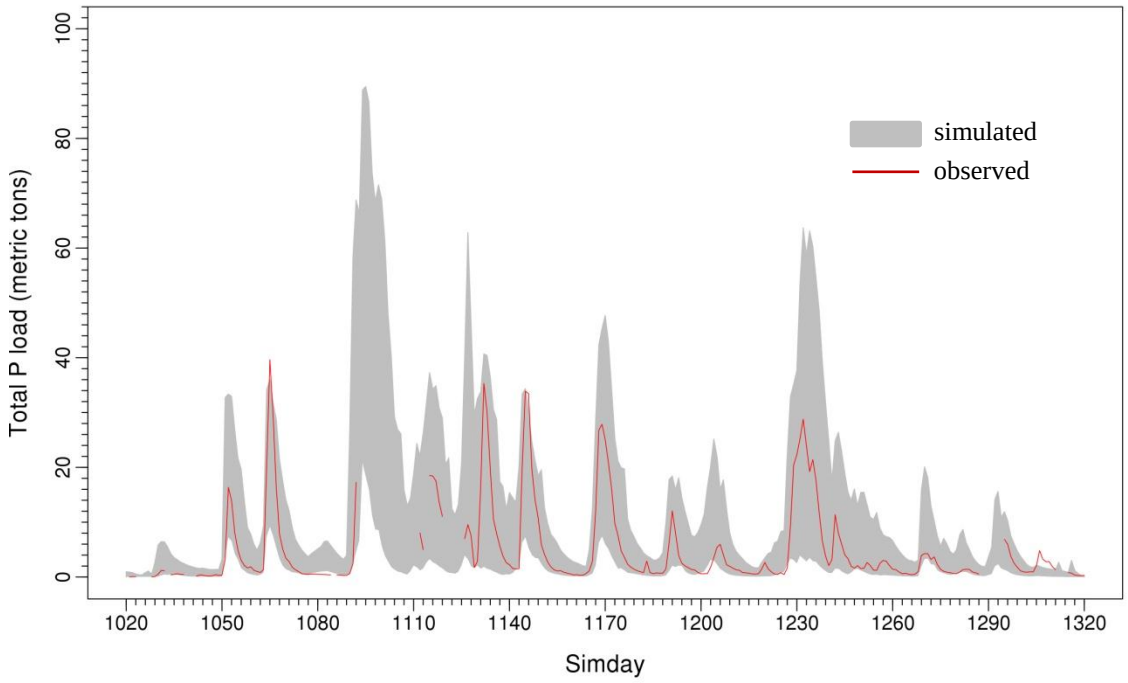

Figure A4.30. Simulated vs. observed total P load in Maumee with in-stream processing. Simday1 = January 01, 2002.

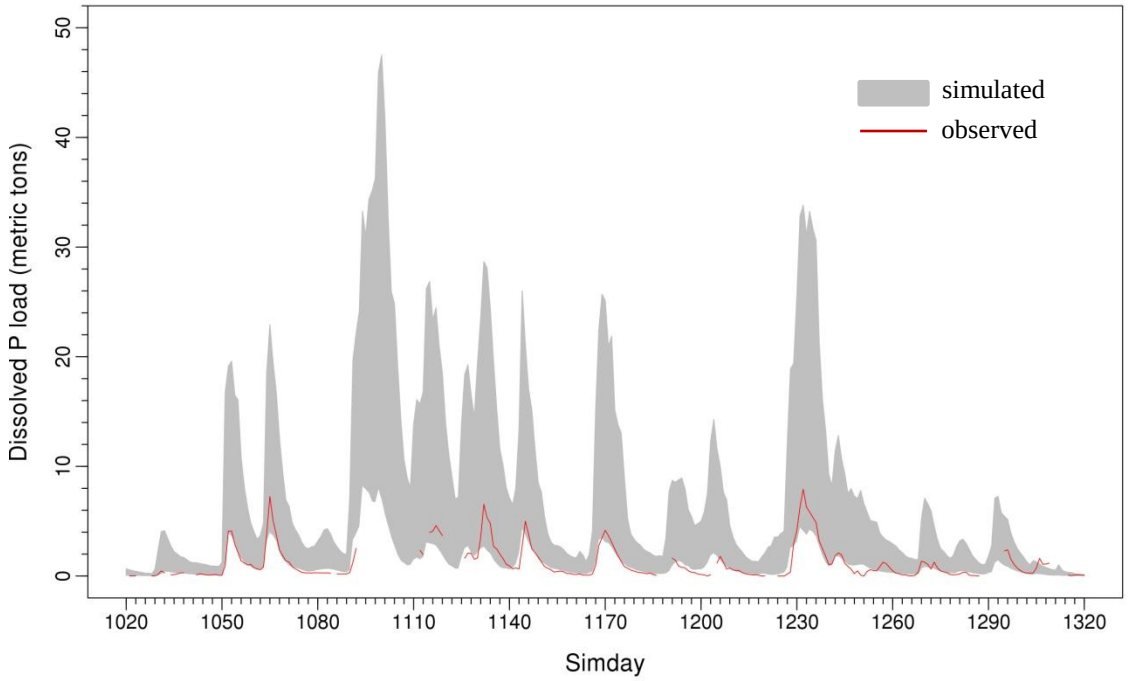

Figure A4.31. Simulated vs. observed dissolved P load in Maumee without in-stream processing. Simday1 = January 01, 2002.

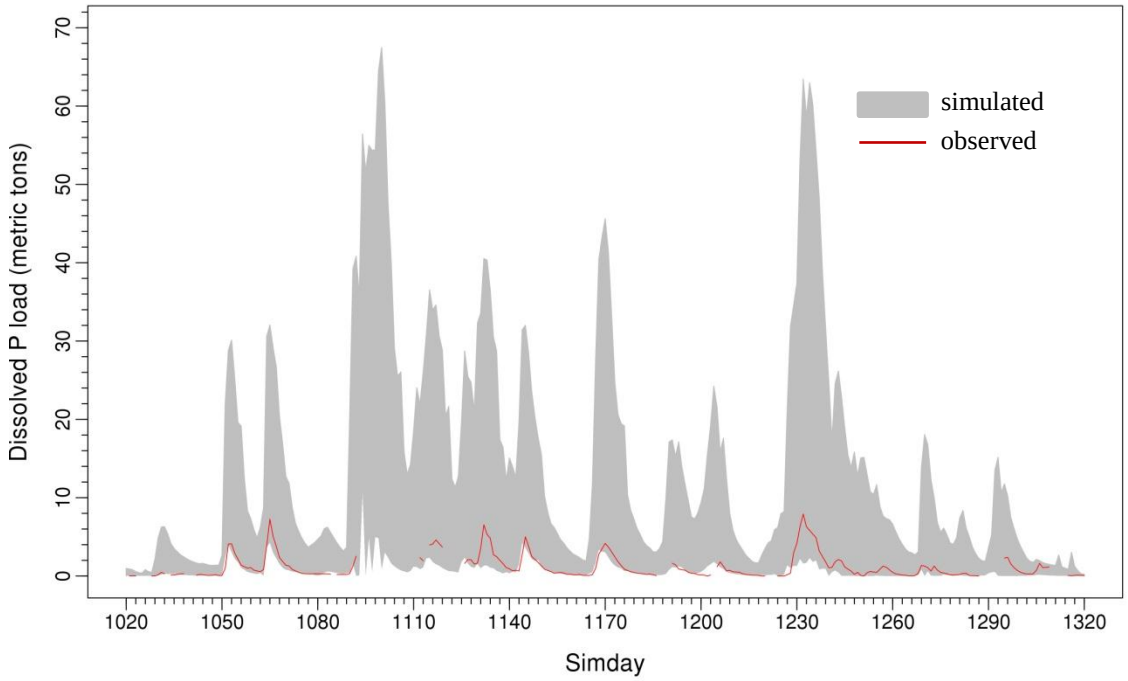

Figure A4.32. Simulated vs. observed dissolved P load in Maumee with in-stream processing. Simday1 = January 01, 2002.